SERI/TR-211-1400
UC Category: 60

The Application of U.S. Upper Wind Data in One Design of Tethered Wind Energy Systems

R.J. O'Doherty
B. W. Roberts

February 1982

Prepared under Task No. 1067.10
WPA No. 172-81

Solar Energy Research Institute
A Division of Midwest Research Institute

1617 Cole Boulevard
Golden, Colorado 80401

Prepared for the
U.S. Department of Energy
Contract No. EG-77-C-01-4042

Printed in the United States of America
Available from:
National Technical Information Service
U.S. Department of Commerce
5285 Port Royal Road
Springfield, VA 22161
Price:
Microfiche $3.00
Printed Copy $7.25

NOTICE

This report was prepared as an account of work sponsored by the United States Government. Neither the United States nor the United States Department of Energy, nor any of their employees, nor any of their contractors, subcontractors, or their employees, makes any warranty, express or implied, or assumes any legal liability or responsibility for the accuracy, completeness or usefulness of any information, apparatus, product or process disclosed, or represents that its use would not infringe privately owned rights.

SERI

FOREWORD

The work summarized in this report was supported through the Advanced and Innovative Wind Energy Concepts task at the Solar Energy Research Institute (SERI) within the Federal Wind Energy Program of the Department of Energy (DOE). Richard L. Mitchell was the technical project manager.

This report was prepared to support SERI subcontractors working in the field of Tethered Wind Energy Concepts. Data from the National Center for Atmospheric Research in Boulder, Colo. were reduced and analyzed by Robert J. O'Doherty (SERI) and Bryan W. Roberts (Visiting Professor from the University of Sydney, Sydney, Australia). Specific sites are described in detail. Additional sites were also analyzed, and results are available from SERI upon request.

Richard L. Mitchell
SERI Project Manager

Approved for

SOLAR ENERGY RESEARCH INSTITUTE

Jack Stone, Manager
Program Office

Donald Ritchie, Manager
Solar Electric Conversion Research
Division

SUMMARY

Objective:

This report assesses the upper atmospheric wind resource for the continental United States, Hawaii, and Alaska.

Discussion:

The document is intended for Solar Energy Research Institute contractors interested in tethered wind energy systems. The raw data were obtained from the National Center for Atmospheric Research, Boulder, Colo.

Conclusion:

The probability distributions of velocity are presented for 54 sites, and detailed calm wind analyses have been undertaken for five of these locations. On the average, the wind lulls about one day per week for a period in excess of about 30 hours.

The report shows that the average power density of this wind resource can be as high as 16 kW/m^2 at northeastern U.S. sites. This power density is at a maximum around the 300-mb pressure level.

TABLE OF CONTENTS

Page

1.0 Introduction 1

2.0 Background of the Concept 3

2.1 Theoretical Foundations 3
2.2 Numerical Techniques 4
2.2.1 Average Wind Speed 5
2.2.2 Average Power Density 5
2.2.3 Cumulative Velocity Distribution 5
2.2.4 Calm Wind Analysis 5
2.2.5 Procedures for Missing Data 6
2.2.6 Sampling Periods 6
2.2.7 Annual and Monthly Average Values of Velocity and Power Density 6
2.3 Detailed Probability Analysis of the U.S. Upper Winds 13
2.4 Power-Duration Curves 15
2.5 The Annual Calm Period Analysis 16
2.6 The Monthly Calm Period Analysis 19
2.7 Lightning Conditions 20
2.8 Conclusions 21

3.0 References 23

Appendix A - Average Values of Velocity and Power 25

Appendix B - Application of U.S. Upper Wind Data in Pre-Design Tethered Wind Energy Systems 55

Appendix C - Annual Calm-Period Charts 111

Appendix D - Use of the Annual Probability Distribution of Velocity Charts 123

LIST OF FIGURES

		Page
2-1	Time-Series Wind Data at a Pressure Altitude of p	4
2-2	Isopleths of Mean Power Density (kW/m^2) at 300 mb	9
2-3	Isopleths of Mean Power Density (kW/m^2) at 400 mb	10
2-4	Isopleths of Mean Power Density (kW/m^2) at 500 mb	11
2-5	Isopleths of Mean Power Density (kW/m^2) at 700 mb	12
2-6	Monthly Average Power Density: Portland, ME	13
2-7	Annual Probability Distribution of Velocity: Portland, ME	14
2-8	Annual Power-Duration Curve: Portland, ME	15
2-9	Annual Calm-Period Analysis: Portland, ME	17
2-10	Annual Calm-Period Analysis: Portland, ME	18
2-11	Number of Occasions per Month Wind Speed is Below 15 m/s: Portland, ME	19
2-12	Average Period Wind Speed is Below 15 m/s: Portland, ME	20
2-13	Annual Average Number of Thunderstorm Days	21

LIST OF TABLES

		Page
2-1	Annual Average Values of Velocity and Power: Portland, ME	7
2-2	U.S. Sites Considered for Annual Average Values of Velocity and Power	8

SECTION 1.0

INTRODUCTION

The Solar Energy Research Institute (SERI) has recently awarded study contracts to assess and to recommend ways to harness the energy in the earth's upper atmospheric wind system.

Jet streams flow continually in mid-latitudes in both hemispheres due to the effect of both solar radiation on the tropics and cooling in the arctic regions with the rotation of the earth on its axis. Reiter, in his classic text on meteorology of the jet streams [1], describes the subtropical and polar-front jet stream systems. Both these jets flow over the United States, but their confluence and meandering patterns lead to a variability in the strength and persistence of the winds at any one fixed site. The variability in the strength and location of these jets is the subject of this report.

Note that an assessment of the winds aloft is integral to the decision about the siting, viability, and practicality of the various types of tethered wind energy systems.

This report is restricted to a statistical assessment of the U.S. upper wind resource. It has been compiled from "Time Series Upper Wind Data," supplied to SERI by the National Center for Atmospheric Research (NCAR), located in Boulder, Colo. These wind data are available for a variety of sites throughout the world, but this study is limited to the continental United States, Hawaii, and Alaska.

SERI

SECTION 2.0

BACKGROUND OF THE CONCEPT

The current statistical survey uses wind energy conversion platforms, if they can be located at sites remote from the earth's surface.

We will show that the availability of this wind energy resource increases with altitude up to around 200 mb. In addition, at favorable U.S. sites, the power density can be as high as 17 kW/m^2, while at sites in the southern hemisphere the power density can be around 19 kW/m^2 [2].

Note that the conversion of mechanical energy from winds invariably produces aerodynamic drag forces. In addition, the conversion of kinetic energy will generate a drag force that will be collinear with the free-stream velocity vector. This drag force must be balanced if a useful energy conversion is to be produced.

These drag loads may be resisted by a tethering cable or cables. One end of the cable would be attached to the platform, and the other end would be fixed to the earth's surface. Subsystems other than a tethering cable might be used to balance the drag load.

Finally, the means by which the converted energy will be transmitted to the earth's surface are left undefined. One can, however, assert that the average power density in the upper atmosphere is highly concentrated when compared to other renewable resources, such as direct solar radiation or wind energy near the surface.

2.1 THEORETICAL FOUNDATIONS

By using standard wind energy techniques, we want to represent the cumulative probability distribution of the wind speed V by an integrated Weibull model:

$$P(V) = 1 - e^{-(V/V_0)^{\alpha}} \quad \text{for } V \geq 0 \qquad (1)$$
$$P(V) = 0 \text{ elsewhere,}$$

where V_0 and α are two constants that give a good fit to the data.

The use of the Weibull distribution is common [3-6] in wind energy applications. Furthermore, the Rayleigh model is a special case of the Weibull model where $\alpha = 2$. The application of these Rayleigh/Weibull models has become an established wind energy practice for the analysis of near-surface winds and is also satisfactory for modeling upper wind data.

However, conventional meteorological techniques represent upper wind data with a bivariant normal distribution [7,8] so that the wind components in the zonal (E-W) and meridional (N-S) directions can be represented by suitable averages and standard deviations. This model allows meteorologists to introduce wind constancy, vector means, and various wind components. However, in this report

it is more appropriate to fit a Weibull distribution to the scalar wind distribution.

These raw rawinsonde data have been used to define the distributions. The standard pressure altitudes of 950, 850, 750, 700, 600, 500, 400, 300, 250, and 200 mb are used to define the various vertical sectors.

In summary, the probability distributions of velocity will be compiled for a series of altitudes at 54 sites selected across the United States and its territories. Then probability distributions can be plotted on a log-log scale. (This graph paper will be referred to as Weibull paper.) Further details of this type of representation can be found in a report by Takle and Brown [3]. On this class of graph paper, the Weibull distribution plots a straight line with a slope of $\alpha/2$, which passes through point $V = V_0$, $P(V) = 1 - 1/e$. This treatment (see Fig. 2-7) allows one to easily evaluate α by use of the side nomogram. The magnitude of V_0 is given by the intersection of appropriate distribution with the 63.2% ordinate (shown as a dotted line in the figures). More details on the use of these charts are given in Appendix D.

2.2 NUMERICAL TECHNIQUES

These raw rawinsonde data were obtained from NCAR. These tapes contained, among other information, a series of one-half day samples of wind velocity and air temperature at the standard pressure altitudes. These data were collected from balloon soundings launched at 0000 and 1200 hours GMT from fixed sites.

The numerical analysis can best be described by reference to Fig. 2-1, which is a segment of the time-series wind data at a pressure altitude p. The data extend from day n to day (n + 4).

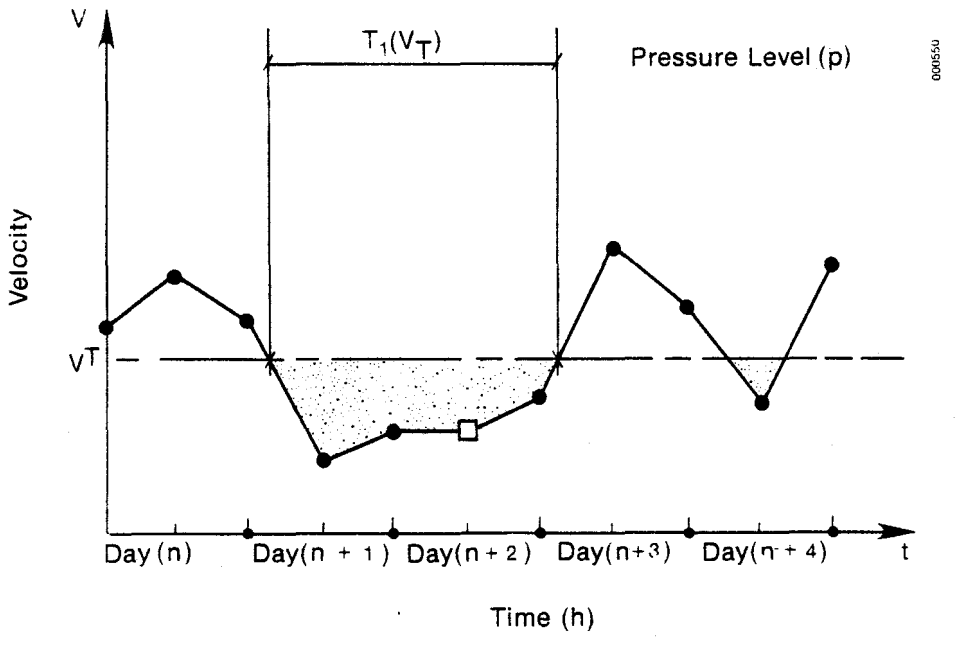

Figure 2-1. Time-Series Wind Data at a Pressure Altitude of p

2.2.1 Average Wind Speed

The average wind speed is the summation of the observations divided by the total number of observations:

$$\overline{V} = \sum_{c=i}^{N} V_i/N \quad . \tag{2}$$

2.2.2 Average Power Density

The average power density is defined as

$$\overline{P} = 1/2 \sum_{i=1}^{N} \rho_i \, V_i^3/N \quad . \tag{3}$$

The air density ρ_i has been derived from the equation of state as

$$\rho_i \simeq 0.35 \; P/(T_i + 273) \quad , \tag{4}$$

where T_i is the ith observation of the air temperature.

2.2.3 Cumulative Velocity Distribution

The cumulative velocity distribution at the velocity V is physically the percentage probability for which the wind velocity will be less than or equal to the value of V:

$$P(V) = 100 \; n(V)/N \quad , \tag{5}$$

where n(V) is the number of observations when the velocity is less than or equal to V. The total number of observations N is approximately 5100 per site in this study.

2.2.4 Calm Wind Analysis

A calm wind survey is important in the design and operation of any tethered system.* Although it is important to know the cumulative probability $P(V_T)$, it is equally significant to know how long, on the average, the wind is below the threshold velocity V_T. Also we would like to know on how many occasions in a given period the winds will fall below the threshold value. In mathematical form, this implies that:

$$P(V_T) \simeq \overline{T}(V_T)N(V_T)100/8760 \quad , \tag{6}$$

---

*The importance of the calm wind analysis will be discussed at length in Secs. 8.0 and 9.0.

where

$P(V_T)$ is the probability the velocity will be equal to or below a speed of V_T;

$N(V_T)$ is the average number of times per year that the wind falls below the threshold speed; and

$\overline{T}(V_T)$ is the average period in hours that the wind speed is below threshold.

If $N(V_T)$ were compiled monthly, then the denominator in Eq. 6 will be 730.

In Fig. 2-1, for example, the first downtime is $T_1(V_T)$ hours. Therefore, a value of unity is accumulated into the count of $N(V_T)$, while a value of $T_1(V_T)$ is counted into the running average of $\overline{T}(V_T)$. A linear interpolation scheme has been used to compute the downtimes. Furthermore, the standard deviation of $T(V_T)$ has been computed and will be discussed later.

2.2.5 Procedures for Missing Data

Of approximately five thousand samples at each site and altitude, we found that about 1% to 2% of data were missing for two reasons.

First, occasionally, the rawinsonde sounding was completely missing due to radar breakdown or poor weather conditions. In this case, the data were effectively moved to the left, on Fig. 2-1, by one day. Thus, no gaps were introduced into the string of soundings. On other rare occasions, three or four soundings were taken in one day. Under these circumstances, the information in Fig. 2-1 was moved to the right to receive the extra data.

Secondly, on some occasions, the rawinsonde flight was abandoned too early, perhaps because of a premature bursting of the balloon. In this case, we assumed the missing data (shown as the open square symbol in Fig. 2-1) were of the same value as those from the previous sounding at the same altitude.

We believe this treatment of the missing data is reasonable. However, other techniques are possible, but the technique used should not significantly affect the result.

2.2.6 Sampling Periods

We have evaluated parameters in Secs. 2.2.1 to 2.2.5 for each month in a seven-year period. We have also assembled annual statistics for the 54 sites in the United States.

2.2.7 Annual and Monthly Average Values of Velocity and Power Density

The average velocity and power density can be determined from the raw data by the use of Eqs. 2 to 4. Average values of both of these variables are given

in Table 2-1. This figure uses Portland, Maine, as an example, and nine altitudes are listed.

Table 2-1. Annual Average Values of Velocity and Power: Portland, ME

Altitude (mb)	Velocity ($\overline{V}$, m/s)	Power ($\overline{P}$, kW/m^2)
900	9.42	1.11
850	10.4	1.36
700	14.8	2.84
600	18.4	4.67
500	22.5	7.53
400	27.6	11.4
300	32.8	14.1
250	33.9	12.9
200	31.2	7.90

The same calculations have been performed for 53 other U.S. sites. The relevant values are given in Appendix A as Tables A-1 through A-54. The appendix considers the sites alphabetically (see Table 2-2).

From the annual average power-density figures given in Appendix A, one can draw resource maps showing the isopleths of power density at the various altitudes. Figures 2-2 to 2-5 show these charts for the 300, 400, 500, and 700 mb levels, respectively.

In the United States, the wind energy resource is primarily concentrated in the Northeast, where the average power density can be in excess of 16 kW/m^2. At 300 mb, the power density falls to about 8 kW/m^2 in the Midwest, and it falls further to about 4 kW/m^2 in equatorial regions.

Note that the jet stream is the dominant influence in the upper air resource. The power density essentially reflects the average residence time that a jet spends above a site as the jet "meanders" over the continent.

Finally, monthly values of power density can be calculated from the raw data. This can be completed for all stations if required, but typical results can be seen in the output for Portland, Maine. Figure 2-6 shows the monthly average power densities for Portland; the results were derived from a seven-year sample.

Figure 2-6 shows that the power density is at a maximum of about 30 kW/m^2 in January and falls to 7 kW/m^2 in July. The maximum and minimum values occur about one month after the winter and summer solstices, respectively [1].

Table 2-2. U.S. Sites Considered for Annual Average Values of Velocity and Power

Albany, NY	Montgomery, AL
Albuquerque, NM	Nashville, TN
Bismarck, ND	New York, NY
Boise, ID	North Platte, NE
Brownsville, TX	Oakland, CA
Buffalo, NY	Oklahoma City, OK
Caribou, ME	Omaha, NE
Charleston, SC	Peoria, IL
Dayton, OH	Pittsburgh, PA
Del Rio, TX	Portland, ME
Denver, CO	Rapid City, SD
Dodge City, KS	St. Cloud, MN
Ely, NV	Salem, IL
Fairbanks, AK	Salem, OR
Fort Worth, TX	Salt Lake City, UT
Glasgow, MT	San Nichols Island, CA
Great Falls, MT	Sault Ste. Marie, MI
Green Bay, WI	Shreveport, LA
Greensboro, NC	Spokane, WA
Guadalupe Island, Mexico	Tampa, FL
Hilo, HI	Topeka, KS
Huntington, WV	Tucson, AZ
International Falls, MN	Wallops Island, VA
Lander, WY	Waycross, GA
Little Rock, AR	Winnemucca, NV
Medford, OR	Winslow, AZ
Midland, TX	Yucca Flats, NV

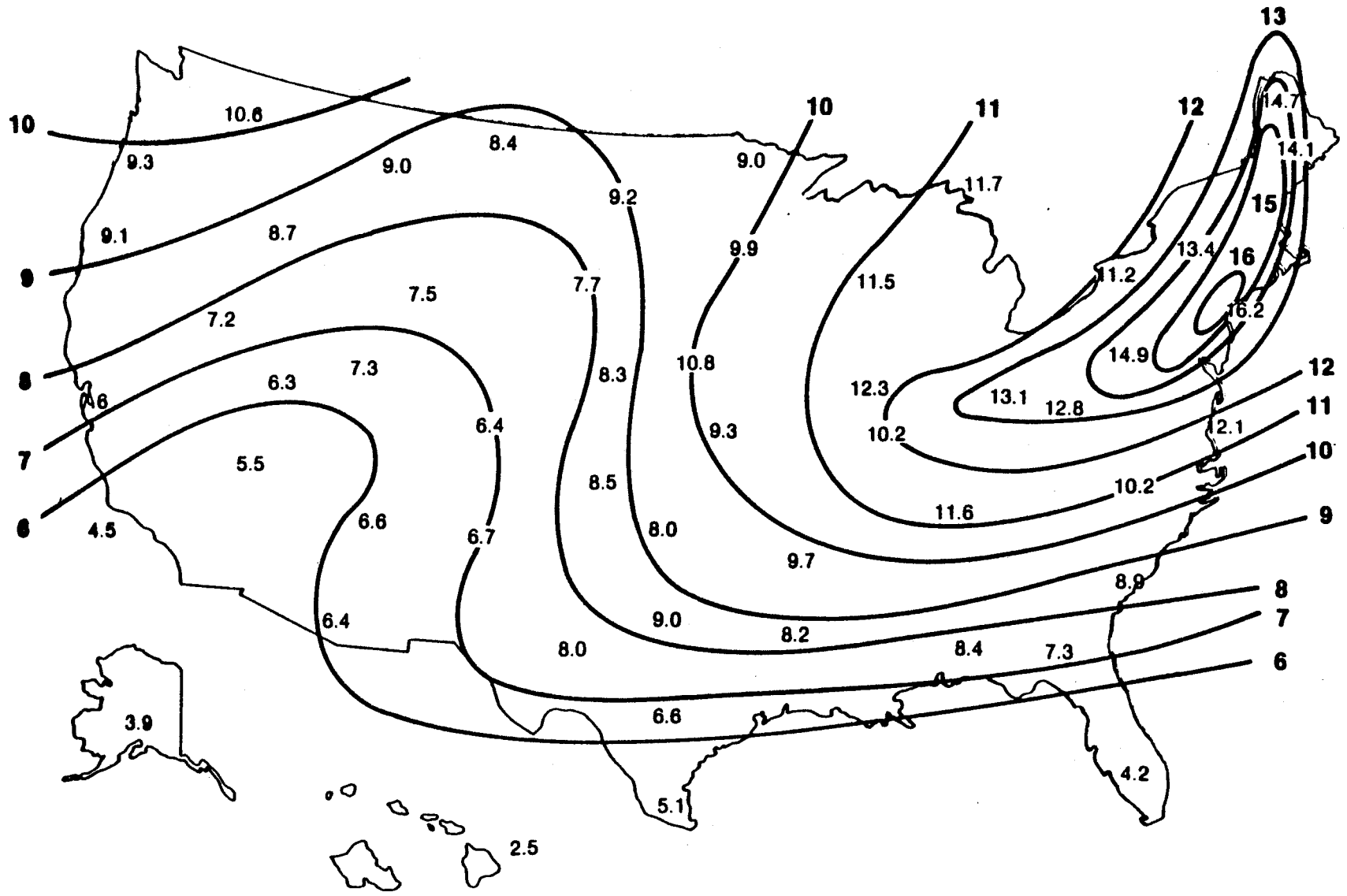

Figure 2-2. Isopleths of Mean Power Density (kW/m^2) at 300 mb

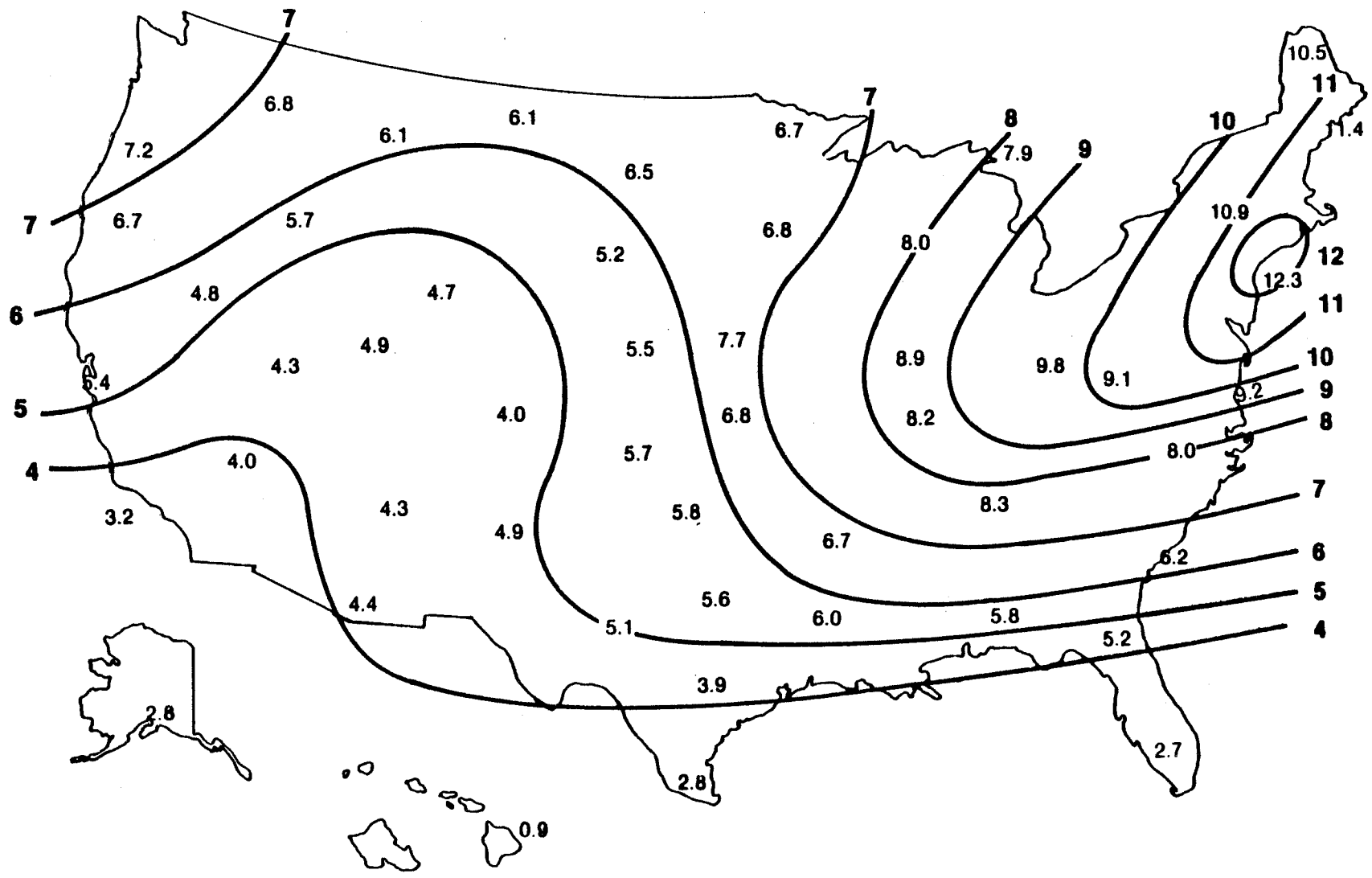

Figure 2-3. Isopleths of Mean Power Density (kW/m²) at 400 mb

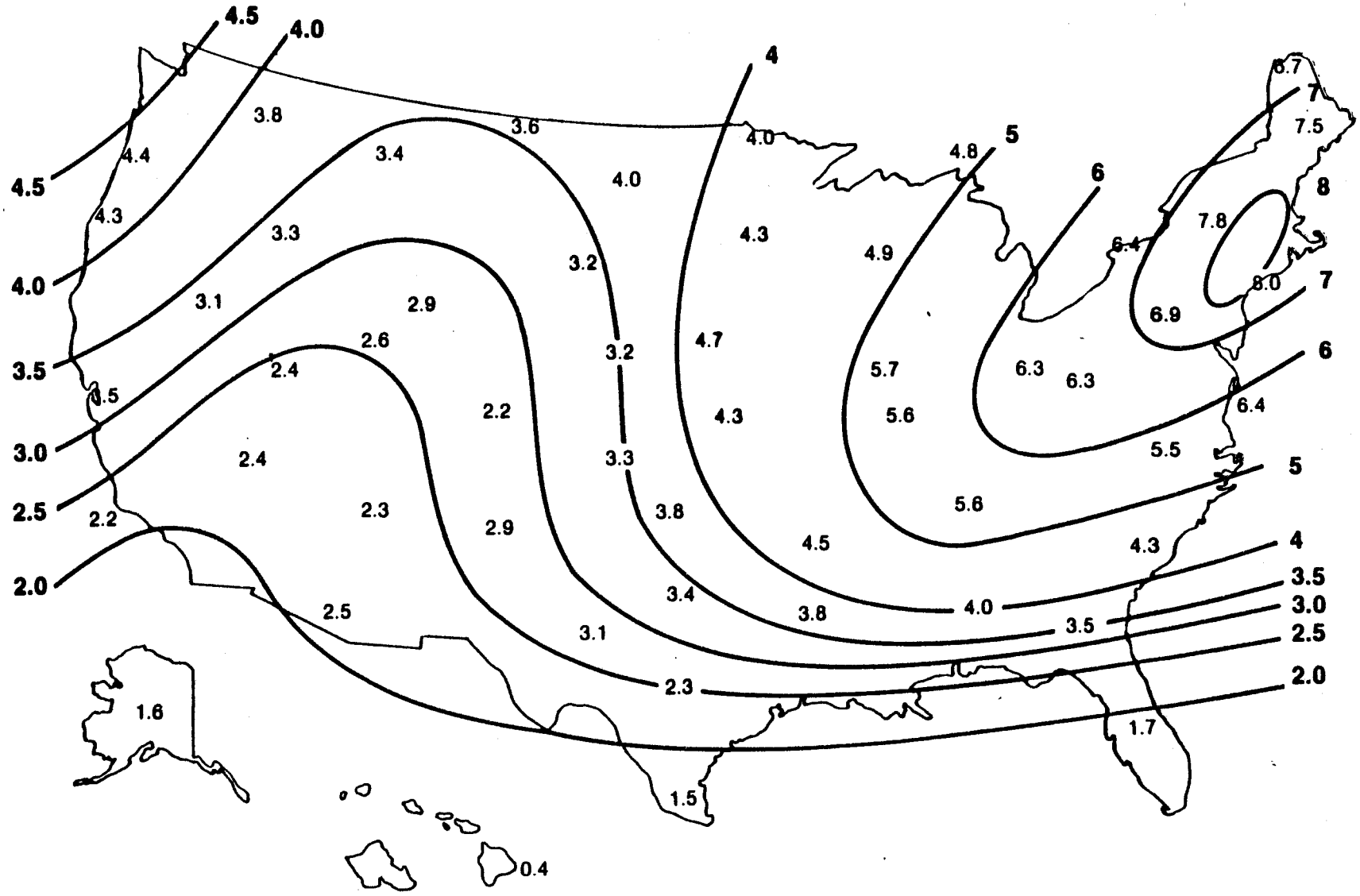

Figure 2-4. Isopleths of Mean Power Density (kW/m²) at 500 mb

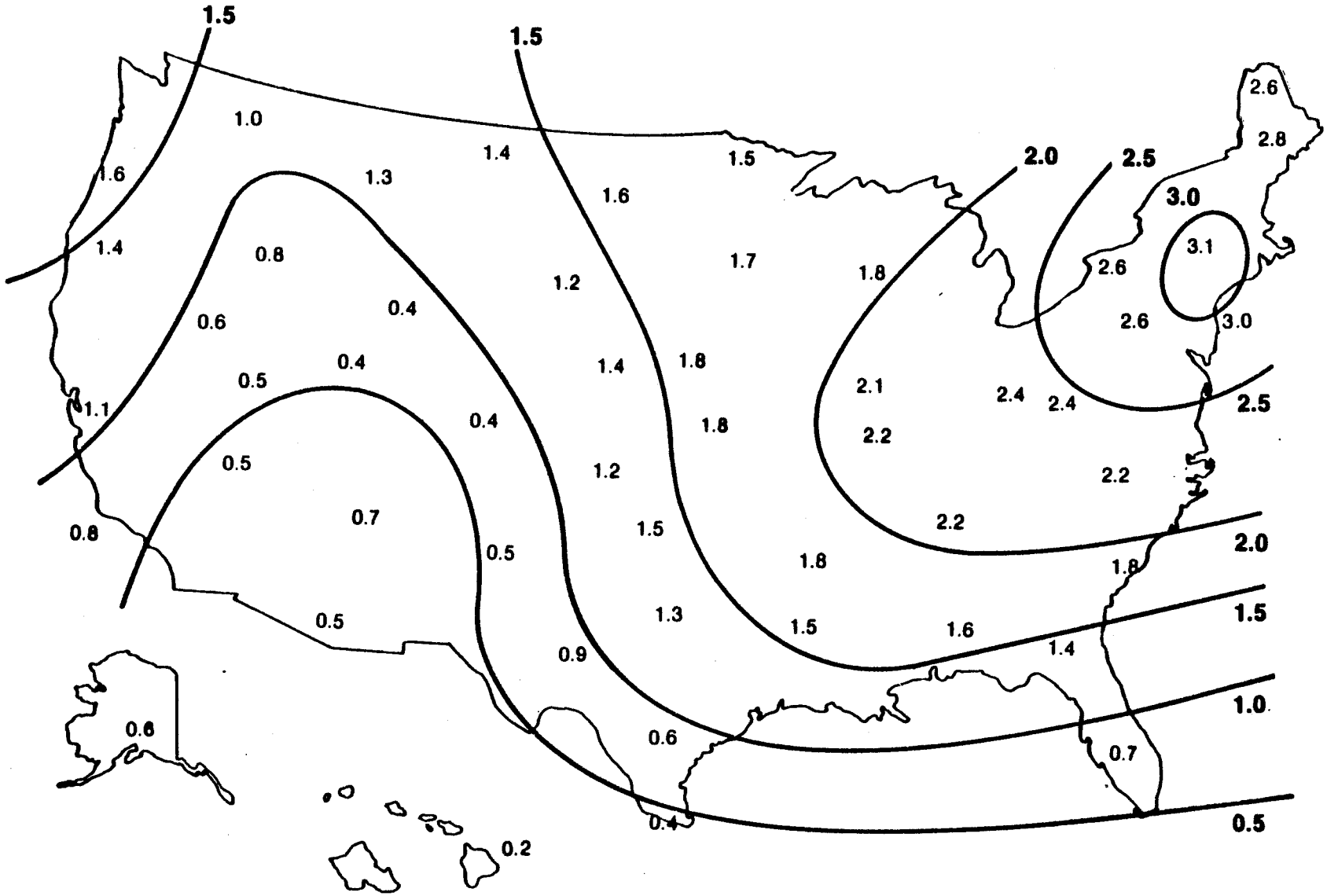

Figure 2-5. Isopleths of Mean Power Density (kW/m²) at 700 mb

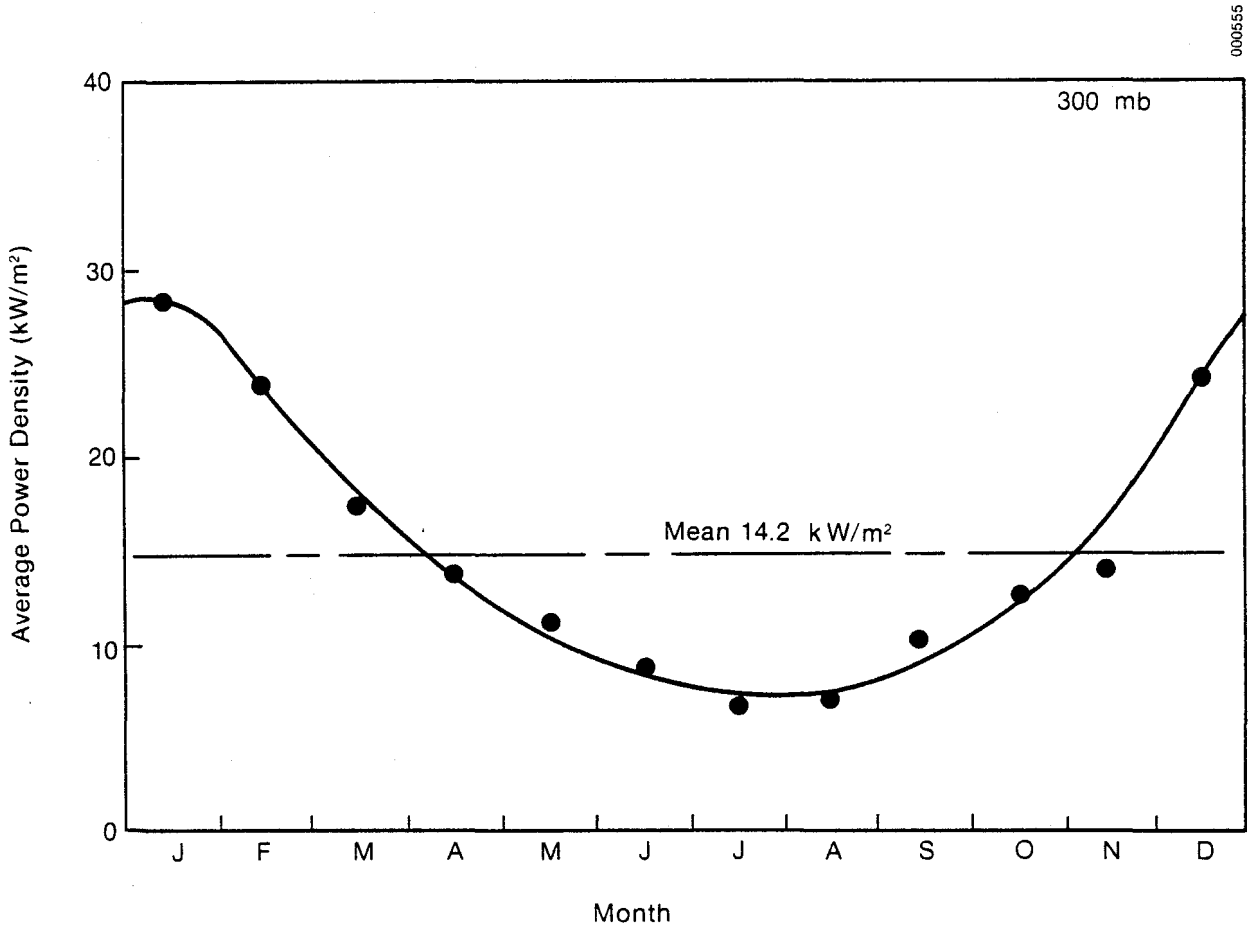

Figure 2-6. Monthly Average Power Density: Portland, ME

2.3 DETAILED PROBABILITY ANALYSIS OF THE U.S. UPPER WINDS

A typical, cumulative probability distribution of velocity is shown in Fig. 2-7 for Portland, Maine. Here distributions for the pressure levels of 700, 500, 400, 300, and 200 mb are approximated by straight-line Weibull distributions. In all cases, the actual distributions are closely modeled by the Weibull distributions. The intersection of the approximating straight line with the dotted line gives the value of V_0 in Eq. 1. The slope of the straight line gives the value of the exponent α which is also in Eq. 1. More details of the distributions for the 54 sites are given in Appendix B as Figs. B-1 through B-54. These figures are relevant to the design of tethered wind energy conversion systems. For example, it is conventional to use figures similar to Figs. B-1 to B-54 in the design of a typical windmill. From the probability distribution of velocity, it is simple to derive the

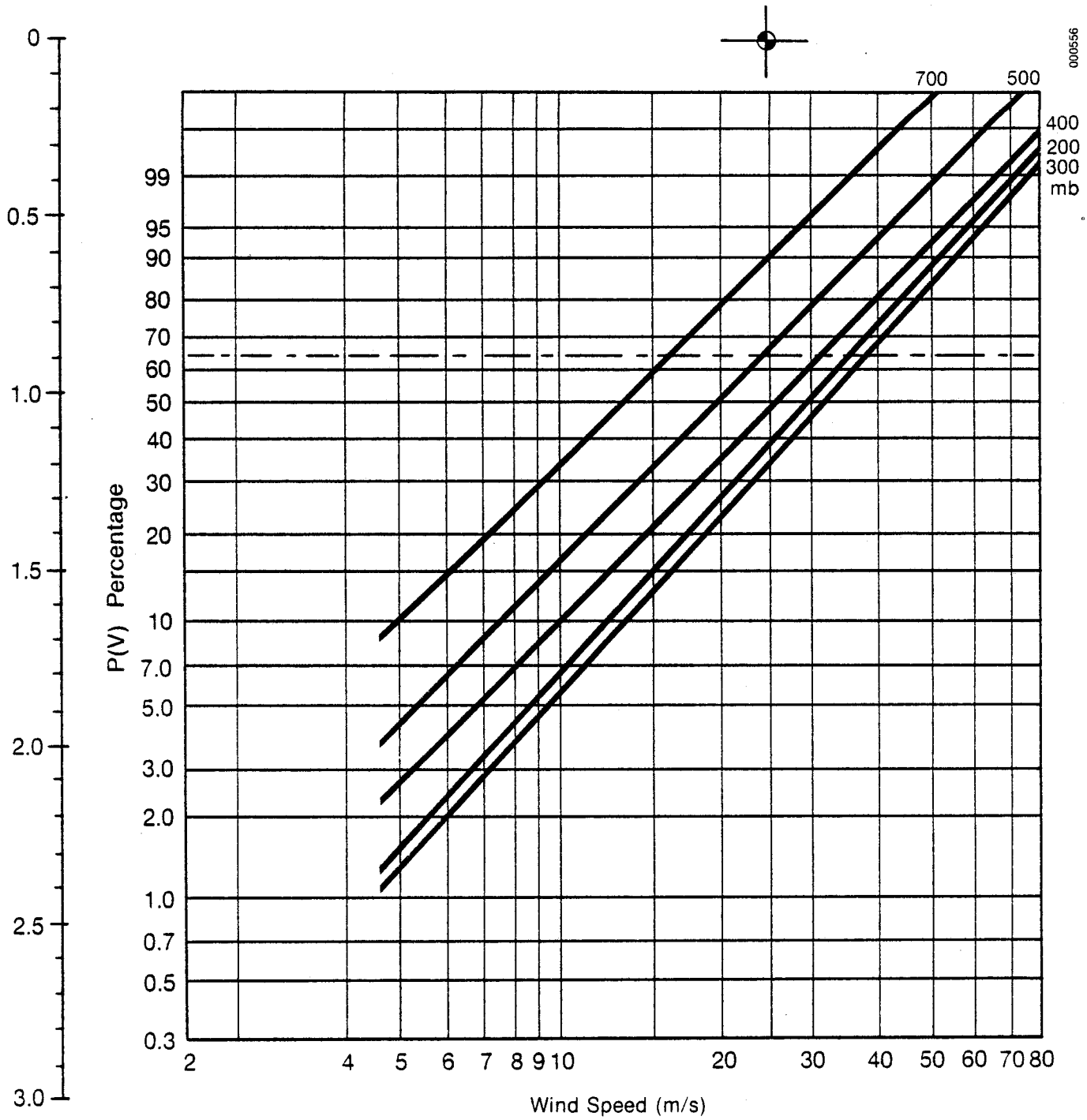

Figure 2-7. Annual Probability Distribution of Velocity: Portland, ME

power-duration curve for that location. These charts may then be used to complete the well-known cost-of-energy calculation. Presumably, an optimal arrangement would minimize this energy cost. An important aspect of this optimization procedure is the manipulation of the probability distribution functions given earlier.

2.4 POWER-DURATION CURVES

The power-duration curve for any of the listed sites, at the relevant altitude, may be determined from the appropriate figure in Appendix B. It is simple to select a series of velocities, form the product $1/2\ \rho\ V^3$, and plot this function against B760 P(V), the effective duration period. The value of ρ can be determined from standard tables or by use of Eq. 4.

A typical annual power-duration calculation is shown in Fig. 2-8 for Portland, Maine, at the altitude of 300 mb. One can determine a similar curve for any other site and altitude.

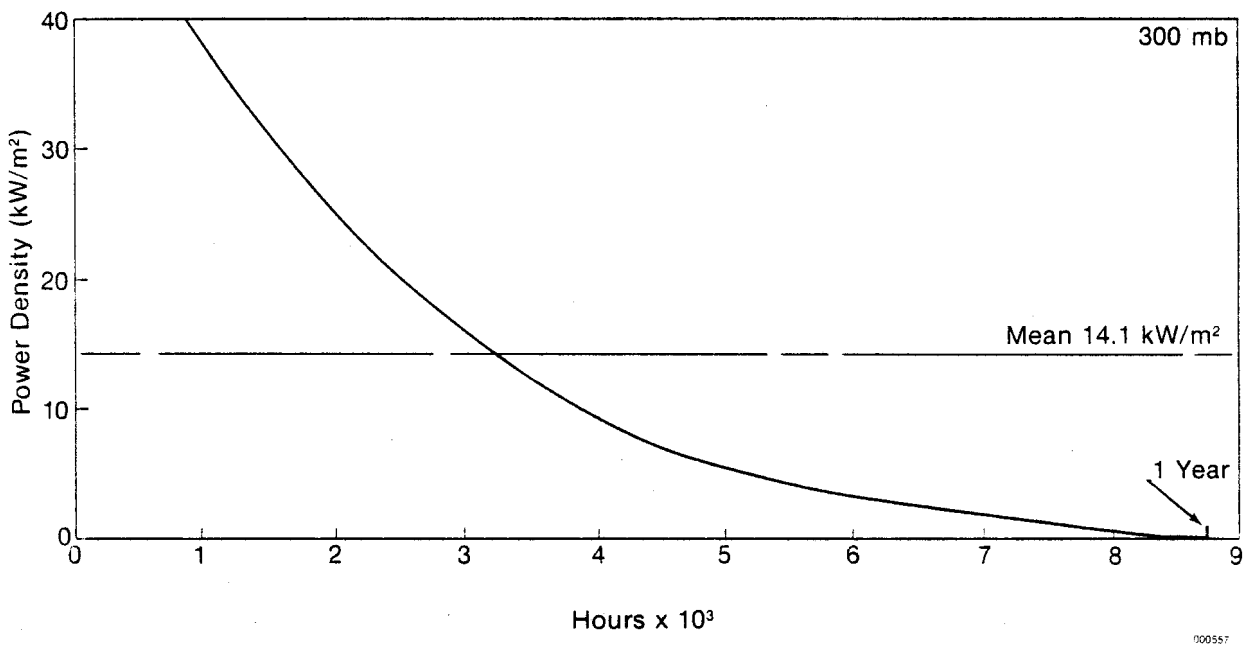

Figure 2-8. Annual Power-Duration Curve: Portland, ME

2.5 THE ANNUAL CALM PERIOD ANALYSIS

The economic and pragmatic conversion of wind energy at an altitude that is remote from the earth's surface is critically dependent on calm periods in the tropopause. A velocity (referred to as the threshold velocity) will be used to define the onset of a calm period aloft. This velocity could be equal to the stalling speed of some fixed wind energy conversion platforms. However, it might be the minimum auto-rotative speed of some rotary wing device. Also, it might be the speed at which a balloon is deployed from a hybrid, fixed wing-balloon platform. This minimum, or threshold, speed will be, in principle, the threshold condition that defines a change in the operating modes of a tethered platform. Furthermore, this report is not intended to discuss the merits of an operating mode in any particular system. This report will stress that low-wind periods are an important variable that can be extracted from the time series wind data.

In Eq. 6 we defined the parameters $N(V_T)$ and $\overline{T}(V_T)$. The former is the total number of individual occasions in a typical year or month that the wind speed drops below the threshold speed. The companion parameter is $\overline{T}(V_T)$; i.e., the number of hours, on the average, that the wind stays below the threshold velocity. The average can be taken over a month or a year, whichever is desired. Note that the product of N and $\overline{T}$, relative to the number of hours in a year or month, is the cumulative probability at the velocity V_T.

A large value for N and a small value for $\overline{T}$ may be an unfavorable combination for tethered systems. The inverse situation may be more attractive. Then the calms would be as long as possible on relatively few occasions.

The current data have been analyzed to evaluate the functions N and $\overline{T}$ through a range of the parameter V_T from 5 to 40 m/s. The annual average values of N and $\overline{T}$ are given in Figs. 2-9 and 2-10. These charts refer to Portland, Maine. Further charts for Denver, Colo.; Guadalupe Island, Mexico; Midland, Texas; and Oakland, Calif., are given in Appendix C as Figs. C-1 through C-10. Curves are given for the pressure levels of 600, 500, 400, 300, and 200 mb. Data for additional locations and levels are available on request from SERI.

Figure 2-9 and other charts in Appendix C show that the value of N decreases with increasing altitude for the velocity in the range $0 < V_T < 25$ m/s. Beyond 25 m/s, the situation is reversed.

In Fig. 2-10 the average time $\overline{T}$ increases steeply with increasing velocity, which occurs at all altitudes. Conversely, as the altitude increases, the time period decreases. One might conclude that at a typical U.S. site the wind lulls approximately below 20 m/s weekly. In addition, the annual average time $\overline{T}$ below 20 m/s is always greater than 30 hours, regardless of the altitude or site location. Furthermore, from the statistical analysis, we have observed that the standard deviation in $T(V_T)$ is of the same order as the mean $\overline{T}(V_T)$, indicating the variation one might expect for $T(V_T)$ in any practical situation.

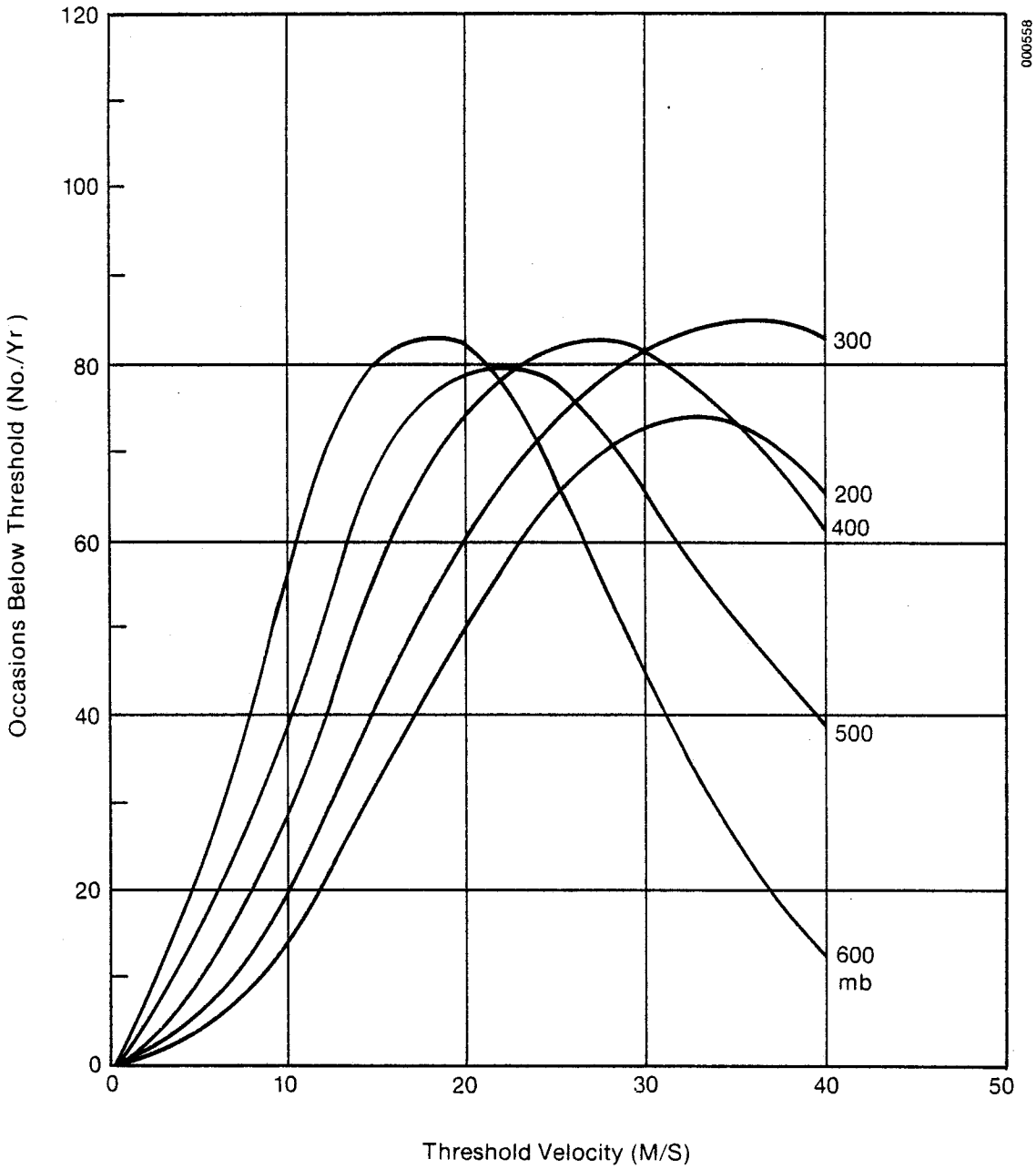

Figure 2-9. Annual Calm-Period Analysis: Portland, ME

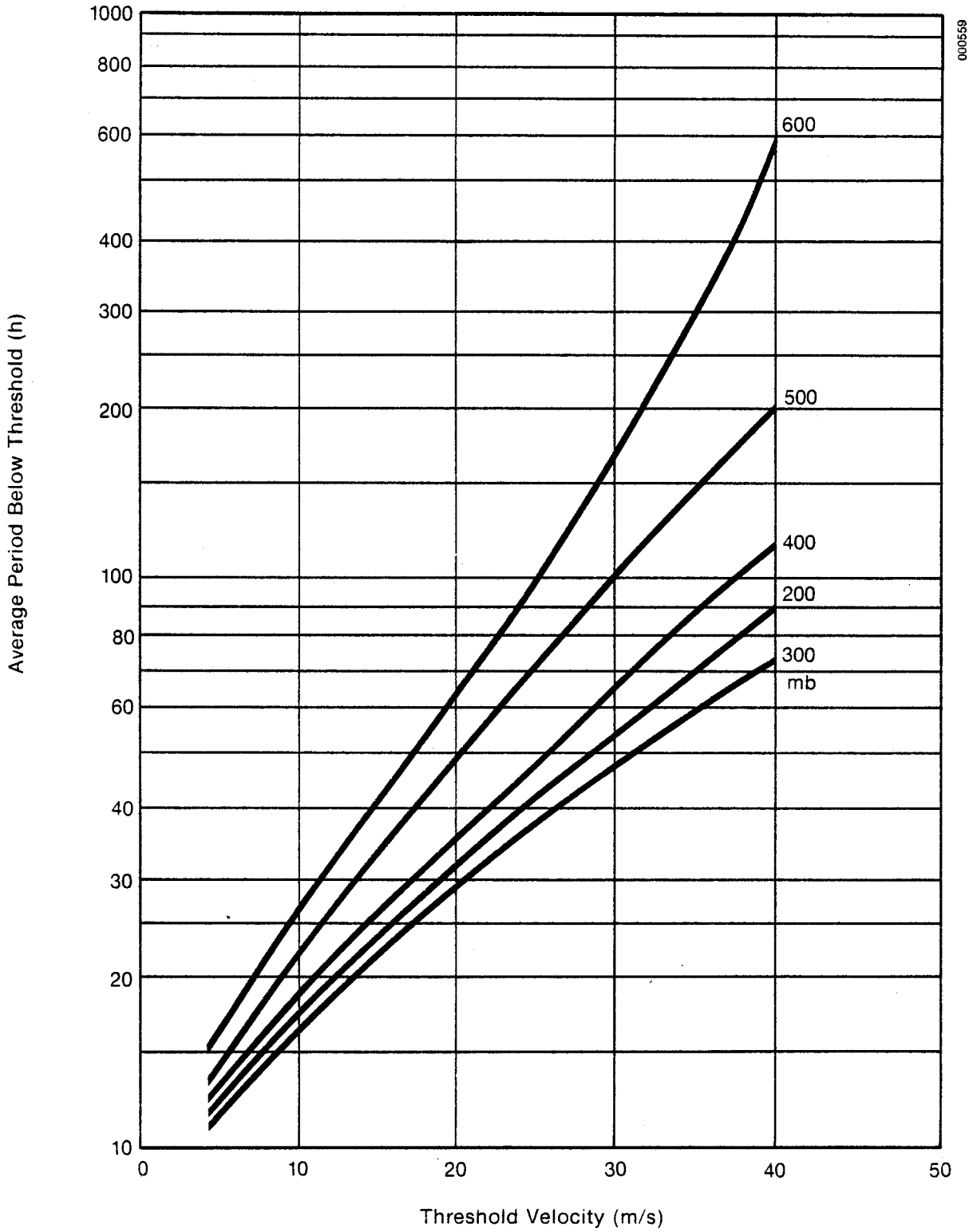

Figure 2-10. Annual Calm-Period Analysis: Portland, ME

2.6 THE MONTHLY CALM PERIOD ANALYSIS

Data for the 54 stations have been analyzed at the monthly level. However, it is impossible to present all data now. Therefore, we suggest that Portland, Maine, might be considered an optimistic U.S. site.

The results of the monthly analysis at 300 mb with V_T = 15 m/s for Portland are shown in Figs. 2-11 and 2-12. Scrutiny of the figures indicates that July, one month past the summer solstice, has the least wind. In July, for a threshold of 15 m/s, the winds will calm on about 6 occasions for about 30 hours each. In the windiest month, January, the wind will fall below 15 m/s on about 1.3 occasions per month for a period of about 10 hours on each occasion.

In summary, if 15 m/s is the stalling speed of a certain aerodynamic platform, then the system will tend to collapse whenever the wind lulls below this speed. In other words, collapse situations will occur according to Fig. 2-11, and the downtime will last for the period indicated in Fig. 2-12.

If the platform's stalling speed is in excess of 15 m/s, the collapse occasions and periods will generally increase. However, the inverse situation will occur for stalling speeds less than 15 m/s.

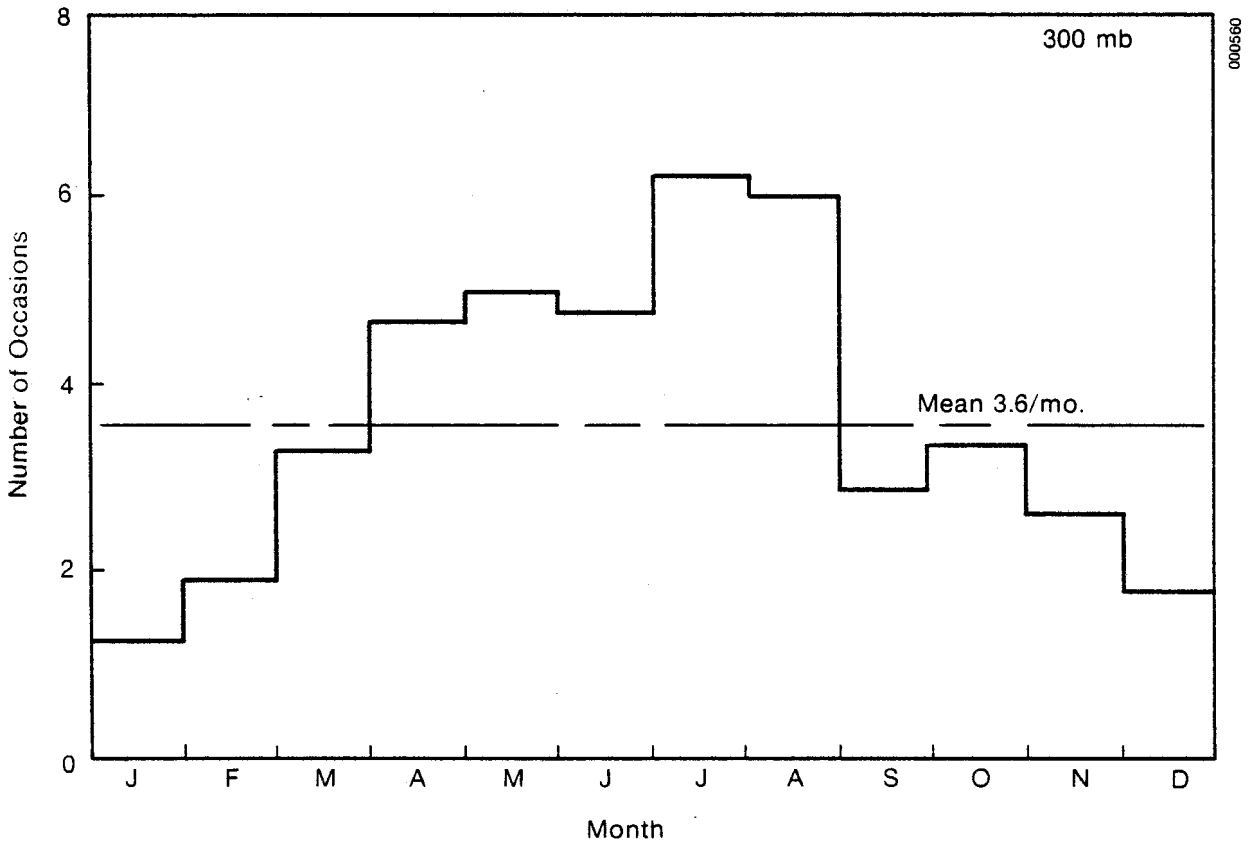

Figure 2-11. Number of Occasions Per Month Wind Speed Falls Below 15 m/s: Portland, ME

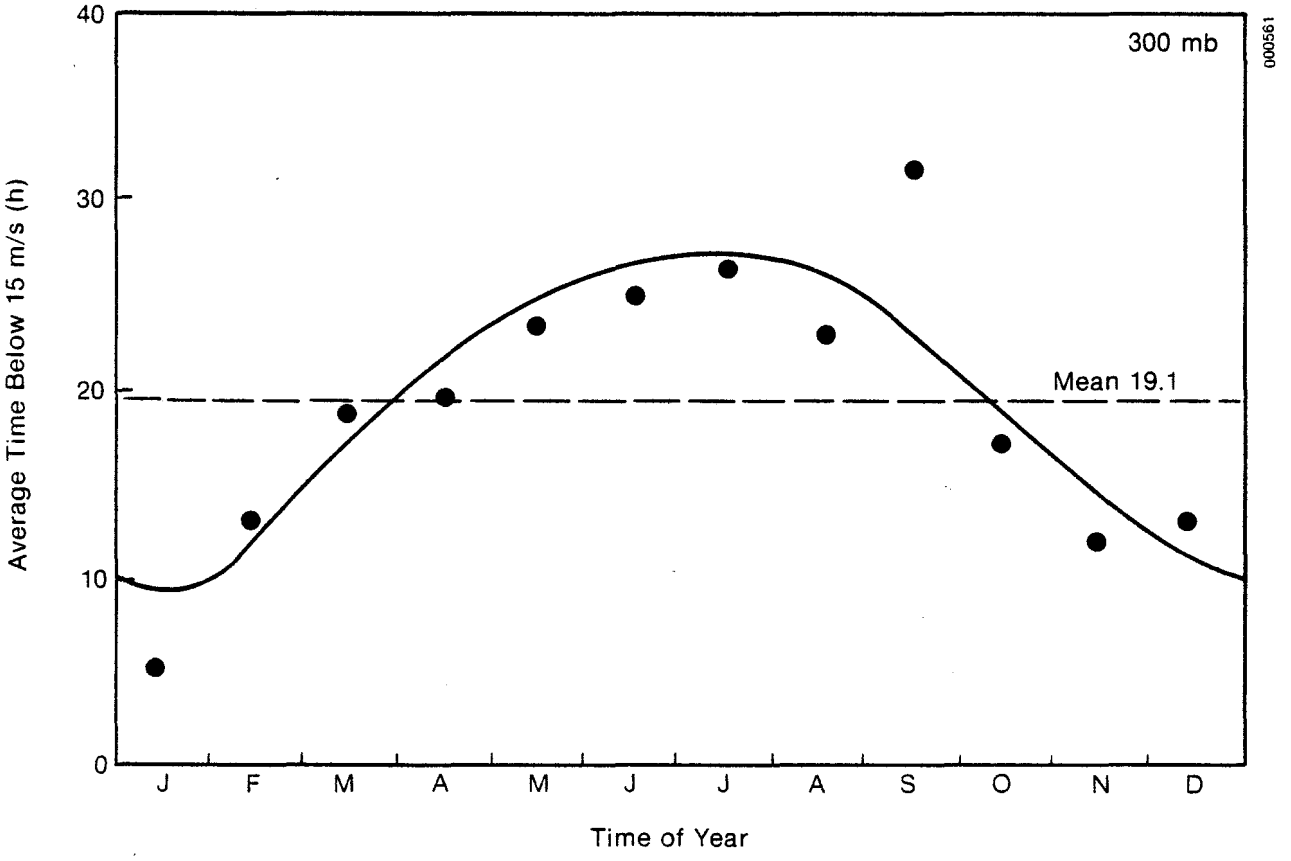

Figure 2-12. Average Period Wind is Below 15 m/s: Portland, ME

2.7 LIGHTNING CONDITIONS

Possible lightning conditions are also important in the design of tethered wind energy systems. The average number of lightning days is essentially the average number of thunder days (which can be found in published charts) [9]. Our report notes that lightning conditions will be important. The occurrence of thunderstorm days is shown in Fig. 2-13.

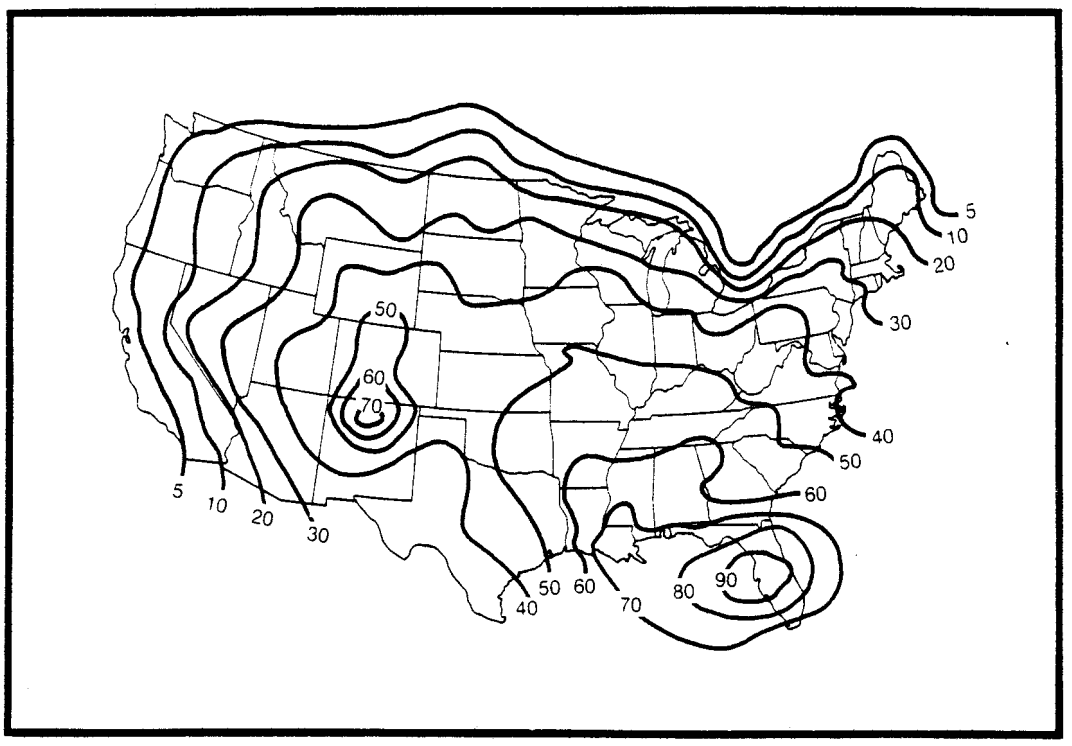

Source: Dodd, C. W. 1977 (Oct.). "Lightning Protection for a Vertical-Axis Wind Turbine." Sand 77-1241; Sandia Labs.

Figure 2-13. The Annual Average Number of Thunderstorm Days

2.8 CONCLUSIONS

This report has attempted to analyze the relevant meteorological data that affect the design of tethered wind energy conversion systems. The United States, as we have shown, is a favorable site for this renewable energy resource. At fixed sites, the annual average power density is 10 to 16 kW/m^2, and over 30% of the continent.

SERI

SECTION 3.0

REFERENCES

1. Reiter, E. R. 1963. Jet Stream Meteorology. Chicago: University of Chicago Press.

2. Atkinson, J. D. et al. The Use of Australian Upper Wind Data in the Design of an Electrical Generating Platform. Charles Kolling Laboratory, Tech, Note D-17. Sydney, Australia: University of Sydney.

3. Takle, E. S.; Brown, J. M. 1978 (Apr.). "Note on the Use of Weibull Statistics to Characterize Wind Speed Data." J. Appl. Met. Vol. 17: pp. 556-559.

4. Hennessey, J. P. 1977 (Feb.). "Some Aspects of Wind Power Statistics." J. Appl. Met. Vol. 16: pp. 119-128.

5. Hennessey, J. P. 1978. "Comparison of Weibull and Rayleigh Distributions for Estimating Wind Power Potential." Wind Eng. Vol. 2 (No. 3): pp. 156-164.

6. Cliff, W. C.; Justus, C. G.; Elderkin, C. E. Simulation of Hourly Wind Speeds for Randomly Dispersed Sites. Rep. PNL-2523. Richland, WA: Battelle-Pacific Northwest Laboratory.

7. Davenport, A. G.; Baynes, C. J. 1972. "An Approach to the Mapping of the Statistical Properties of Gradient Winds (over Canada)." Atmosphere. Vol. 10 (No. 3): pp. 80-92.

8. Maher, J. V.; Lee, D. M. 1977 (Apr.). "Upper Air Statistics - Australia." Bureau of Met. Department of Science.

9. Dodd, C. W. 1977 (Oct.). Lightning Protection for a Vertical-Axis Wind Turbine. SAND 77-1241. Albuquerque, NM: Sandia Laboratories.

SERI

APPENDIX A

AVERAGE VALUES OF VELOCITY AND POWER

SERI

Table A-1. Annual Average Values of Velocity and Power

Albany, NY

Altitude (mb)	Velocity ($\overline{V}$, m/s)	Power ($\overline{P}$, kW/m^2)
900	10.1	1.19
850	11.3	1.63
700	15.2	3.10
600	18.7	5.04
500	22.6	7.78
400	27.0	10.9
300	31.9	13.4
250	33.1	12.2
200	31.4	8.13

Table A-2. Annual Average Values of Velocity and Power

Albuquerque, NM

Pressure Altitude (mb)	Mean Velocity ($\overline{V}$, m/s)	Mean Power ($\overline{P}$, kW/m^2)
900	--	--
850	2.50	0.01
700	8.19	0.53
600	11.4	1.31
500	15.1	2.91
400	18.8	4.85
300	23.4	6.73
250	26.0	7.31
200	26.7	5.80

Table A-3. Annual Average Values of Velocity and Power

Bismarck, ND

Altitude (mb)	Velocity ($\overline{V}$, m/s)	Power ($\overline{P}$, kW/m^2)
900	8.78	0.75
850	9.52	0.97
700	12.2	1.59
600	14.9	2.50
500	18.3	4.04
400	22.6	6.51
300	27.6	9.17
250	28.7	8.49
200	26.5	5.08

Table A-4. Annual Average Values of Velocity and Power

Boise, ID

Altitude (mb)	Velocity ($\overline{V}$, m/s)	Power ($\overline{P}$, kW/m^2)
900	4.37	0.11
850	6.05	0.29
700	9.56	0.77
600	13.2	1.72
500	17.1	3.29
400	21.6	5.70
300	27.0	8.71
250	28.6	8.69
200	26.1	5.16

Table A-5. Annual Average Values of Velocity and Power

Brownsville, TX

Altitude (mb)	Velocity ($\overline{V}$, m/s)	Power ($\overline{P}$, kW/m^2)
900	8.77	0.77
850	7.93	0.57
700	7.4	0.42
600	9.05	0.75
500	11.7	1.46
400	15.5	2.79
300	20.9	5.07
250	24.2	6.53
200	26.6	6.75

Table A-6. Annual Average Values of Velocity and Power

Buffalo, NY

Altitude (mb)	Velocity ($\overline{V}$, m/s)	Power ($\overline{P}$, kW/m^2)
900	9.79	1.20
850	10.7	1.44
700	14.5	2.60
600	17.5	4.04
500	21.1	6.39
400	25.3	9.39
300	29.8	11.2
250	31.6	10.8
200	29.6	6.8

Table A-7. Annual Average Values of Velocity and Power

Caribou, ME

Altitude (mb)	Velocity ($\overline{V}$, m/s)	Power ($\overline{P}$, kW/m^2)
900	10.4	1.22
850	11.2	1.52
700	14.6	2.57
600	17.7	4.16
500	21.6	6.72
400	26.5	10.5
300	32.5	14.7
250	33.9	14.1
200	30.8	8.35

Table A-8. Annual Average Values of Velocity and Power

Charleston, SC

Altitude (mb)	Velocity ($\overline{V}$, m/s)	Power ($\overline{P}$, kW/m^2)
900	8.15	0.77
850	8.67	0.89
700	11.6	1.79
600	13.9	2.77
500	16.8	4.30
400	20.3	6.19
300	25.2	8.86
250	28.5	10.3
200	30.9	9.96

Table A-9. Annual Average Values of Velocity and Power

Dayton, OH

Altitude (mb)	Velocity ($\overline{V}$, m/s)	Power ($\overline{P}$, kW/m^2)
900	8.91	0.95
850	9.85	1.24
700	13.7	2.37
600	16.9	3.87
500	20.6	6.33
400	25.1	9.84
300	30.5	13.1
250	32.9	13.1
200	32.2	9.47

Table A-10. Annual Average Values of Velocity and Power

Del Rio, TX

Altitude (mb)	Velocity ($\overline{V}$, m/s)	Power ($\overline{P}$, kW/m^2)
900	8.09	0.50
850	7.91	0.47
700	8.44	0.61
600	10.9	1.24
500	13.9	2.32
400	17.8	3.94
300	23.4	6.58
250	26.7	7.98
200	28.4	7.43

Table A-11. Annual Average Values of Velocity and Power

Denver, CO

Altitude (mb)	Velocity ($\overline{V}$, m/s)	Power ($\overline{P}$, kW/m^2)
900	--	--
850	--	--
700	7.01	0.41
600	10.7	1.08
500	14.5	2.18
400	18.6	3.98
300	23.9	6.40
250	25.9	6.48
200	25.5	4.60

Table A-12. Annual Average Values of Velocity and Power

Dodge City, KS

Altitude (mb)	Velocity ($\overline{V}$, m/s)	Power ($\overline{P}$, kW/m^2)
900	8.58	0.59
850	10.3	1.21
700	10.8	1.20
600	13.1	1.90
500	16.3	3.30
400	20.6	5.66
300	25.9	8.52
250	28.5	9.11
200	28.7	6.93

Table A-13. Annual Average Values of Velocity and Power

Ely, NV

Altitude (mb)	Velocity ($\overline{V}$, m/s)	Power ($\overline{P}$, kW/m^2)
900	--	--
850	--	--
700	7.29	0.52
600	10.8	1.12
500	14.6	2.41
400	18.8	4.34
300	23.4	6.28
250	25.3	6.24
200	24.6	4.30

Table A-14. Annual Average Values of Velocity and Power

Fairbanks, AK

Altitude (mb)	Velocity ($\overline{V}$, m/s)	Power ($\overline{P}$, kW/m^2)
900	5.72	0.28
850	6.40	0.38
700	8.31	0.63
600	9.72	0.88
500	12.0	1.58
400	15.4	2.76
300	18.3	3.90
250	17.3	3.11
200	14.3	1.23

Table A-15. Annual Average Values of Velocity and Power

Fort Worth, TX

Altitude (mb)	Velocity ($\overline{V}$, m/s)	Power ($\overline{P}$, kW/m^2)
900	9.26	0.95
850	9.20	0.90
700	10.8	1.28
600	13.1	2.09
500	16.2	3.43
400	20.3	5.58
300	26.0	9.04
250	29.4	10.7
200	31.5	10.0

Table A-16. Annual Average Values of Velocity and Power

Glasgow, MT

Altitude (mb)	Velocity ($\overline{V}$, m/s)	Power ($\overline{P}$, kW/m^2)
900	7.61	0.48
850	8.73	0.80
700	11.7	1.42
600	14.5	2.23
500	17.8	3.58
400	22.3	6.07
300	27.1	8.41
250	28.0	7.69
200	25.1	4.31

Table A-17. Annual Average Values of Velocity and Power

Great Falls, MT

Altitude (mb)	Velocity ($\overline{V}$, m/s)	Power ($\overline{P}$, kW/m^2)
900	3.13	0.30
850	8.40	0.72
700	10.7	1.31
600	13.7	2.08
500	17.3	3.43
400	22.0	6.11
300	27.3	8.99
250	28.2	8.20
200	25.2	4.53

Table A-18. Annual Average Values of Velocity and Power

Green Bay, WI

Altitude (mb)	Velocity ($\overline{V}$, m/s)	Power ($\overline{P}$, kW/m^2)
900	9.25	0.92
850	9.67	0.99
700	13.0	1.81
600	16.0	3.00
500	19.4	4.85
400	24.0	7.97
300	30.0	11.53
250	31.1	10.87
200	28.8	6.71

Table A-19. Annual Average Values of Velocity and Power

Greensboro, NC

Altitude (mb)	Velocity ($\overline{V}$, m/s)	Power ($\overline{P}$, kW/m^2)
900	8.34	0.76
850	9.13	1.02
700	13.0	2.23
600	15.8	3.48
500	19.3	5.48
400	23.3	8.03
300	27.9	10.2
250	30.3	10.7
200	30.8	8.61

Table A-20. Annual Average Values of Velocity and Power

Guadalupe Island, Mexico

Altitude (mb)	Velocity ($\overline{V}$, m/s)	Power ($\overline{P}$, kW/m^2)
900	4.81	0.15
850	5.48	0.21
700	7.45	0.45
600	9.00	0.75
500	10.7	1.08
400	12.8	1.50
300	16.1	2.25
250	17.9	2.69
200	19.0	2.63

Table A-21. Annual Average Values of Velocity and Power

Hilo, HI

Altitude (mb)	Velocity ($\overline{V}$, m/s)	Power ($\overline{P}$, kW/m^2)
900	4.27	0.096
850	4.16	0.088
700	5.64	0.191
600	6.02	0.242
500	7.58	0.413
400	10.9	0.900
300	17.2	2.47
250	21.7	3.95
200	25.0	4.80

Table A-22. Annual Average Values of Velocity and Power

Huntington, WV

Altitude (mb)	Velocity ($\overline{V}$, m/s)	Power ($\overline{P}$, kW/m^2)
900	8.18	0.77
850	9.32	1.06
700	13.6	2.37
600	16.9	3.96
500	20.5	6.32
400	24.7	9.13
300	30.3	12.8
250	32.9	13.1
200	32.8	10.1

Table A-23. Annual Average Values of Velocity and Power

International Falls, MN

Altitude (mb)	Velocity ($\overline{V}$, m/s)	Power ($\overline{P}$, kW/m^2)
900	8.64	0.73
850	9.38	0.92
700	12.2	1.50
600	15.1	2.45
500	18.4	4.00
400	22.9	6.70
300	27.6	9.00
250	28.6	8.20
200	25.8	4.64

Table A-24. Annual Average Values of Velocity and Power

Lander, WY

Altitude (mb)	Velocity ($\overline{V}$, m/s)	Power ($\overline{P}$, kW/m^2)
900	--	--
850	--	--
700	6.83	0.42
600	12.3	1.56
500	15.9	2.87
400	20.0	4.72
300	25.4	7.49
250	27.0	7.31
200	25.5	4.79

Table A-25. Annual Average Values of Velocity and Power

Little Rock, AR

Altitude (mb)	Velocity ($\overline{V}$, m/s)	Power ($\overline{P}$, kW/m^2)
900	8.58	0.86
850	9.20	1.02
700	12.0	1.78
600	14.7	2.92
500	17.7	4.48
400	21.5	6.68
300	26.8	9.68
250	29.9	11.1
200	31.4	9.95

Table A-26. Annual Average Values of Velocity and Power

Medford, OR

Altitude (mb)	Velocity ($\overline{V}$, m/s)	Power ($\overline{P}$, kW/m^2)
900	3.63	0.087
850	4.87	0.19
700	10.9	1.42
600	14.2	2.49
500	18.0	4.25
400	22.3	6.70
300	26.8	9.05
250	28.1	8.56
200	26.1	5.19

Table A-27. Annual Average Values of Velocity and Power

Midland, TX

Altitude (mb)	Velocity ($\overline{V}$, m/s)	Power ($\overline{P}$, kW/m^2)
900	6.63	0.25
850	8.77	0.68
700	9.42	0.87
600	12.4	1.72
500	15.5	3.12
400	19.4	5.14
300	24.9	7.98
250	27.9	9.18
200	29.1	8.03

Table A-28. Annual Average Values of Velocity and Power

Montgomery, AL

Altitude (mb)	Velocity ($\overline{V}$, m/s)	Power ($\overline{P}$, kW/m^2)
900	7.57	0.60
850	8.28	0.74
700	11.1	1.59
600	13.4	2.52
500	16.4	3.96
400	19.9	5.83
300	24.7	8.44
250	27.8	9.80
200	30.1	9.48

Table A-29. Annual Average Values of Velocity and Power

Nashville, TN

Altitude (mb)	Velocity ($\overline{V}$, m/s)	Power ($\overline{P}$, kW/m^2)
900	8.48	0.89
850	9.31	1.09
700	13.0	2.20
600	15.8	3.59
500	19.2	5.63
400	23.3	8.33
300	28.8	11.6
250	31.8	12.5
200	32.5	10.4

Table A-30. Annual Average Values of Velocity and Power

New York, NY

Altitude (mb)	Velocity ($\overline{V}$, m/s)	Power ($\overline{P}$, kW/m^2)
900	9.94	1.28
850	10.7	1.46
700	15.0	3.03
600	18.5	1.85
500	22.4	7.98
400	27.5	12.3
300	33.2	16.2
250	35.5	16.3
200	34.6	11.6

Table A-31. Annual Average Values of Velocity and Power

North Platte, NE

Altitude (mb)	Velocity ($\overline{V}$, m/s)	Power ($\overline{P}$, kW/m^2)
900	6.20	0.25
850	9.74	0.96
700	11.4	1.34
600	13.9	2.05
500	16.9	3.24
400	20.9	5.51
300	26.1	8.29
250	28.3	8.55
200	27.6	6.04

Table A-32. Annual Average Values of Velocity and Power

Oakland, CA

Altitude (mb)	Velocity ($\overline{V}$, m/s)	Power ($\overline{P}$, kW/m^2)
900	6.18	0.33
850	6.80	0.43
700	9.99	1.11
600	13.0	2.12
500	16.3	3.54
400	20.3	5.43
300	25.1	7.62
250	27.0	7.57
200	26.3	5.44

Table A-33. Annual Average Values of Velocity and Power

Oklahoma City, OK

Altitude (mb)	Velocity ($\overline{V}$, m/s)	Power ($\overline{P}$, kW/m^2)
900	10.0	1.21
850	9.9	1.18
700	11.2	1.49
600	13.6	2.41
500	16.5	3.84
400	20.4	5.80
300	25.6	8.04
250	27.8	8.59
200	27.8	6.94

Table A-34. Annual Average Values of Velocity and Power

Omaha, NE

Altitude (mb)	Velocity ($\overline{V}$, m/s)	Power ($\overline{P}$, kW/m^2)
900	10.3	1.67
850	10.5	3.12
700	12.6	1.78
600	15.4	2.96
500	18.6	4.72
400	22.8	7.66
300	28.1	10.8
250	30.1	10.5
200	29.0	6.96

Table A-35. Annual Average Values of Velocity and Power

Peoria, IL

Altitude (mb)	Velocity ($\overline{V}$, m/s)	Power ($\overline{P}$, kW/m^2)
900	9.33	1.00
850	9.87	1.12
700	13.4	2.13
600	16.5	3.59
500	19.9	5.72
400	24.3	8.86
300	29.8	12.31
250	32.1	12.35
200	31.4	8.83

Table A-36. Annual Average Values of Velocity and Power

Pittsburgh, PA

Altitude (mb)	Velocity ($\overline{V}$, m/s)	Power ($\overline{P}$, kW/m^2)
900	8.57	0.79
850	9.89	1.15
700	14.5	2.640
600	17.8	4.30
500	21.6	6.91
400	26.3	10.8
300	32.2	14.9
250	34.4	14.8
200	33.1	10.0

Table A-37. Annual Average Values of Velocity and Power

Portland, ME

Altitude (mb)	Velocity ($\overline{V}$, m/s)	Power ($\overline{P}$, kW/m^2)
900	9.42	1.11
850	10.4	1.36
700	14.8	2.84
600	18.4	4.67
500	22.5	7.53
400	27.6	11.38
300	32.8	14.1
250	33.9	12.9
200	31.2	7.9

Table A-38. Annual Average Values of Velocity and Power

Rapid City, SD

Altitude (mb)	Velocity ($\overline{V}$, m/s)	Power ($\overline{P}$, kW/m^2)
900	5.27	0.22
850	8.31	0.73
700	12.3	1.23
600	19.4	1.94
500	17.1	3.17
400	21.3	5.23
300	26.2	7.74
250	27.7	7.60
200	26.1	4.82

Table A-39. Annual Average Values of Velocity and Power

St. Cloud, MN

Altitude (mb)	Velocity ($\overline{V}$, m/s)	Power ($\overline{P}$, kW/m^2)
900	9.19	0.88
850	9.66	0.98
700	12.7	1.69
600	15.4	2.70
500	18.7	4.29
400	22.9	6.82
300	28.3	9.88
250	29.8	9.42
200	27.5	5.61

Table A-40. Annual Average Values of Velocity and Power

Salem, IL

Altitude (mb)	Velocity ($\overline{V}$, m/s)	Power ($\overline{P}$, kW/m^2)
900	9.24	1.02
850	9.86	1.16
700	13.4	2.19
600	16.2	3.56
500	19.5	5.55
400	23.6	8.24
300	28.0	10.2
250	30.0	10.1
200	29.4	7.39

Table A-41. Annual Average Values of Velocity and Power

Salem, OR

Altitude (mb)	Velocity ($\overline{V}$, m/s)	Power ($\overline{P}$, kW/m^2)
900	6.91	0.63
850	7.96	0.89
700	11.9	1.63
600	15.0	2.59
500	18.8	4.44
400	23.2	7.15
300	27.8	9.31
250	28.3	8.05
200	25.3	4.40

Table A-42. Annual Average Values of Velocity and Power

Salt Lake City, UT

Altitude (mb)	Velocity ($\overline{V}$, m/s)	Power ($\overline{P}$, kW/m^2)
900	--	--
850	4.79	0.15
700	7.65	0.41
600	11.6	1.15
500	15.6	2.61
400	20.0	4.87
300	24.8	7.32
250	26.7	7.50
200	25.6	4.94

Table A-43. Annual Average Values of Velocity and Power

San Nichols Island, CA

Altitude (mb)	Velocity ($\overline{V}$, m/s)	Power ($\overline{P}$, kW/m^2)
900	5.05	0.23
850	5.72	0.29
700	8.50	0.75
600	10.7	1.41
500	13.0	2.16
400	16.0	3.16
300	20.6	4.53
250	22.7	5.00
200	23.4	4.14

Table A-44. Annual Average Values of Velocity and Power

Sault Ste. Marie, MI

Altitude (mb)	Velocity ($\overline{V}$, m/s)	Power ($\overline{P}$, kW/m^2)
900	9.13	0.85
850	9.82	1.00
700	13.2	1.92
600	16.0	2.99
500	19.4	4.81
400	23.8	7.87
300	29.5	11.70
250	31.1	11.29
200	28.7	6.95

Table A-45. Annual Average Values of Velocity and Power

Shreveport, LA

Altitude (mb)	Velocity ($\overline{V}$, m/s)	Power ($\overline{P}$, kW/m^2)
900	8.44	0.84
850	9.03	0.99
700	11.3	1.49
600	13.8	2.44
500	16.7	3.84
400	20.5	5.99
300	25.4	8.24
250	28.4	9.52
200	29.9	8.62

Table A-46. Annual Average Values of Velocity and Power

Spokane, WA

Altitude (mb)	Velocity ($\overline{V}$, m/s)	Power ($\overline{P}$, kW/m^2)
900	6.32	0.34
850	7.34	0.61
700	10.0	0.98
600	13.7	2.05
500	17.7	3.77
400	22.8	6.78
300	28.7	10.6
250	29.6	10.0
200	26.3	5.57

Table A-47. Annual Average Values of Velocity and Power

Tampa, FL

Altitude (mb)	Velocity ($\overline{V}$, m/s)	Power ($\overline{P}$, kW/m^2)
900	6.43	0.35
850	6.57	0.39
700	7.76	0.67
600	9.56	1.08
500	12.1	1.74
400	15.2	2.70
300	19.4	4.24
250	22.4	5.26
200	25.2	5.58

Table A-48. Annual Average Values of Velocity and Power

Topeka, KS

Altitude (mb)	Velocity ($\overline{V}$, m/s)	Power ($\overline{P}$, kW/m^2)
900	9.70	1.08
850	9.96	1.14
700	12.4	1.75
600	15.0	2.76
500	18.0	4.30
400	22.0	6.80
300	26.9	9.25
250	29.0	9.24
200	28.6	6.55

Table A-49. Annual Average Values of Velocity and Power

Tucson, AZ

Pressure Altitude (mb)	Mean Velocity ($\overline{V}$, m/s)	Mean Power ($\overline{P}$, kW/m^2)
900	4.47	0.13
850	5.12	0.19
700	7.68	0.50
600	10.7	1.23
500	14.0	2.54
400	17.9	4.43
300	22.8	6.44
250	25.6	7.49
200	26.7	6.37

Table A-50. Annual Average Values of Velocity and Power

Wallops Island, VA

Altitude (mb)	Velocity ($\overline{V}$, m/s)	Power ($\overline{P}$, kW/m^2)
900	9.71	1.20
850	10.2	1.24
700	14.0	2.43
600	17.2	4.08
500	20.7	6.37
400	24.9	9.24
300	29.7	12.1
250	32.0	12.2
200	32.1	9.67

Table A-51. Annual Average Values of Velocity and Power

Waycross, GA

Altitude (mb)	Velocity ($\overline{V}$, m/s)	Power ($\overline{P}$, kW/m^2)
900	7.50	0.60
850	7.92	0.71
700	10.4	1.41
600	12.5	2.23
500	15.3	3.45
400	18.8	5.20
300	23.5	7.31
250	26.6	8.54
200	29.2	8.58

Table A-52. Annual Average Values of Velocity and Power

Winnemucca, NV

Altitude (mb)	Velocity ($\overline{V}$, m/s)	Power ($\overline{P}$, kW/m^2)
900	--	--
850	4.52	0.11
700	8.21	0.64
600	12.2	1.57
500	16.1	3.08
400	19.9	4.84
300	24.9	7.22
250	26.1	6.76
200	24.6	4.28

Table A-53. Annual Average Values of Velocity and Power

Winslow, AZ

Altitude (mb)	Velocity ($\overline{V}$, m/s)	Power ($\overline{P}$, kW/m^2)
900	--	--
850	3.13	0.05
700	8.31	0.68
600	10.7	1.22
500	14.0	2.32
400	18.1	4.29
300	23.3	6.59
250	25.6	7.00
200	25.8	5.27

Table A-54. Annual Average Values of Velocity and Power

Yucca Flats, NV

Altitude (mb)	Velocity ($\overline{V}$, m/s)	Power ($\overline{P}$, kW/m^2)
900	--	--
850	5.06	0.19
700	7.81	0.50
600	10.4	1.11
500	14.1	2.39
400	17.9	3.97
300	22.4	5.47
250	24.3	5.48
200	24.1	4.17

SERI

APPENDIX B

APPLICATION OF U.S. UPPER WIND DATA IN PRE-DESIGN TETHERED WIND ENERGY SYSTEMS

SERI

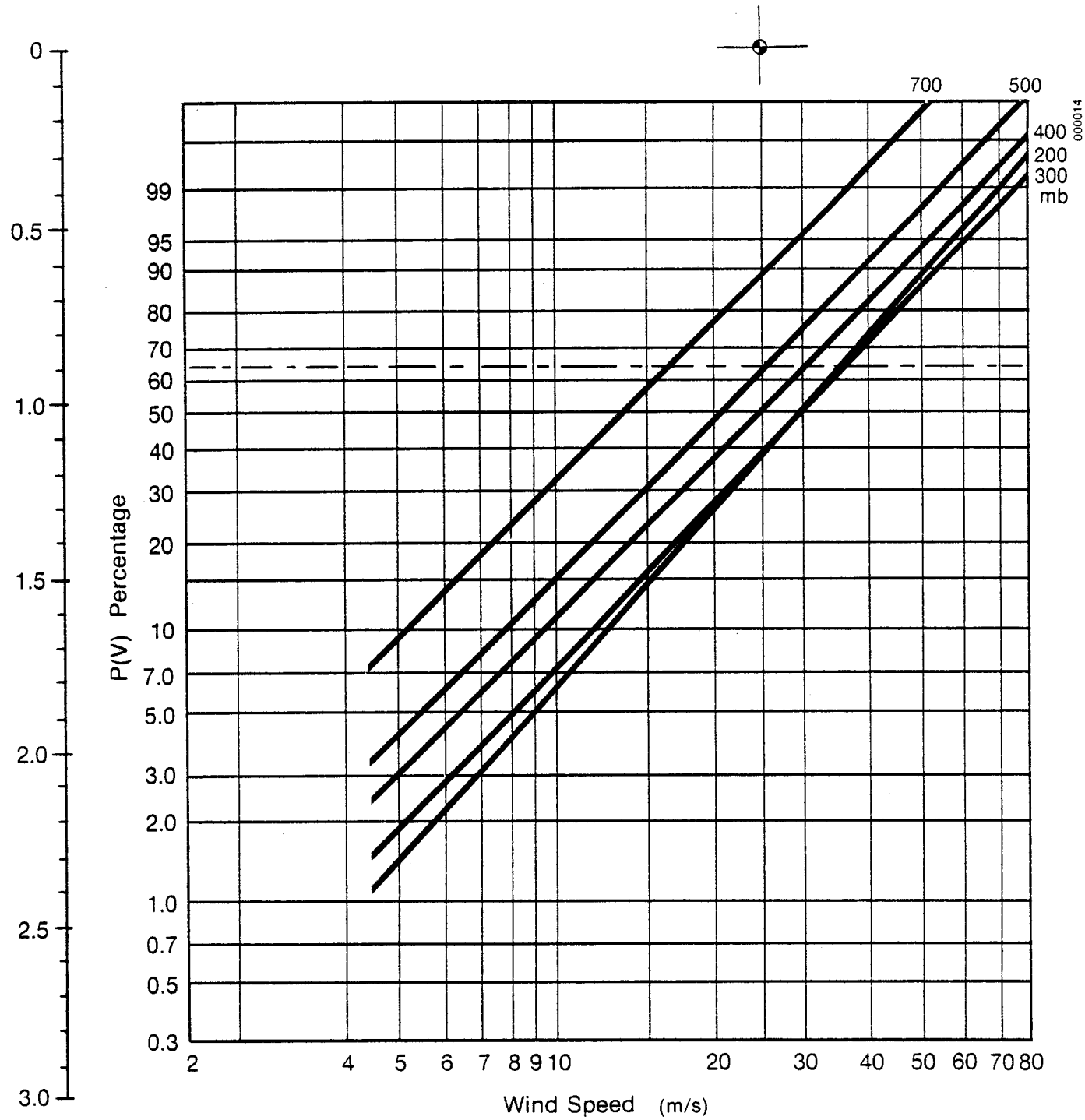

Figure B-1. Annual Probability Distribution of Velocity: Albany, NY

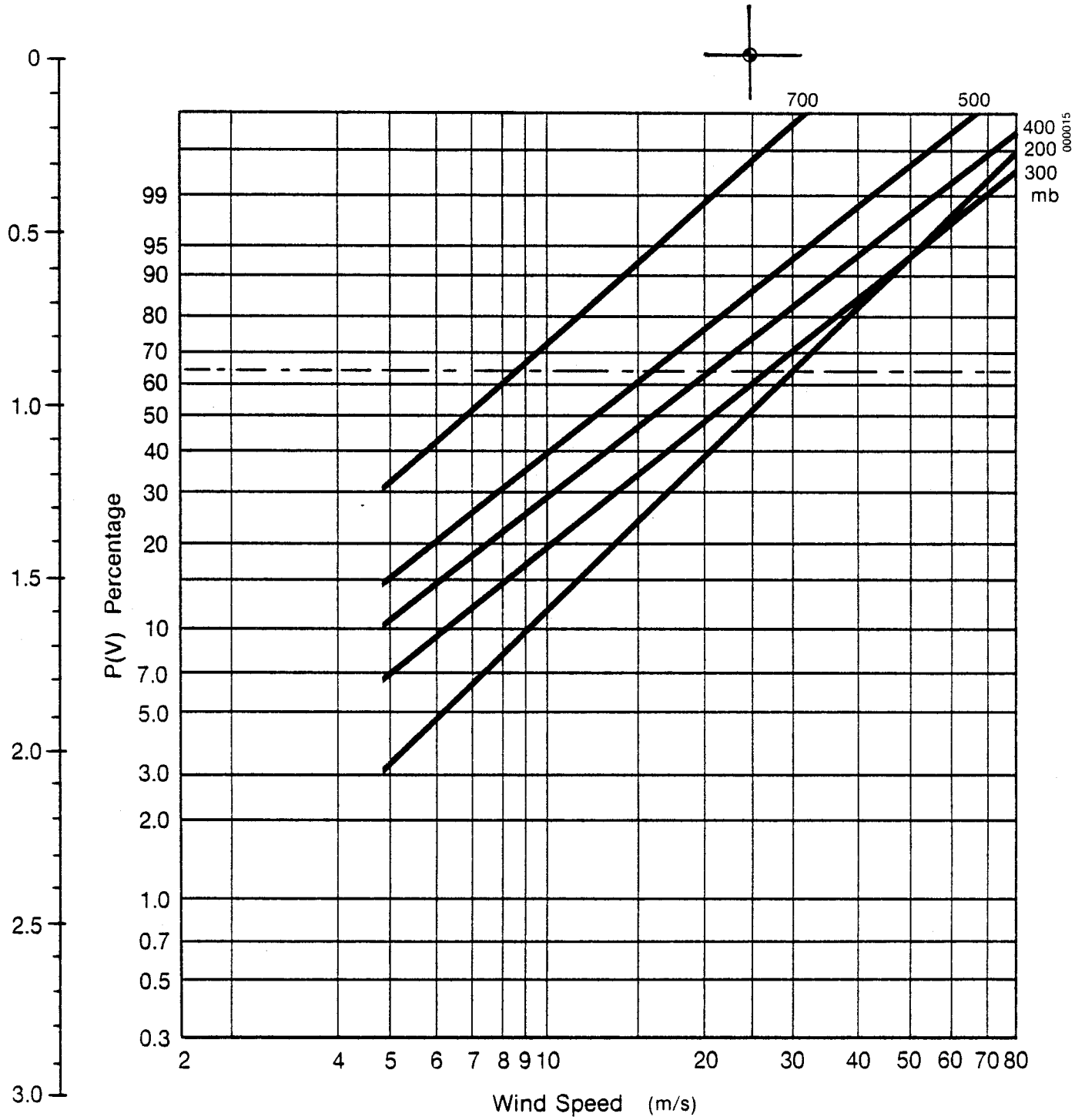

Figure B-2. Annual Probability Distribution of Velocity: Albuquerque, NM

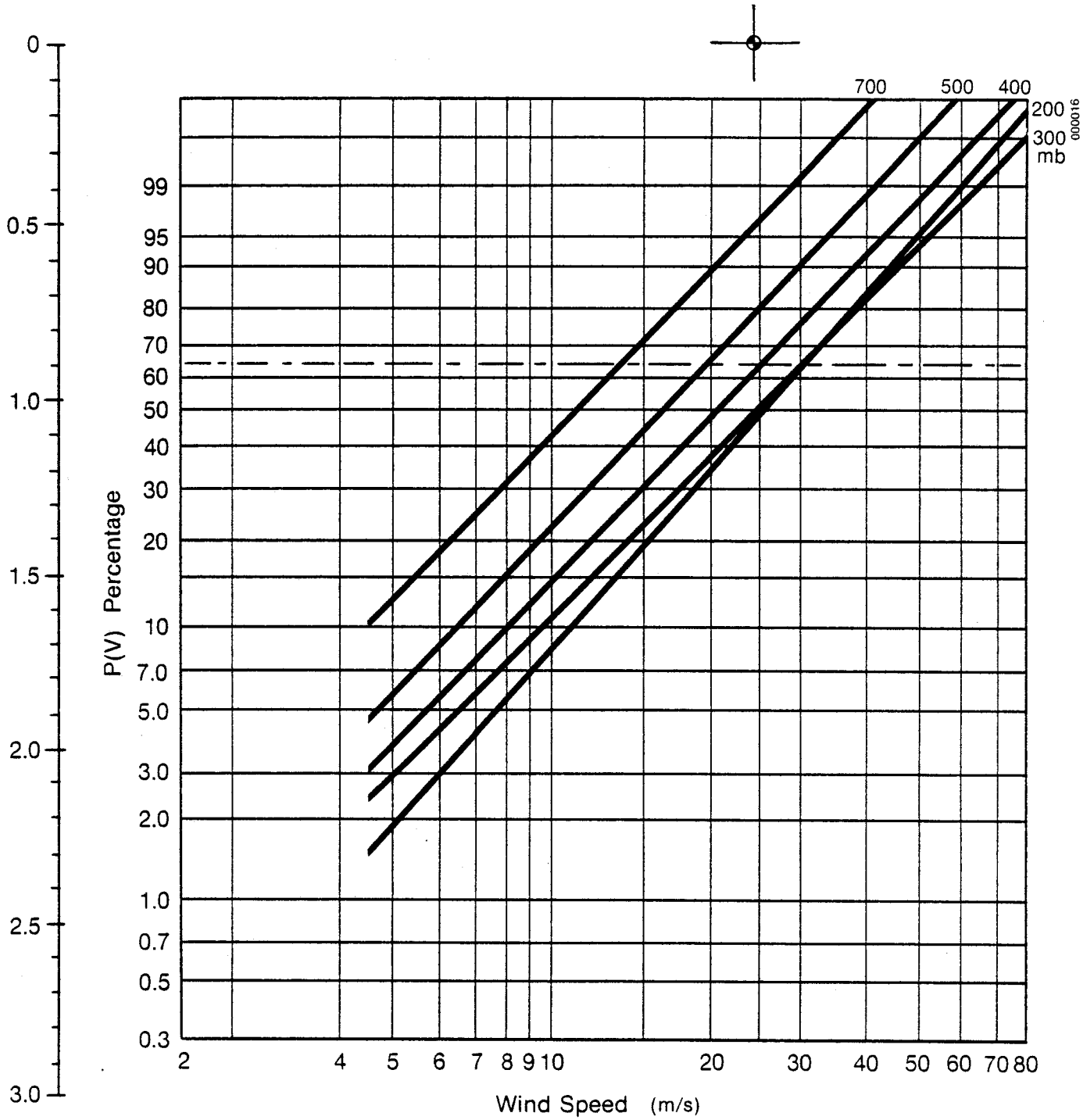

Figure B-3. Annual Probability Distribution of Velocity: Bismarck, ND

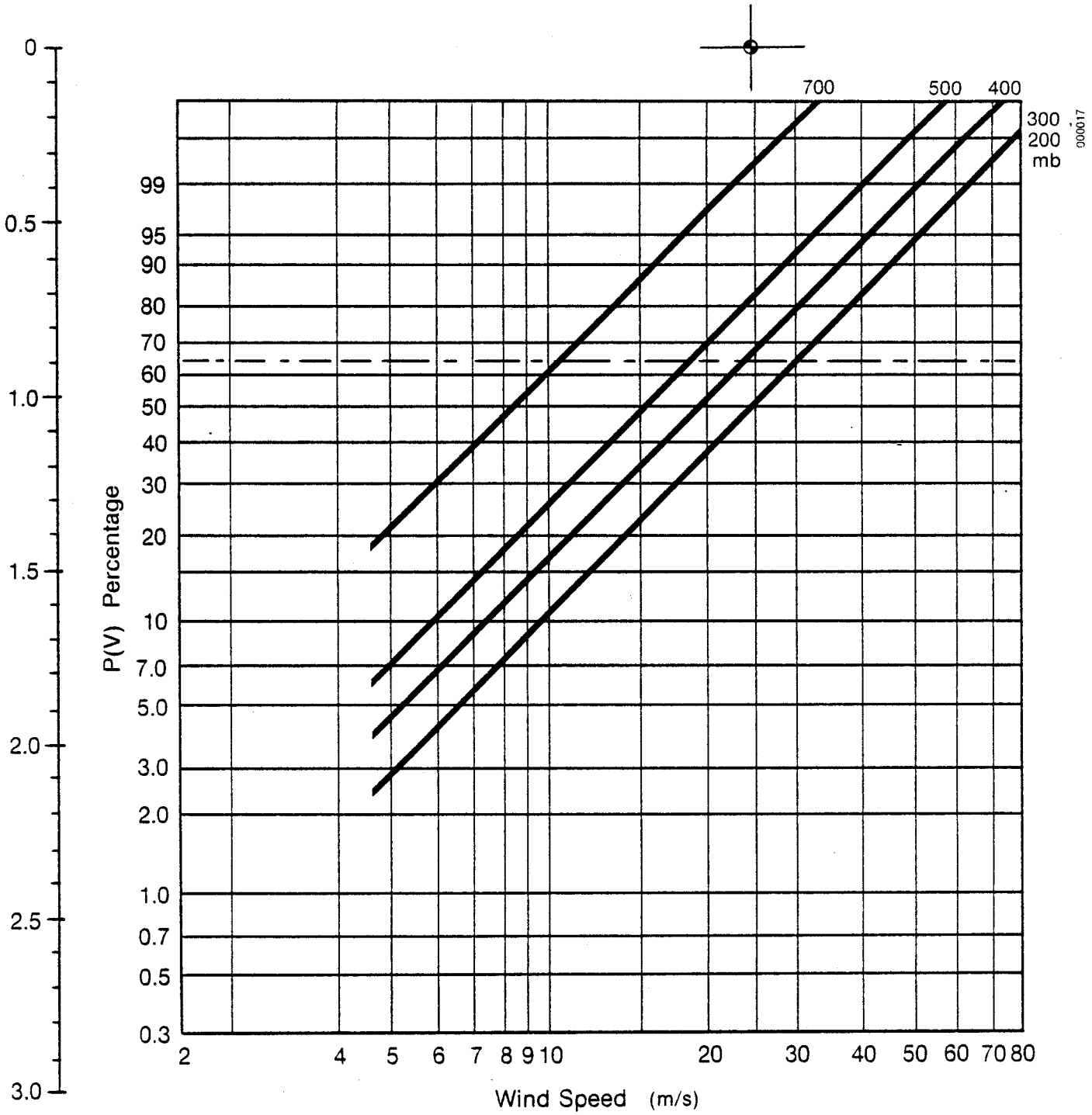

Figure B-4. Annual Probability Distribution of Velocity: Boise, ID

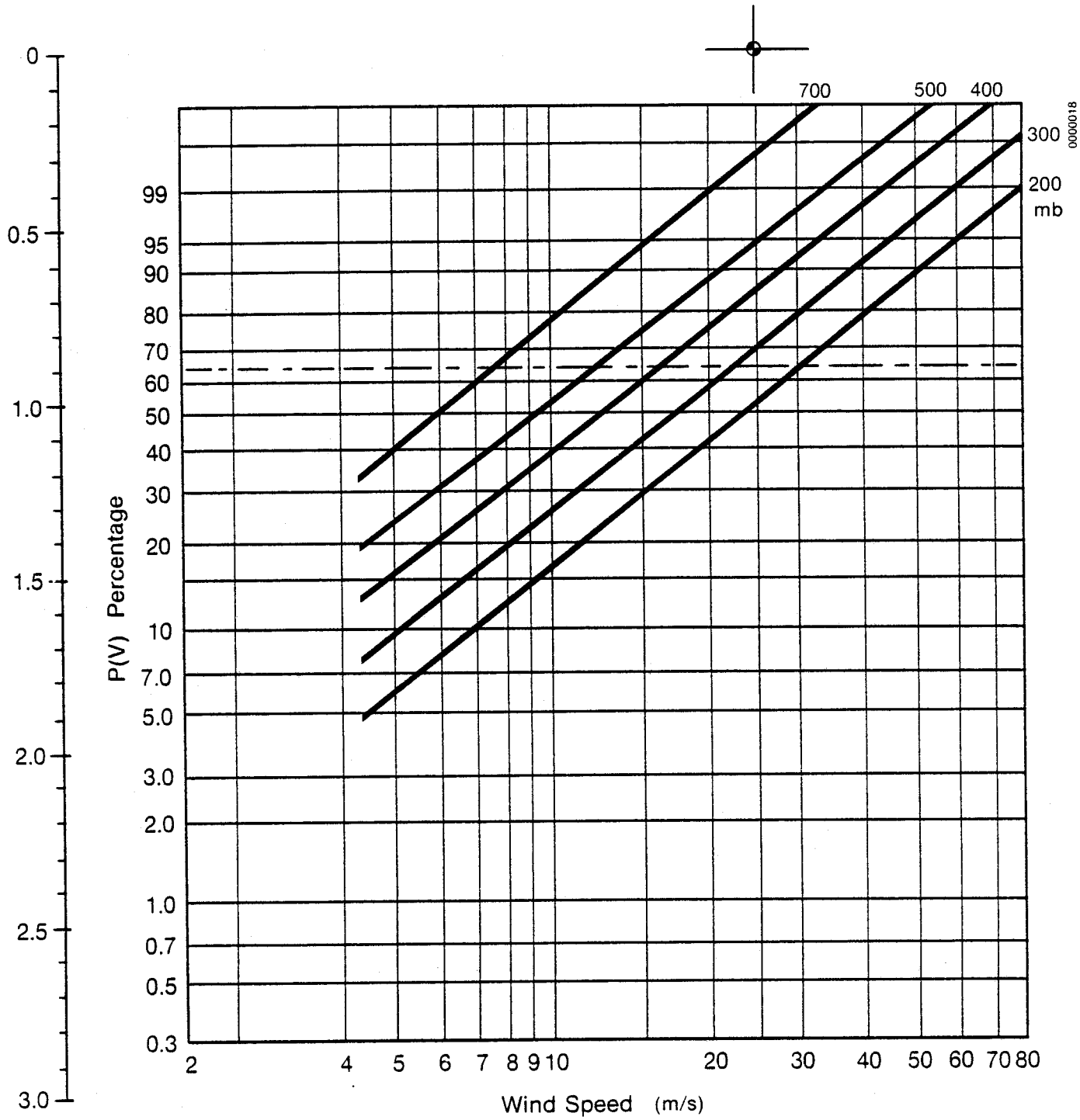

Figure B-5. Annual Probability Distribution of Velocity: Brownsville, TX

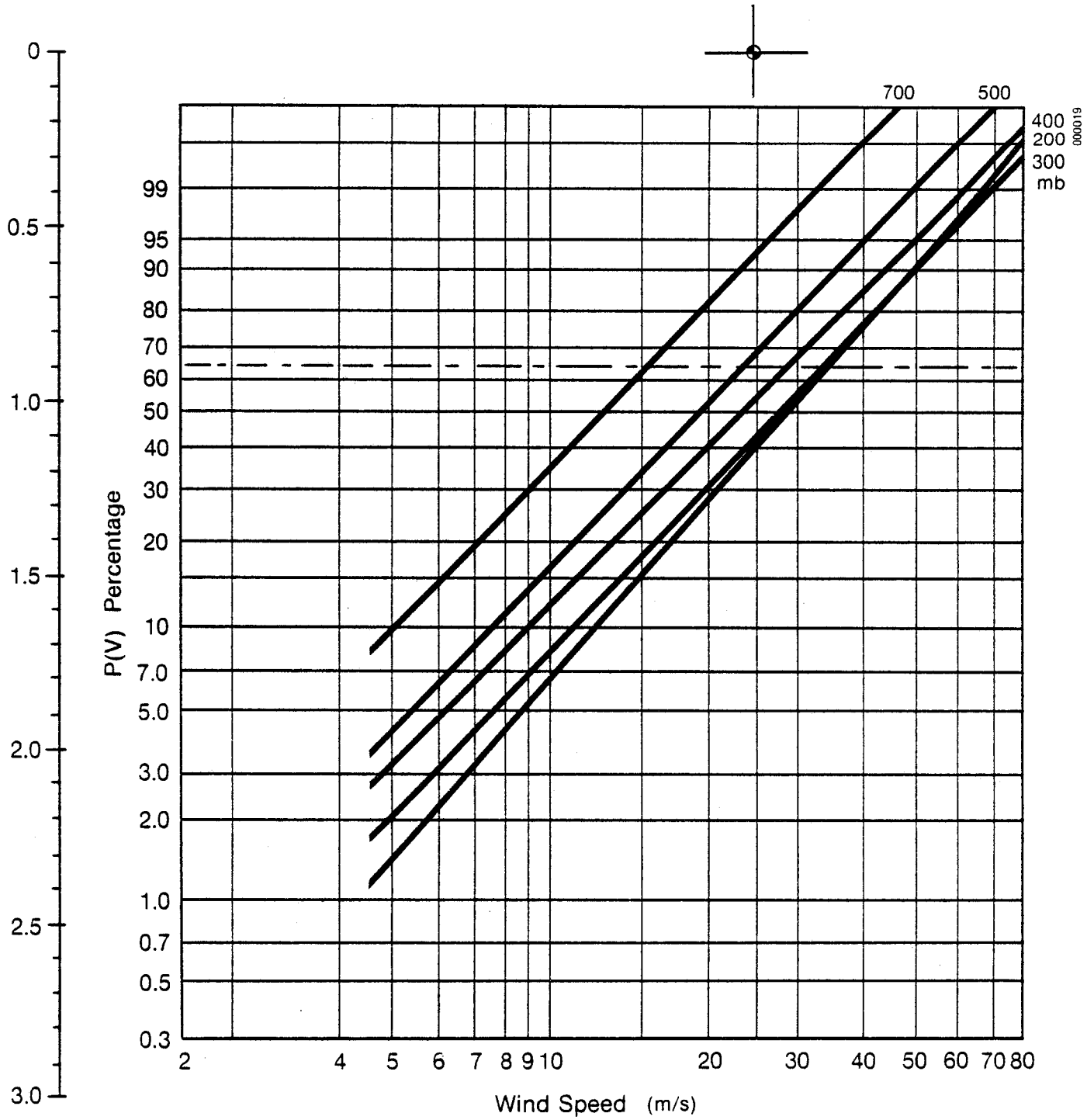

Figure B-6. Annual Probability Distribution of Velocity: Buffalo, NY

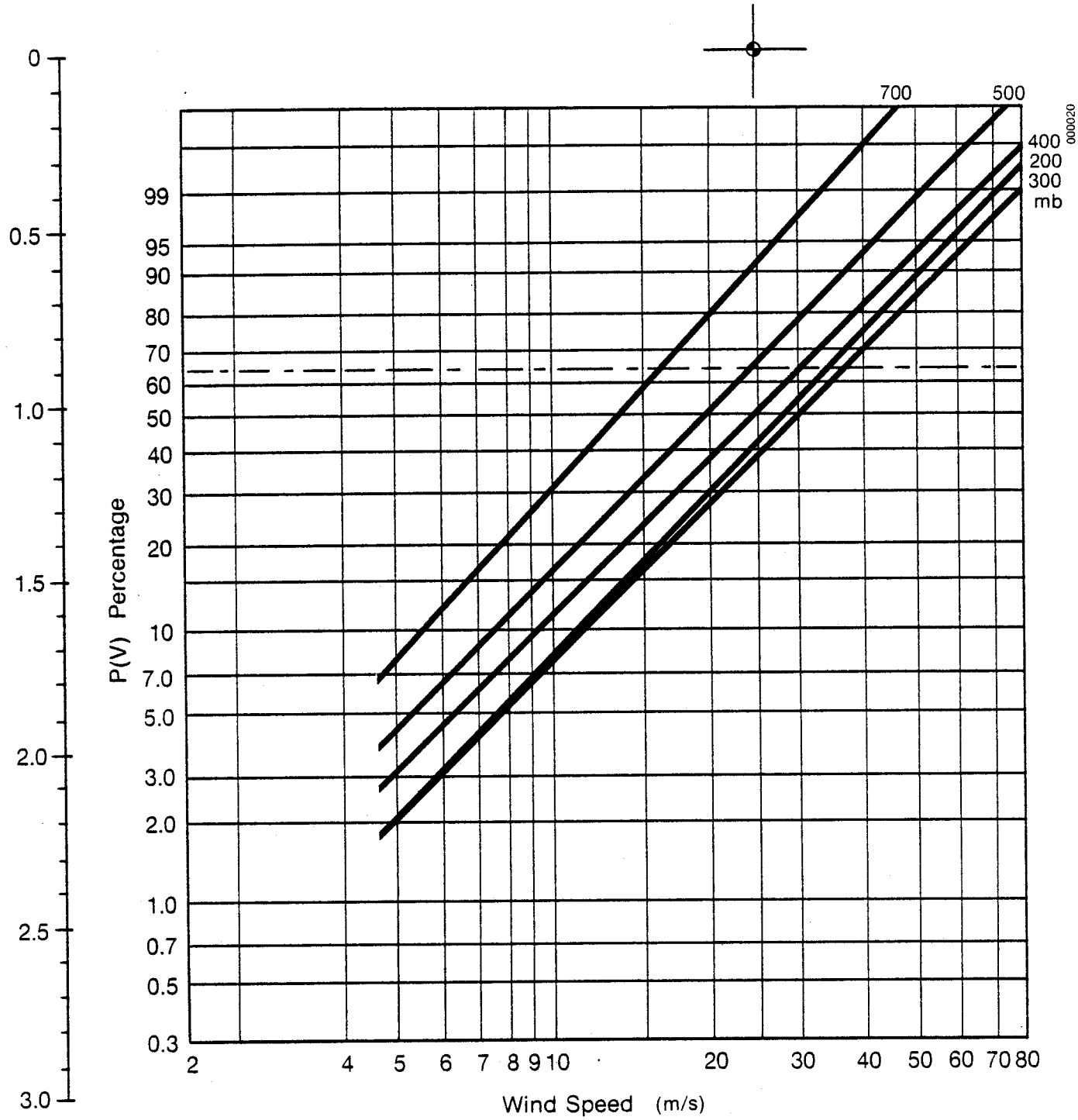

Figure B-7. Annual Probability Distribution of Velocity: Caribou, ME

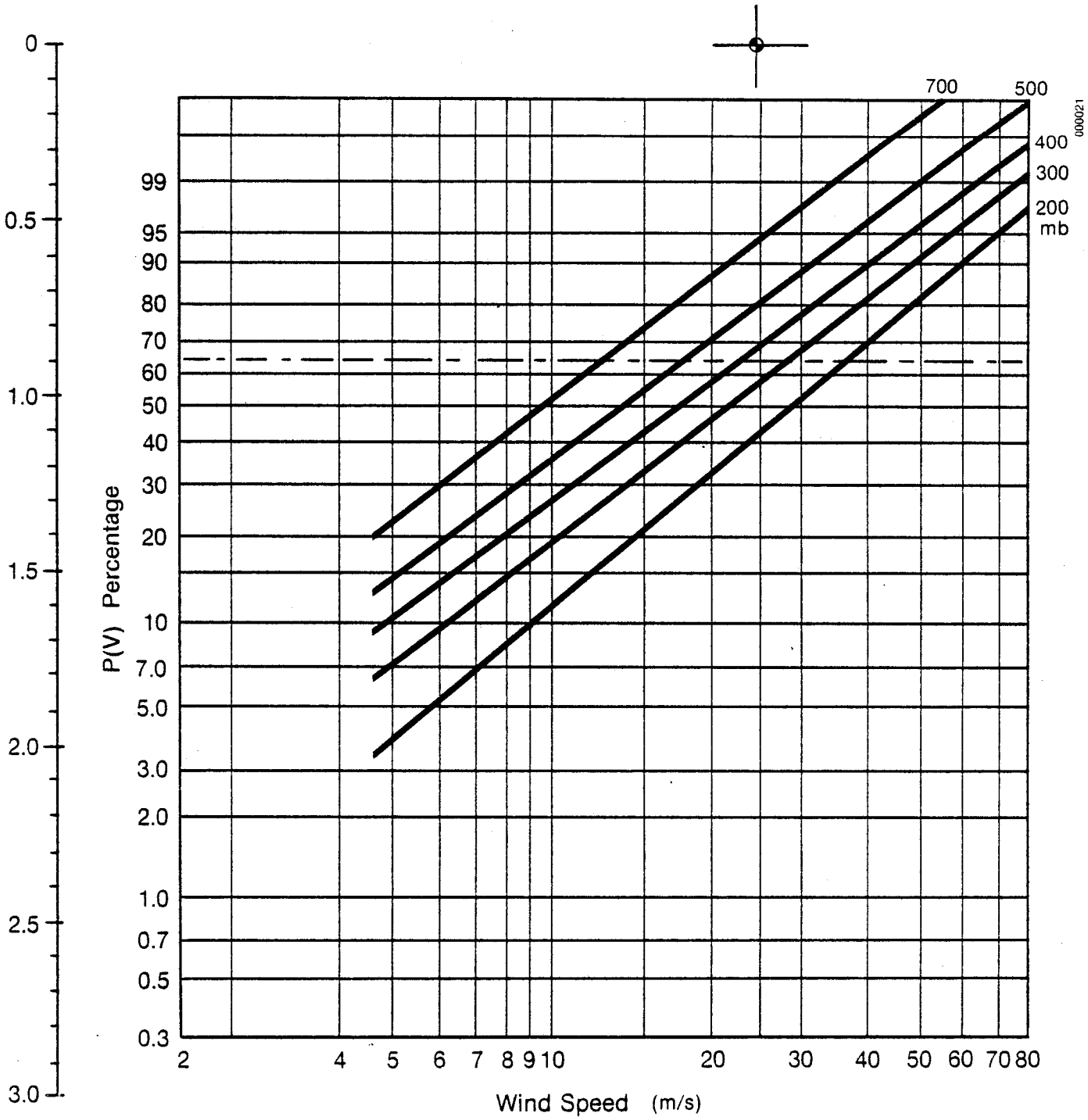

Figure B-8. Annual Probability Distribution of Velocity: Charleston, SC

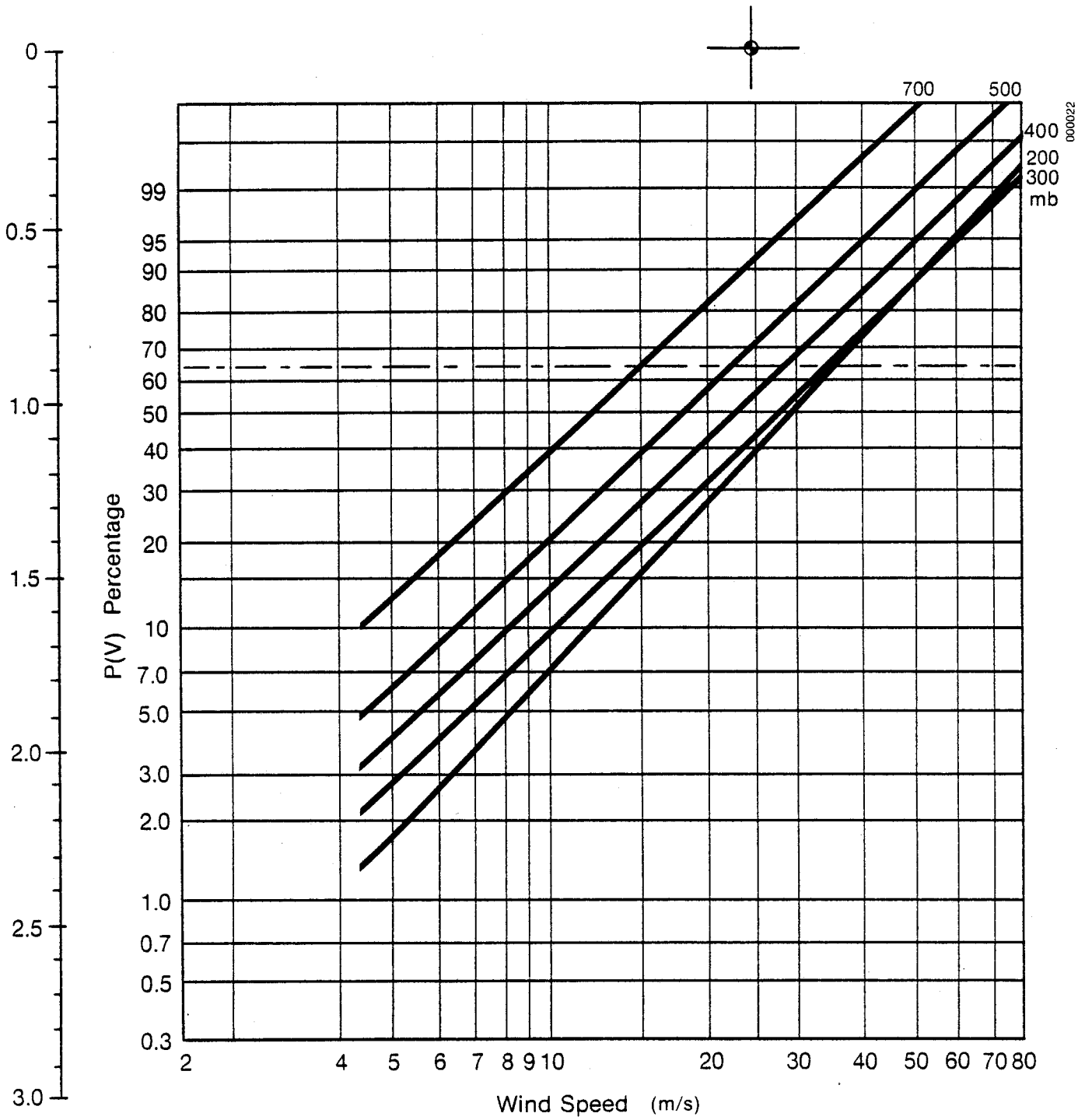

Figure B-9. Annual Probability Distribution of Velocity: Dayton, OH

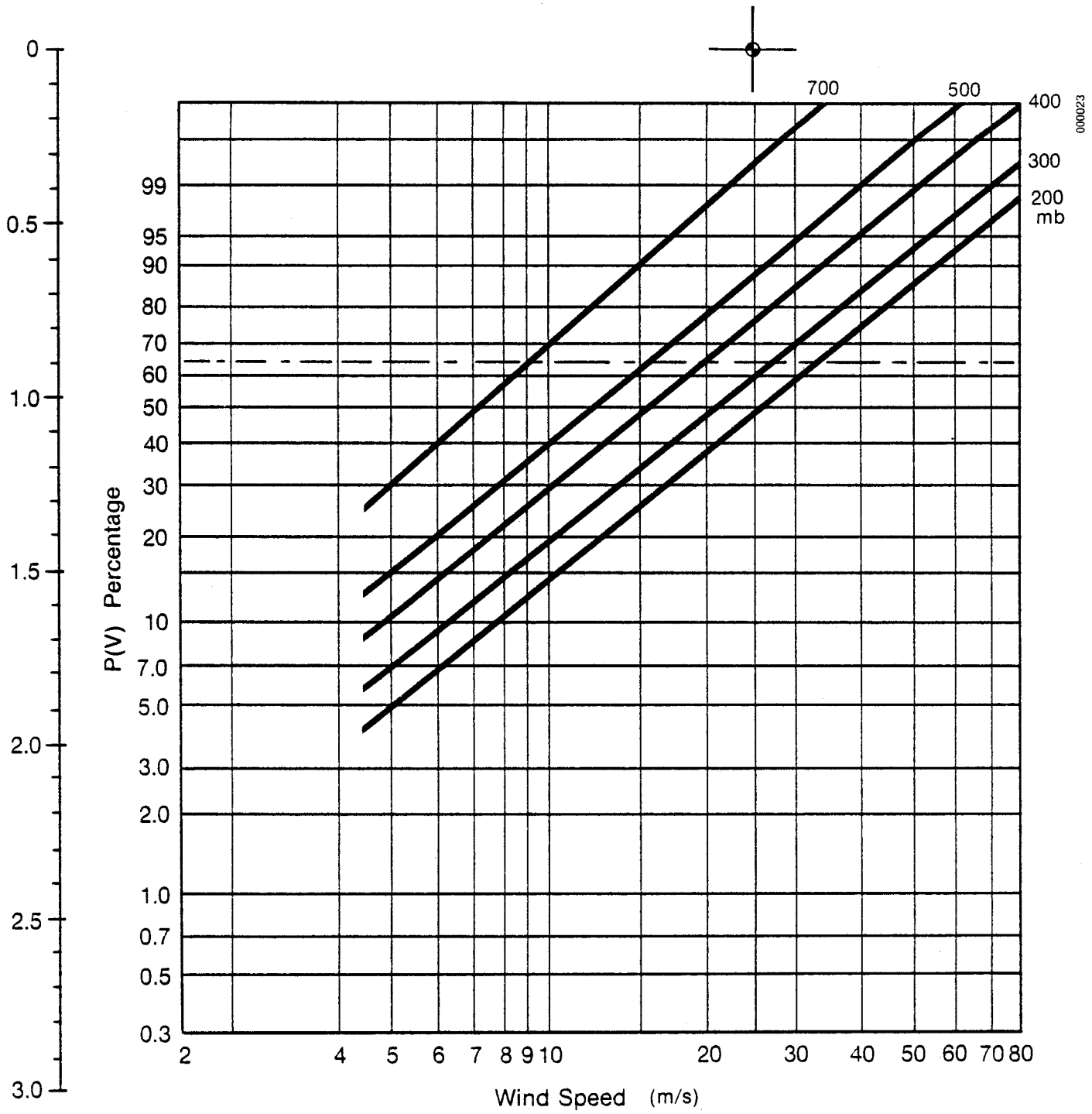

Figure B-10. Annual Probability Distribution of Velocity: Del Rio, TX

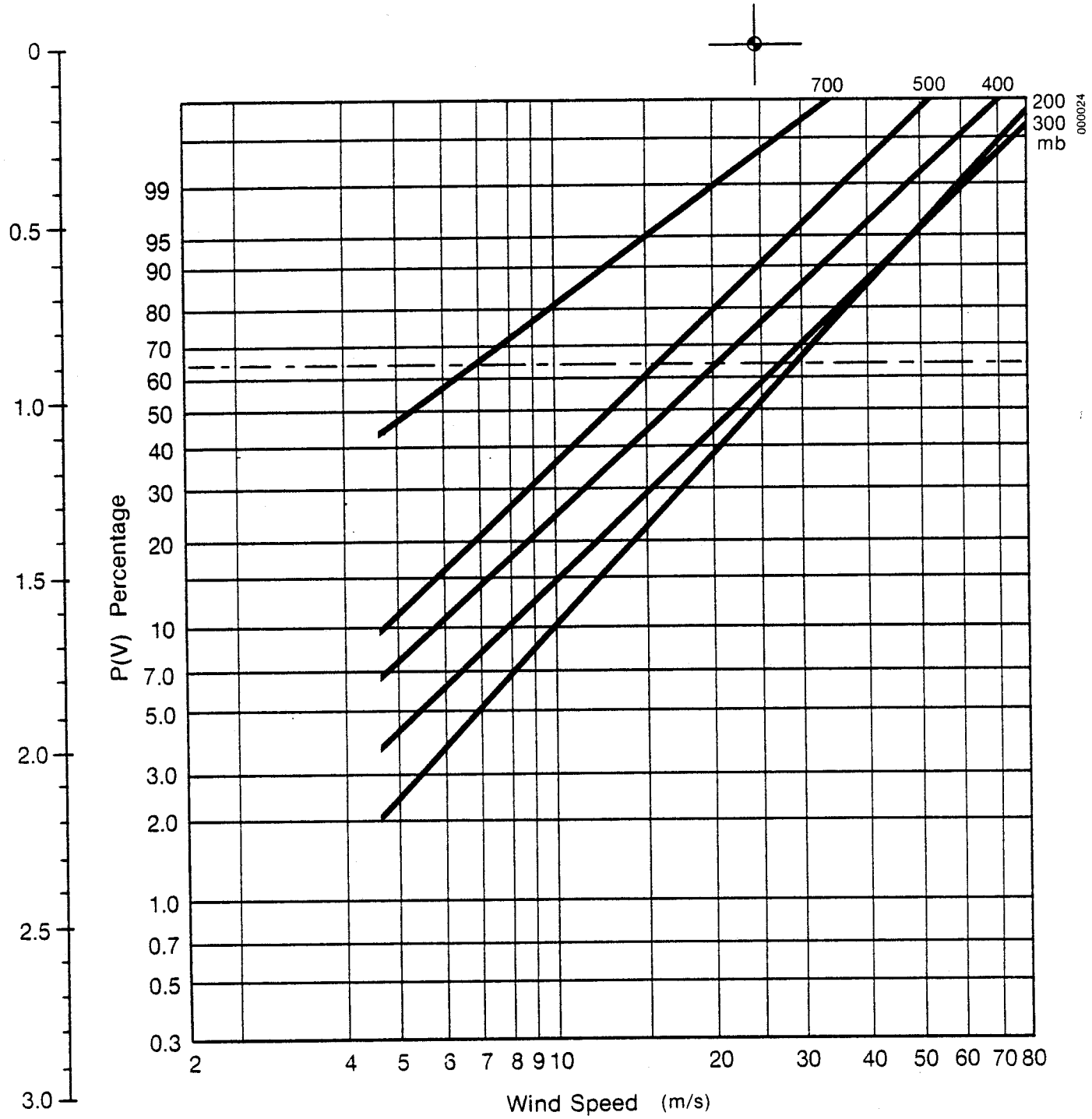

Figure B-11. Annual Probability Distribution of Velocity: Denver, CO

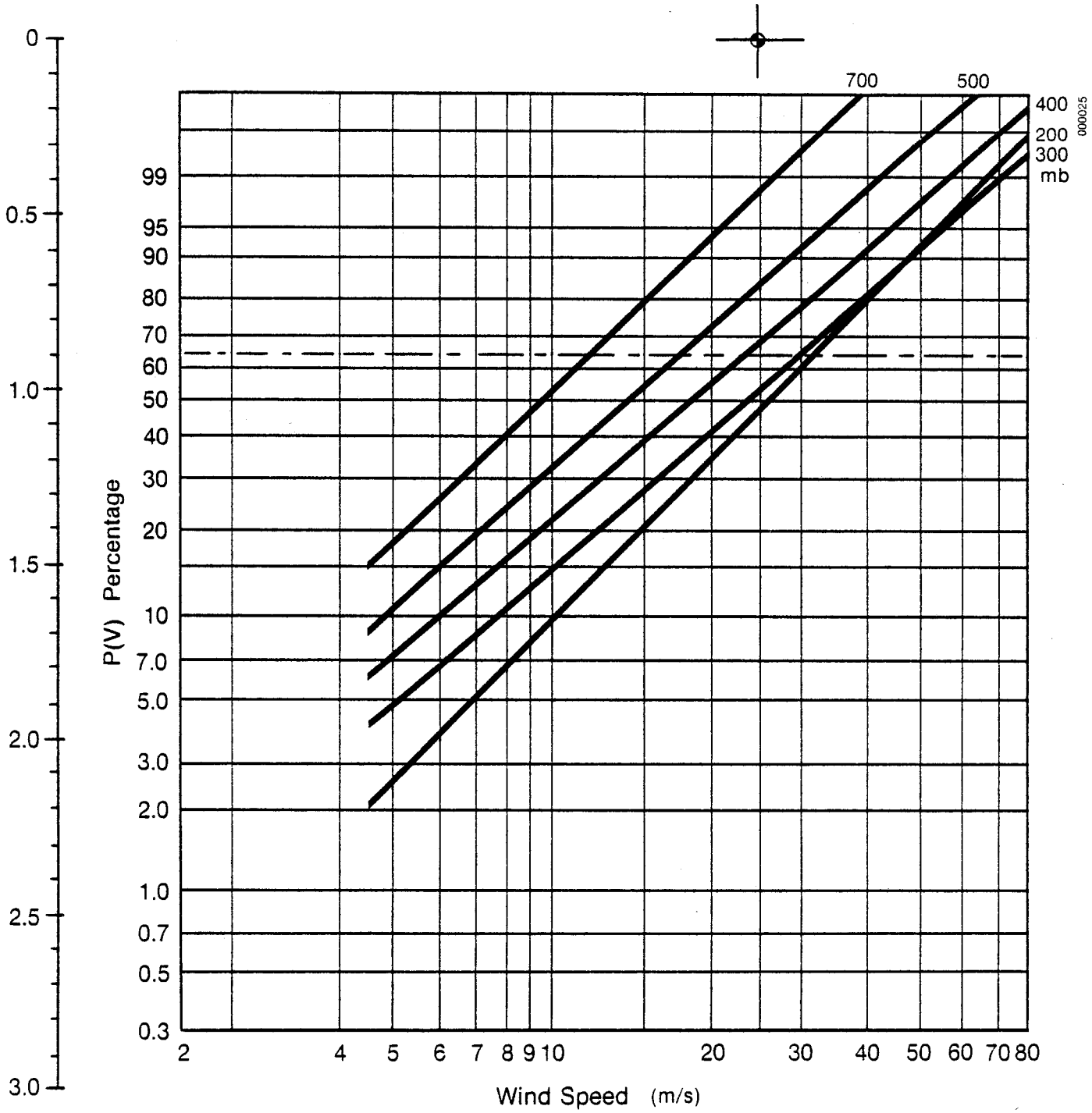

Figure B-12. Annual Probability Distribution of Velocity: Dodge City, KS

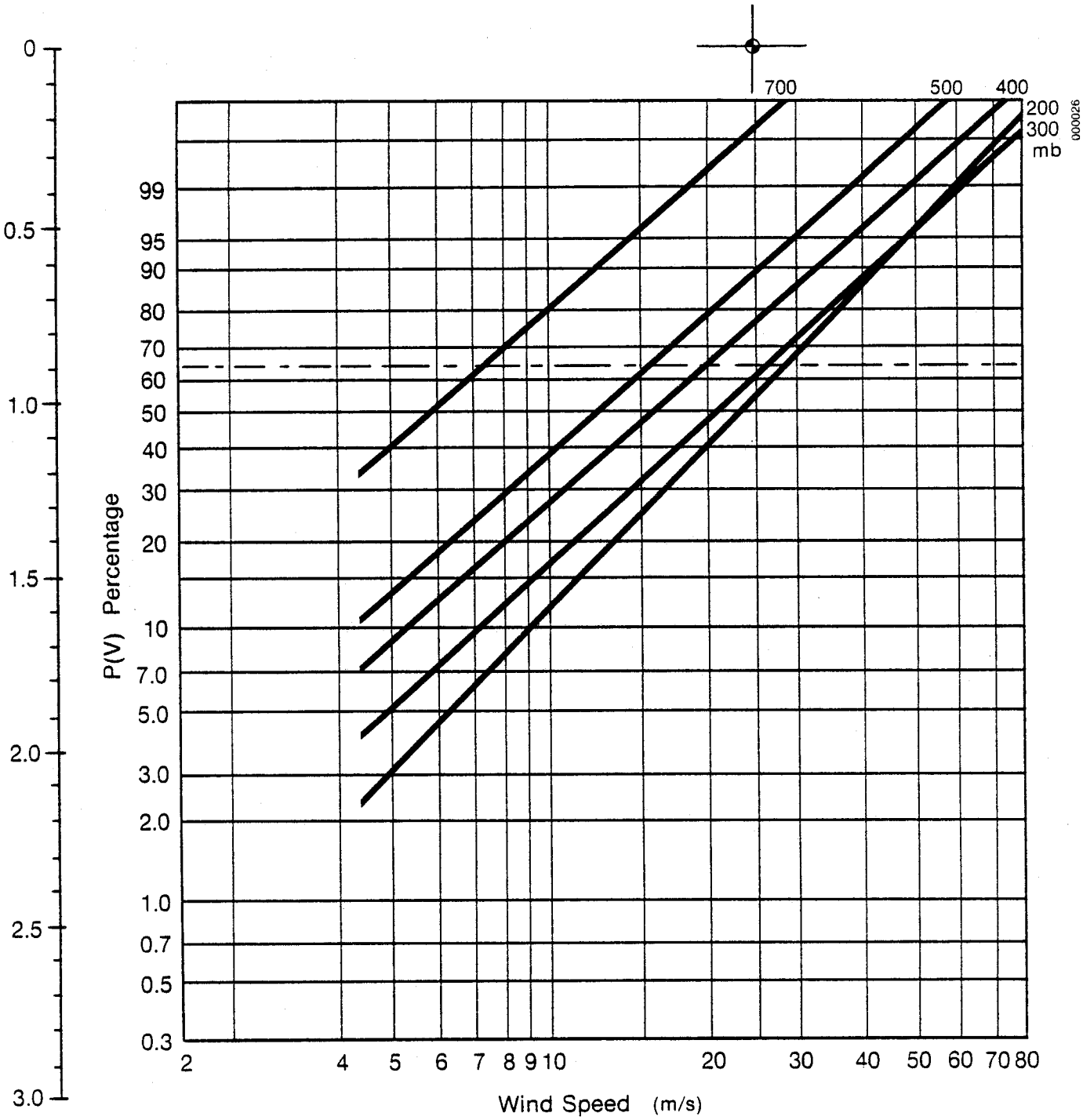

Figure B-13. Annual Probability Distribution of Velocity: Ely, NV

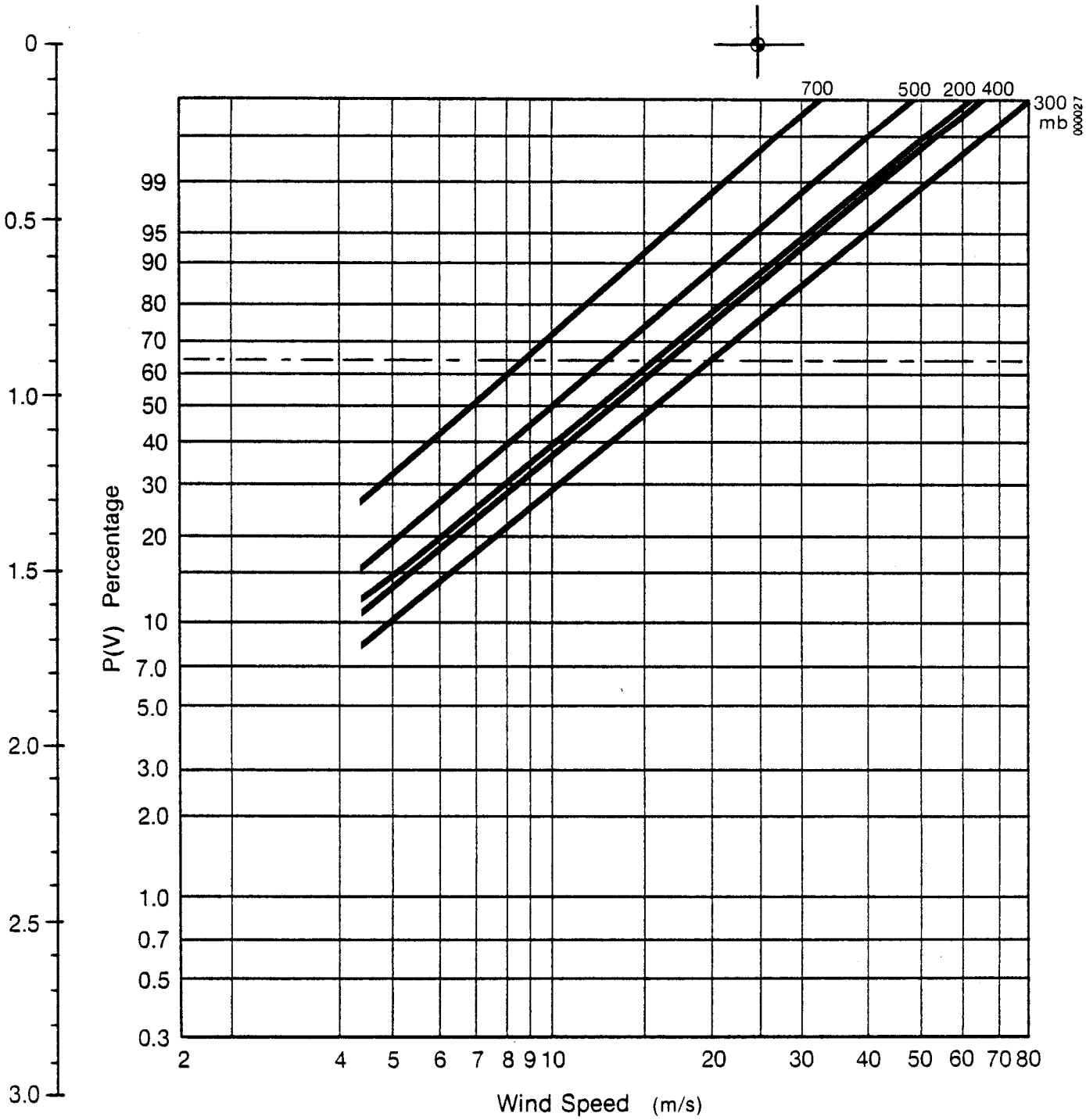

Figure B-14. Annual Probability Distribution of Velocity: Fairbanks, AK

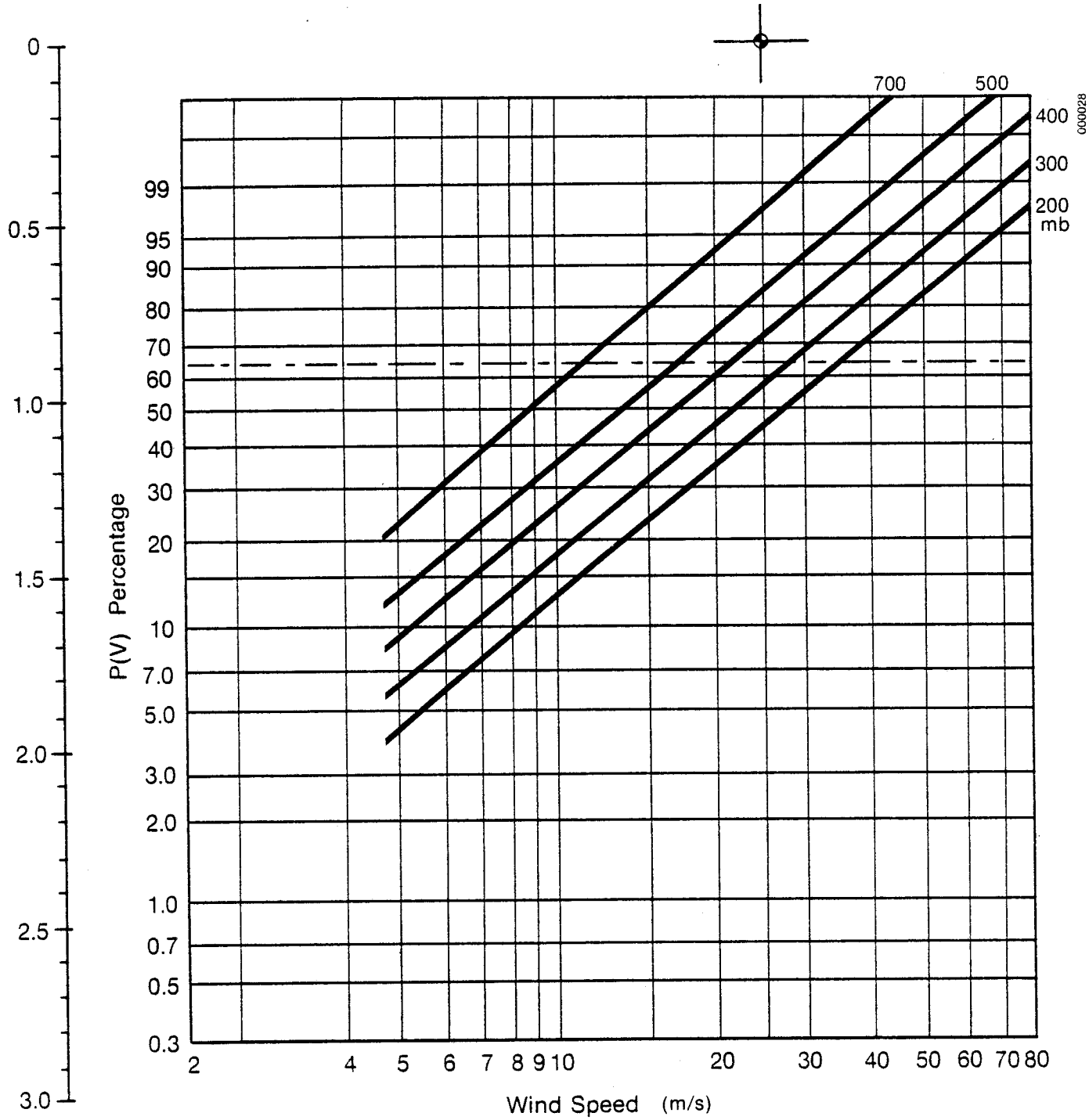

Figure B-15. Annual Probability Distribution of Velocity: Ft. Worth, TX

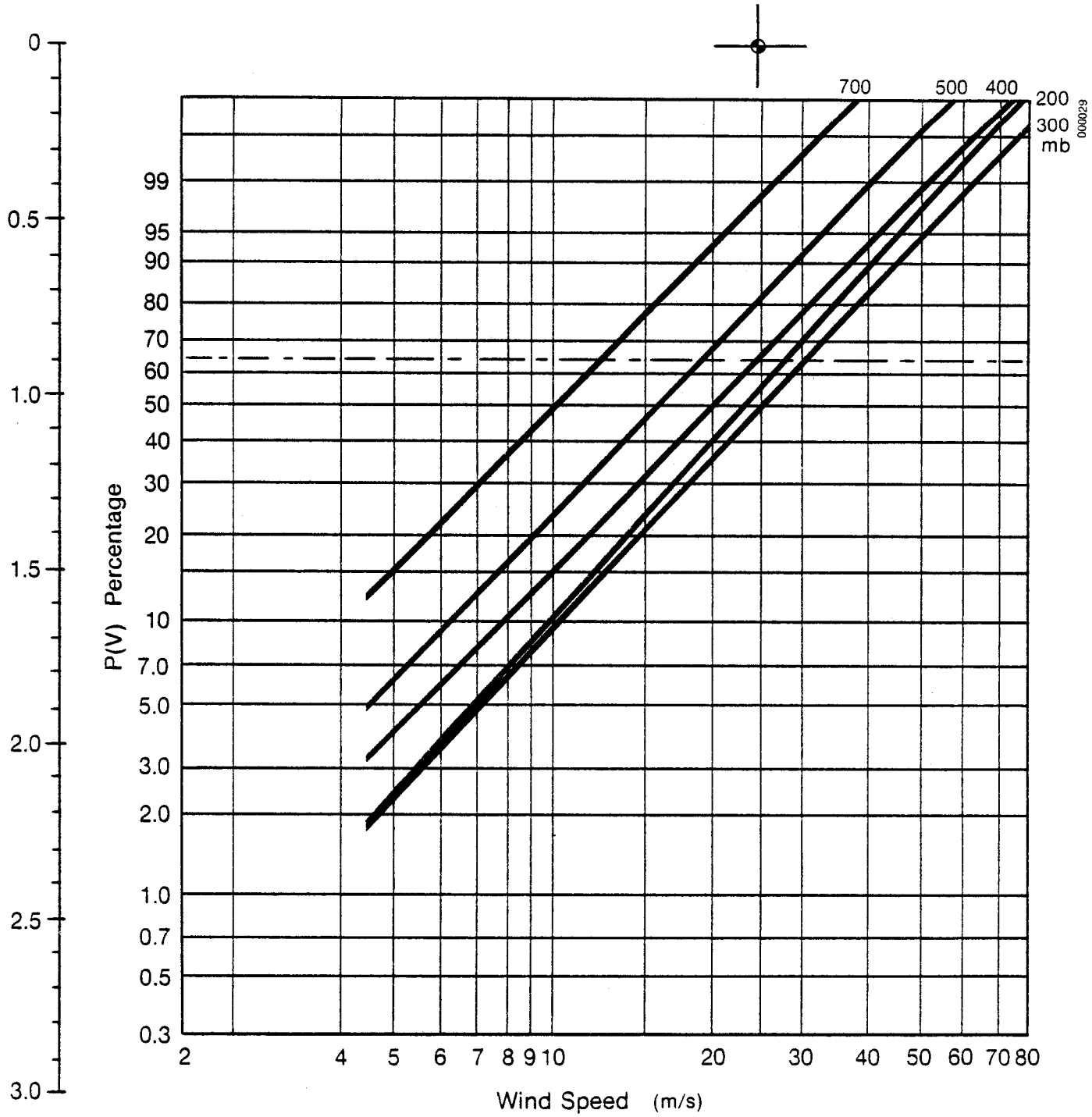

Figure B-16. Annual Probability Distribution of Velocity: Glasgow, ME

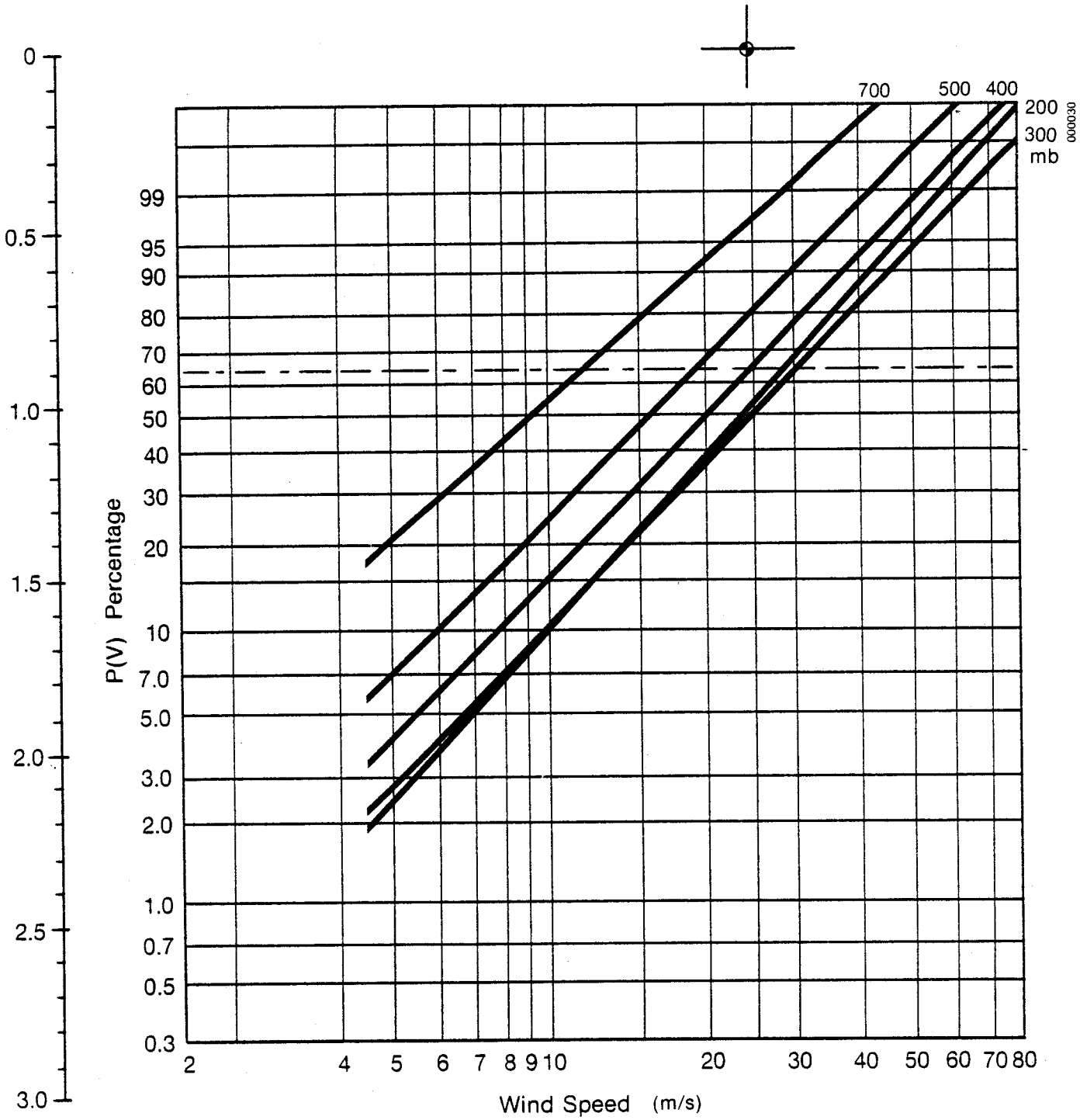

Figure B-17. Annual Probability Distribution of Velocity: Great Falls, MT

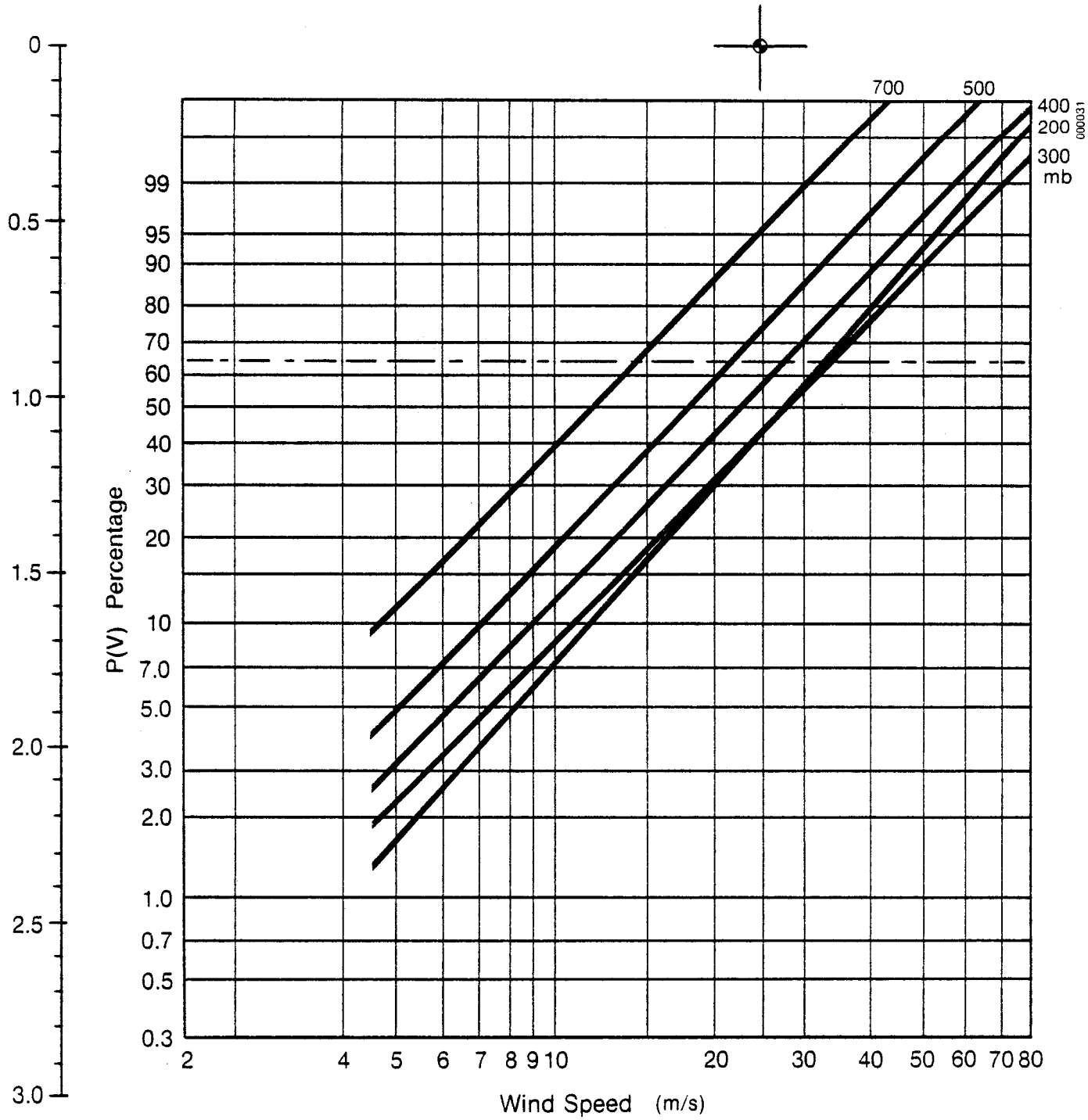

Figure B-18. Annual Probability Distribution of Velocity: Green Bay, WI

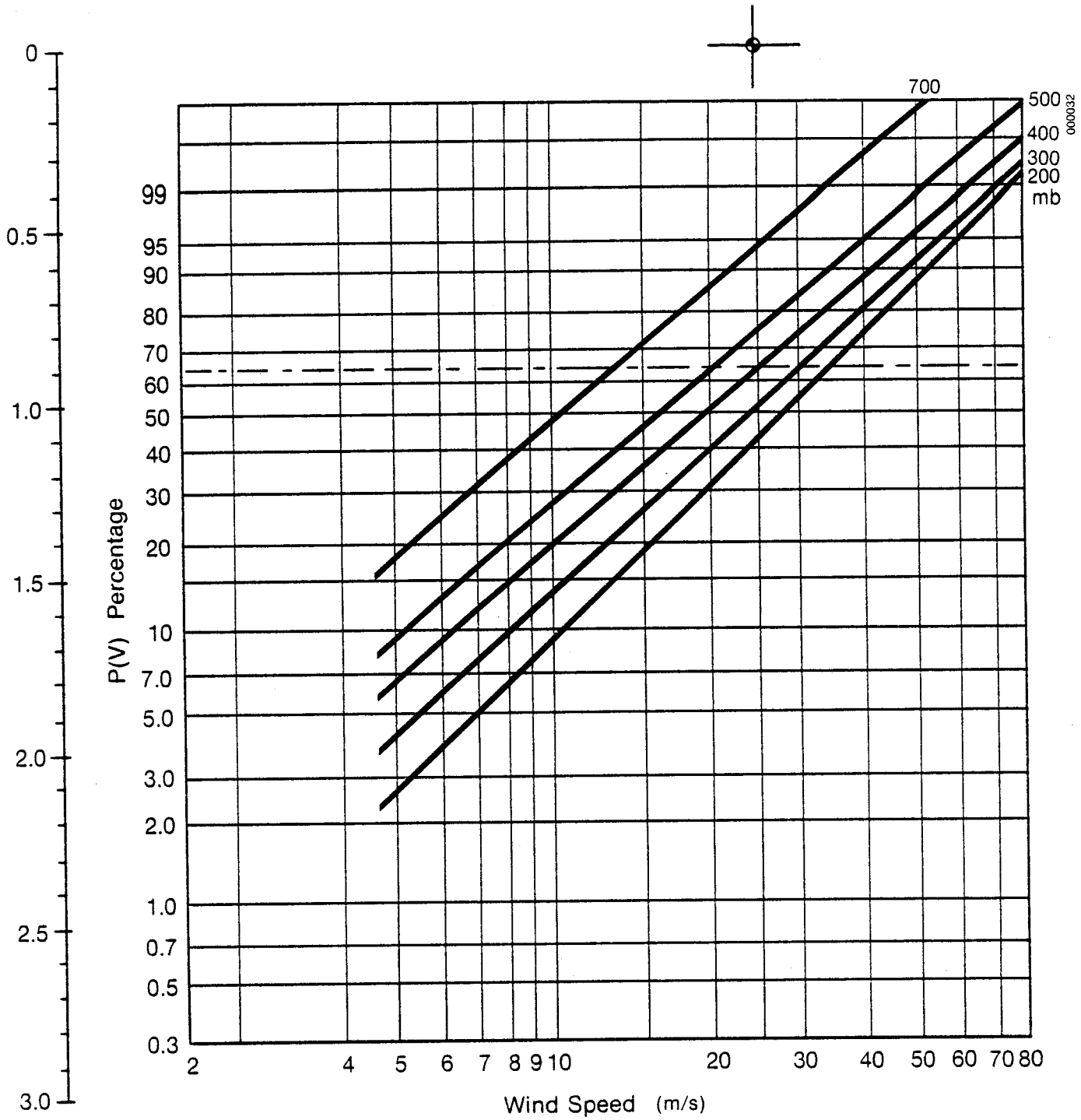

Figure B-19. Annual Probability Distribution of Velocity: Greensboro, NC

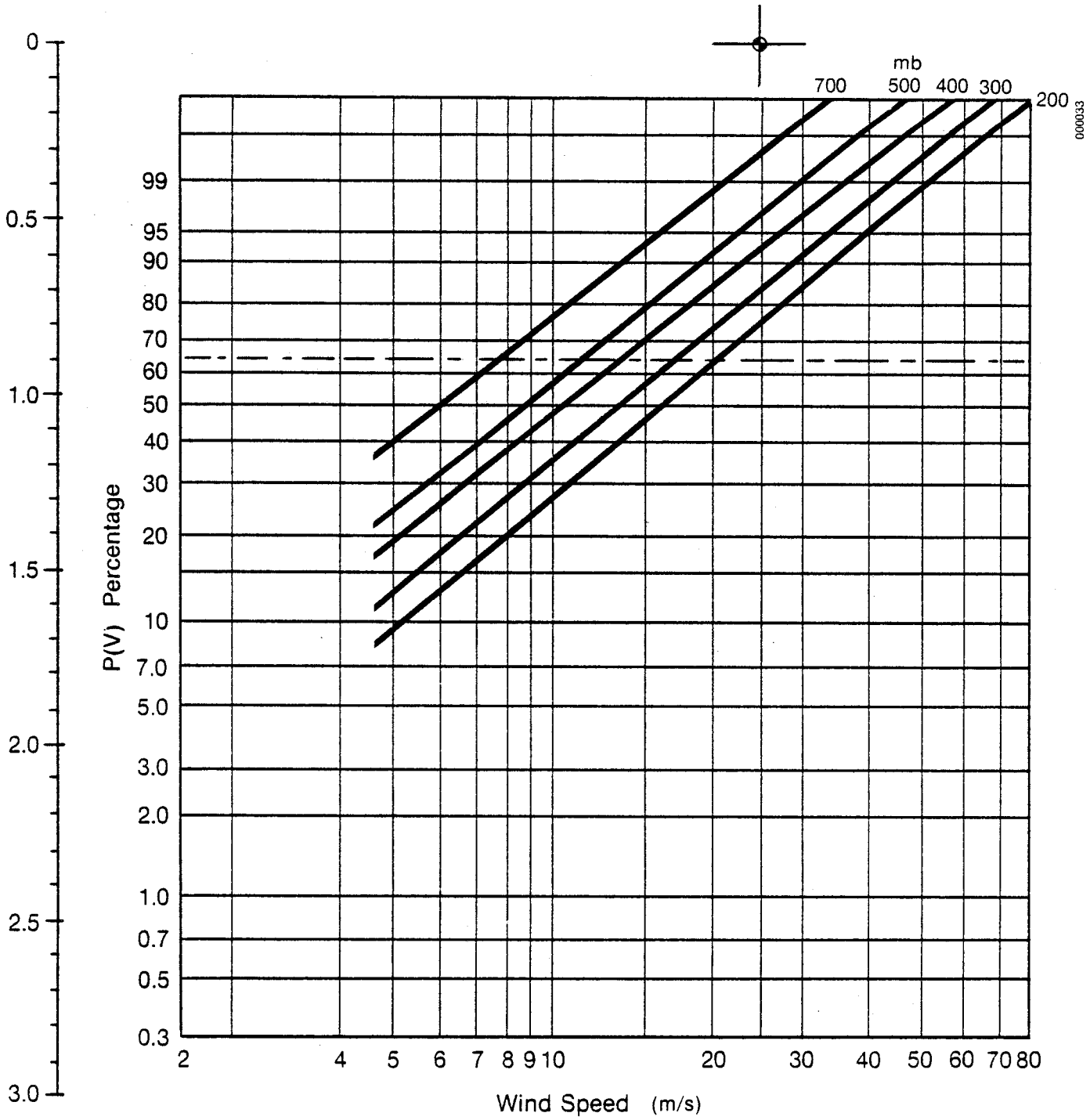

Figure B-20. Annual Probability Distribution of Velocity: Guadalupe Island, Mexico

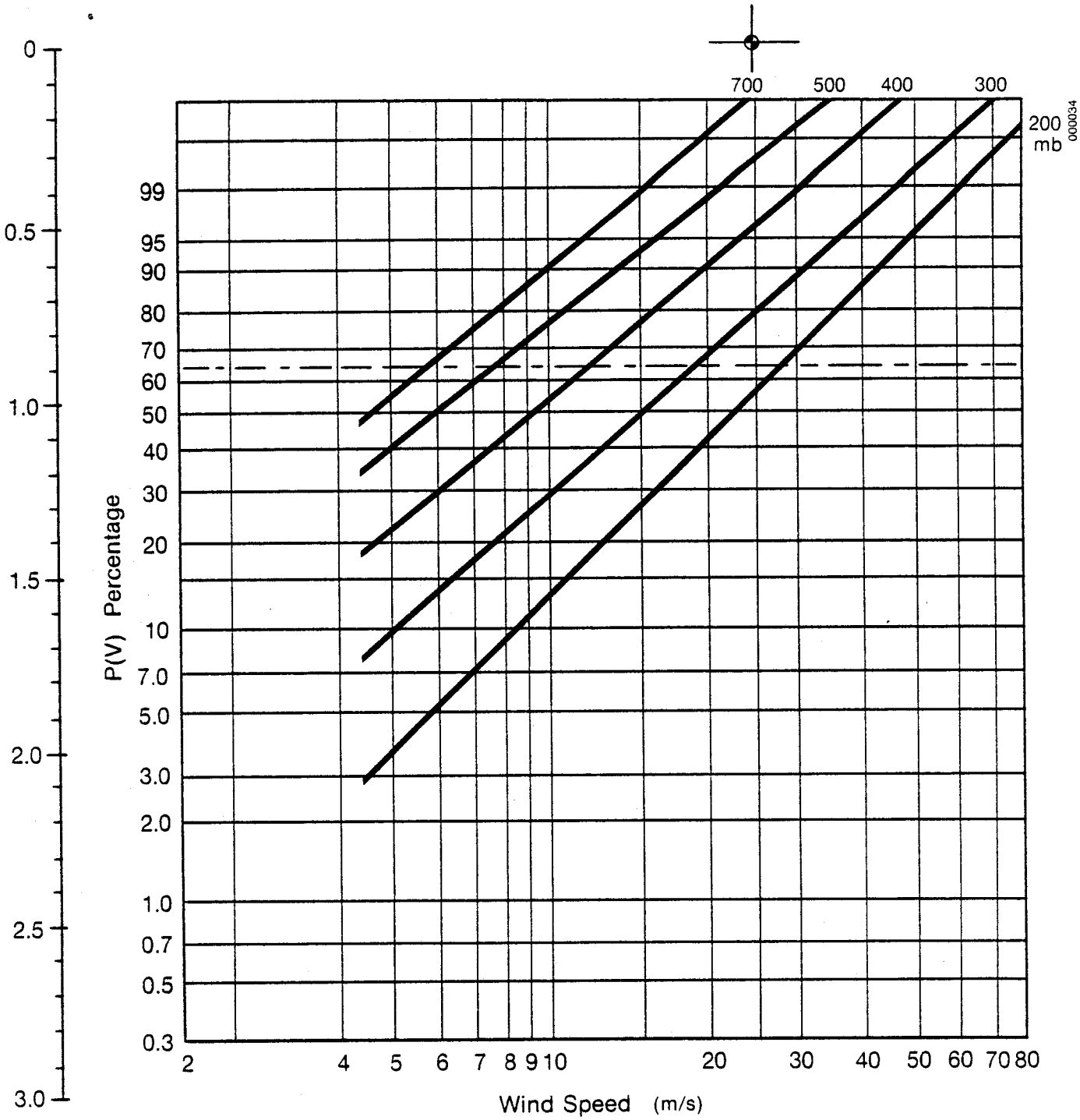

Figure B-21. Annual Probability Distribution of Velocity: Hilo, HI

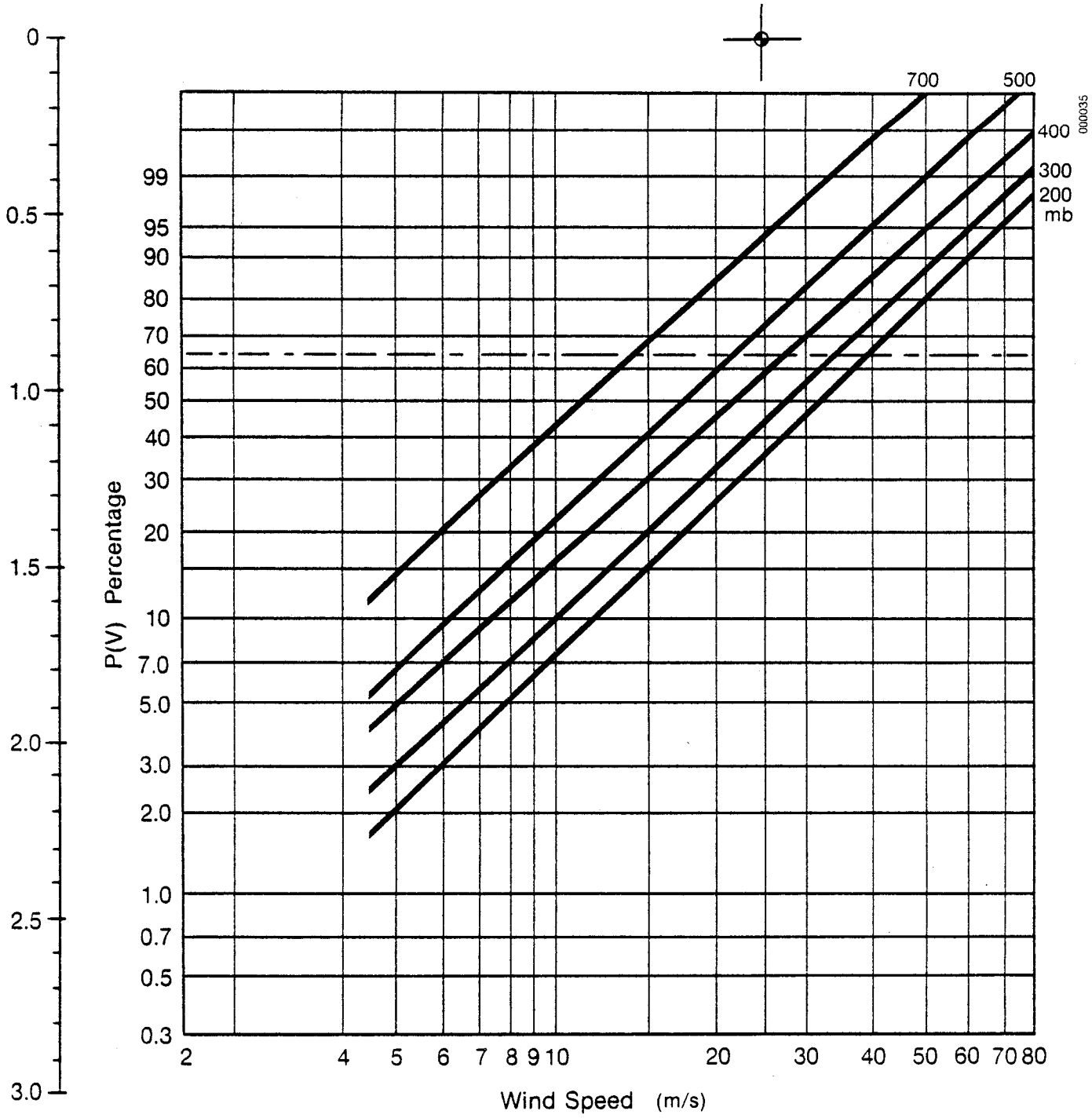

Figure B-22. Annual Probability Distribution of Velocity: Huntington, WV

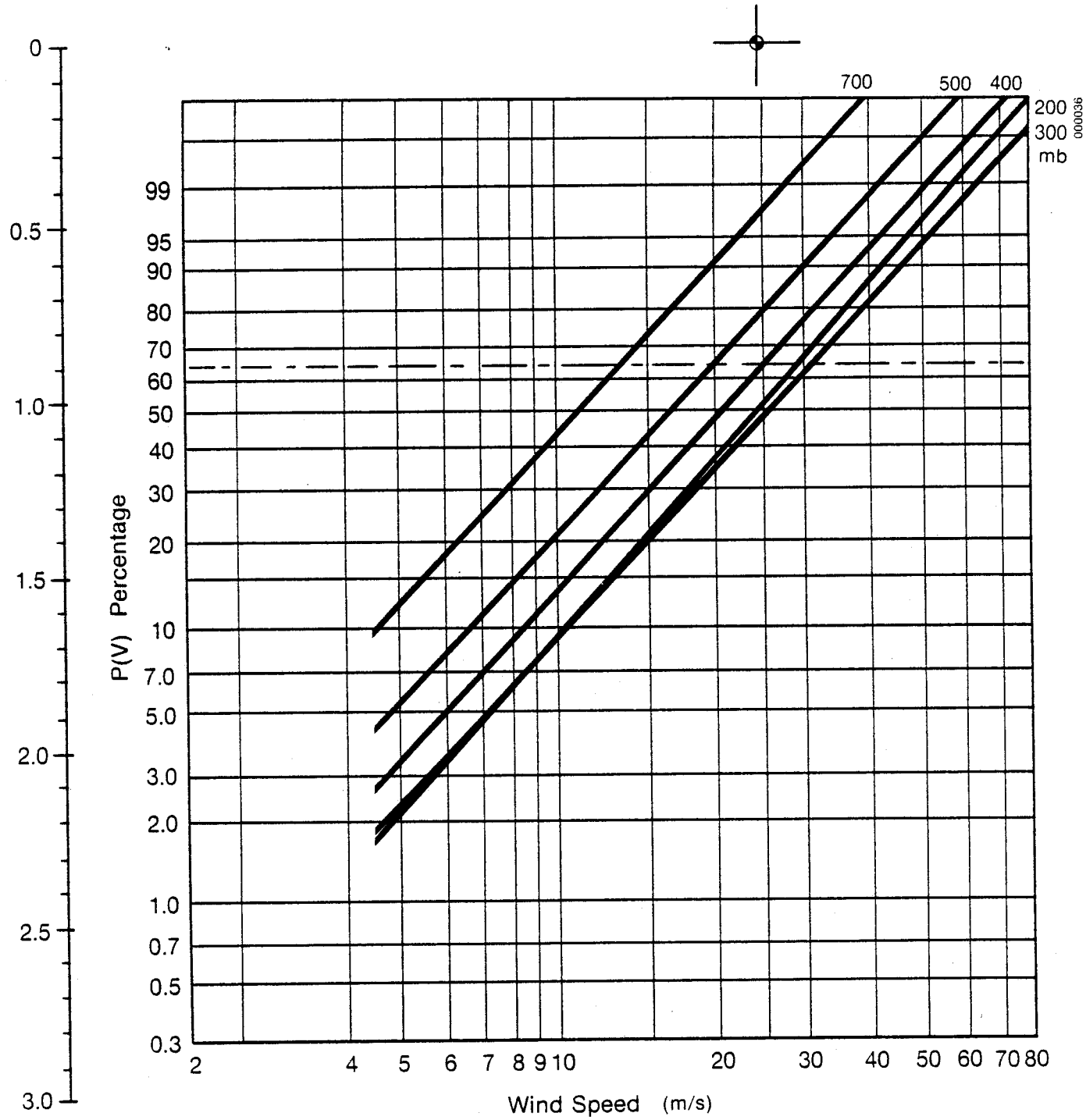

Figure B-23. Annual Probability Distribution of Velocity: International Falls, MN

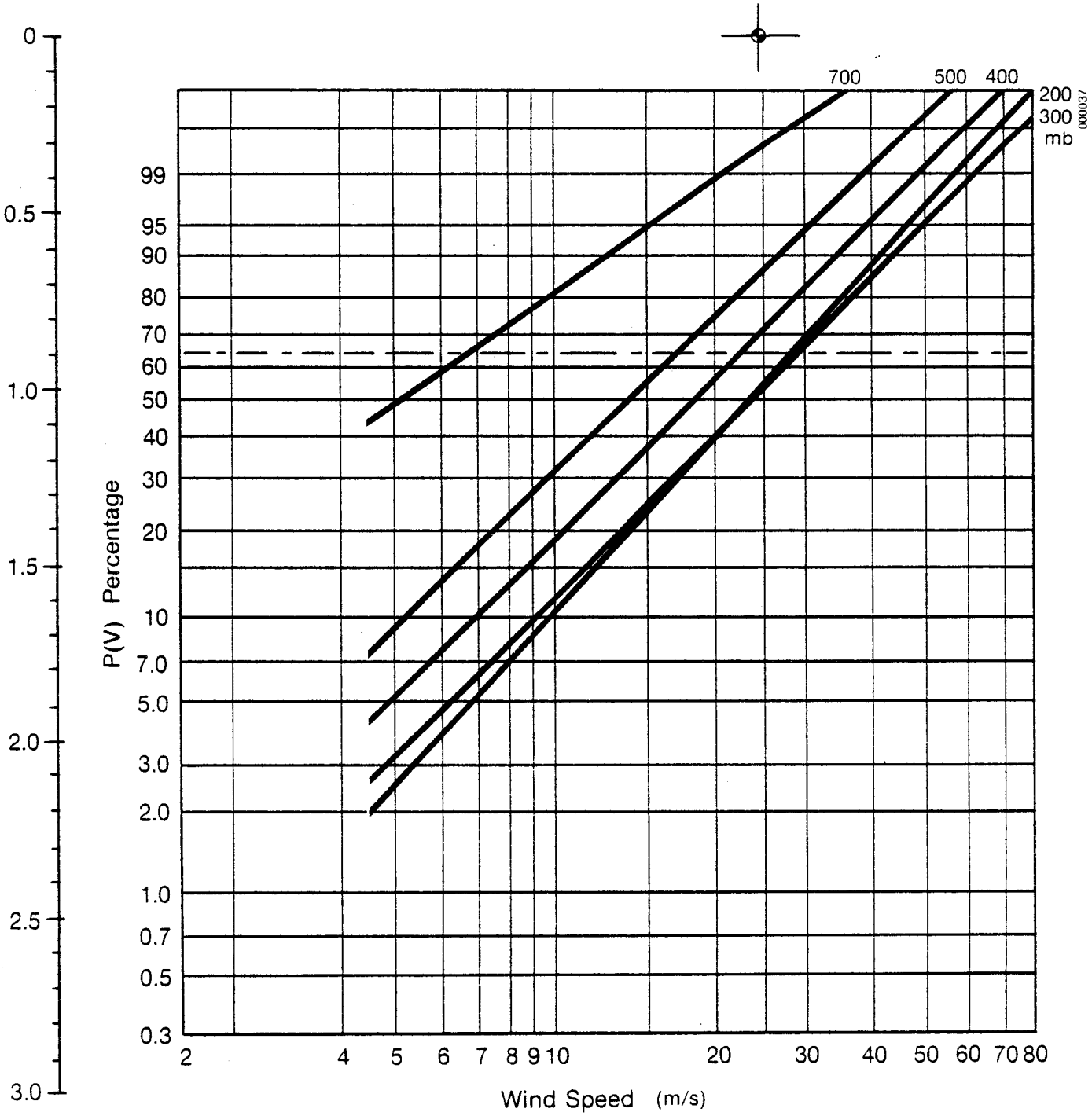

Figure B-24. Annual Probability Distribution of Velocity: Lander, WY

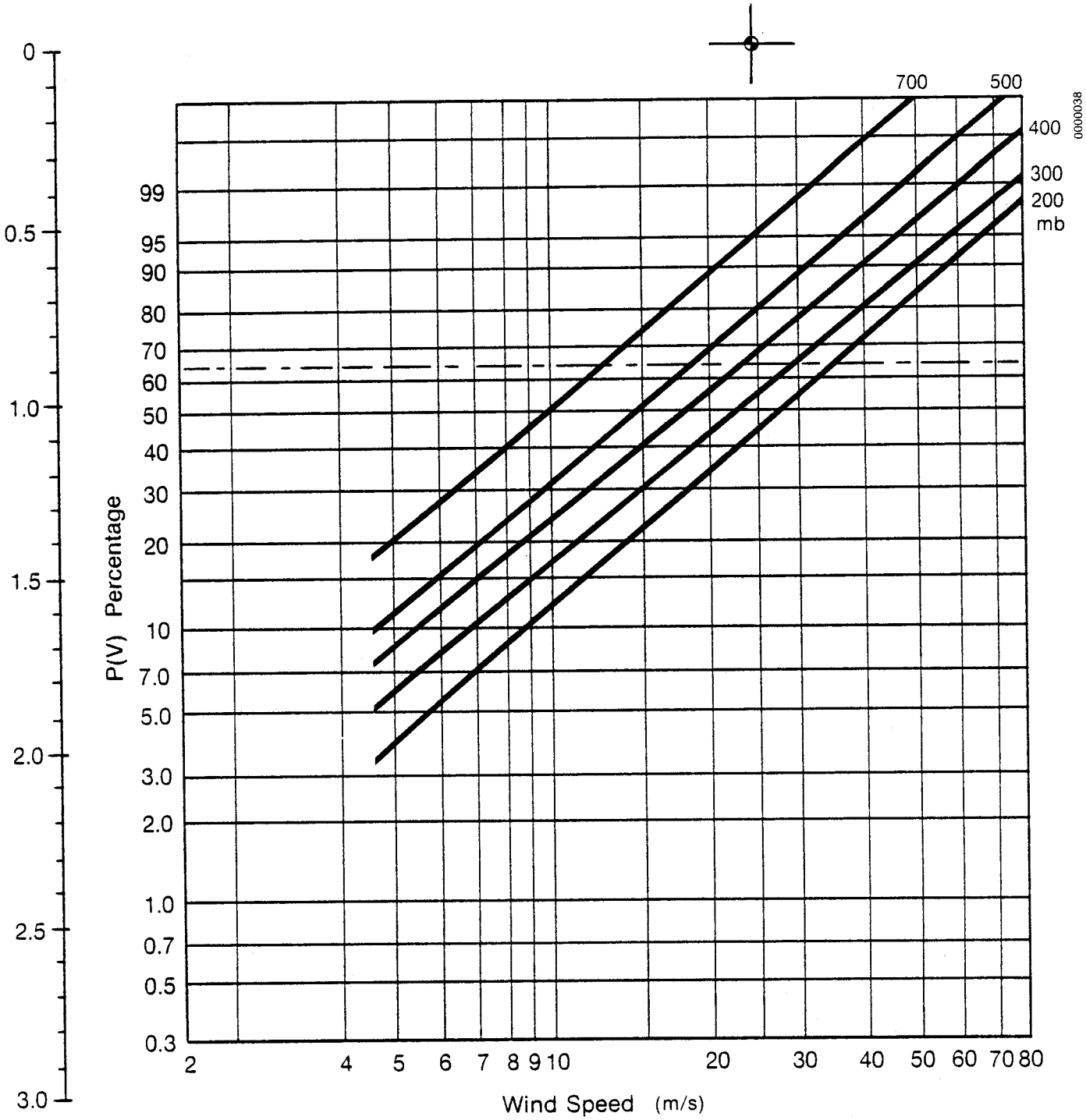

Figure B-25. Annual Probability Distribution of Velocity: Little Rock, AR

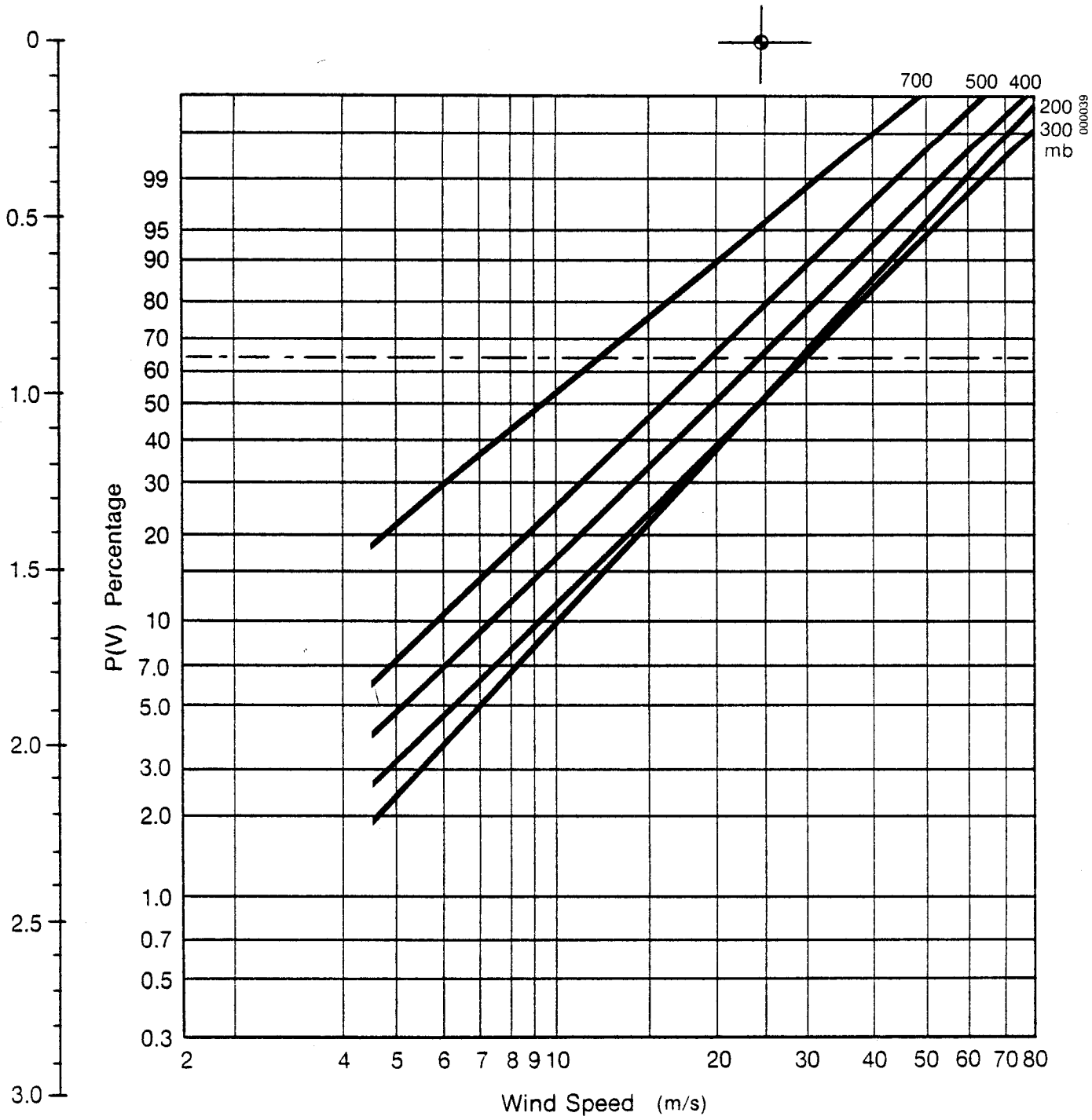

Figure B-26. Annual Probability Distribution of Velocity: Medford, OR

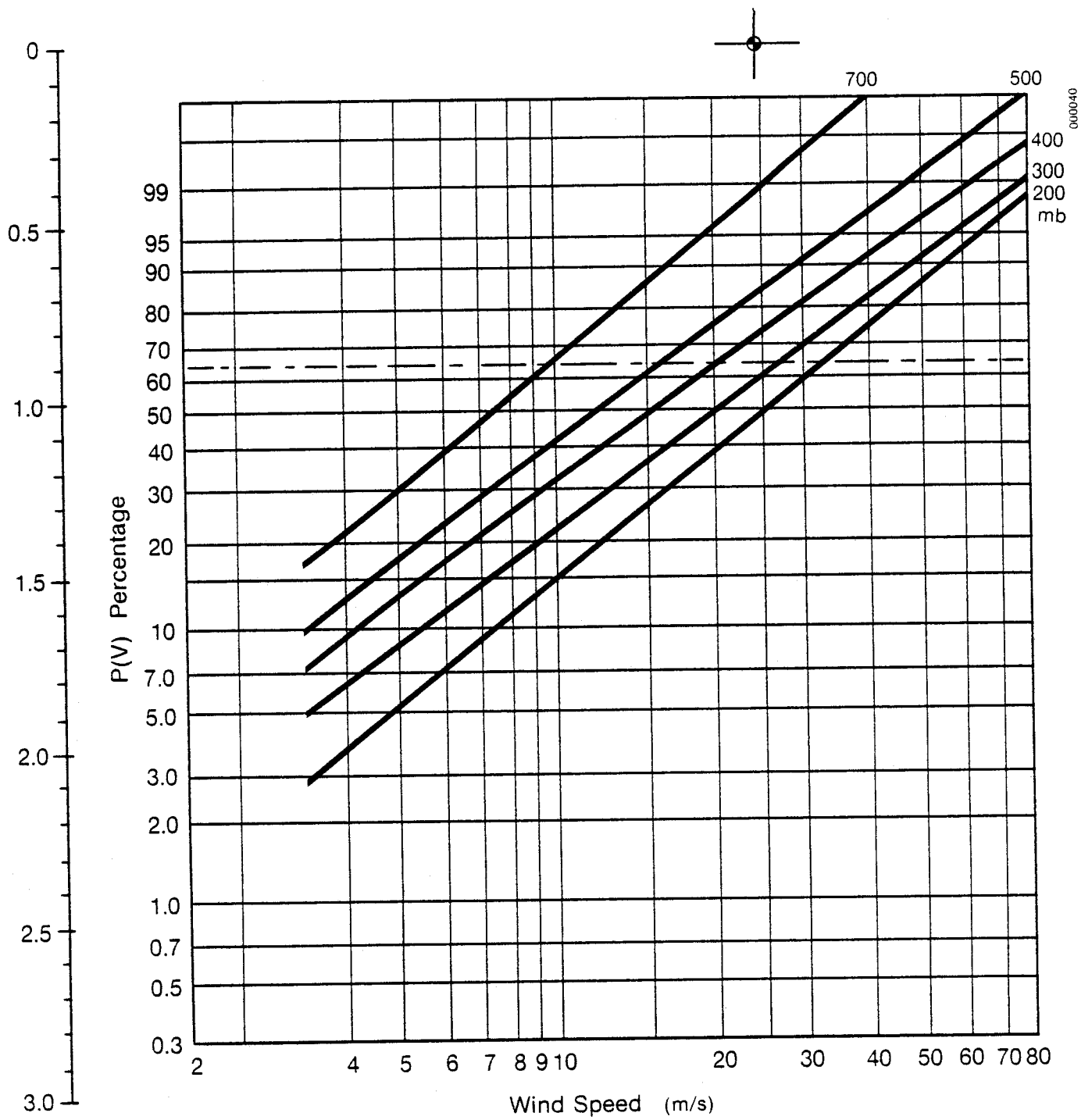

Figure B-27. Annual Probability Distribution of Velocity: Midland, TX

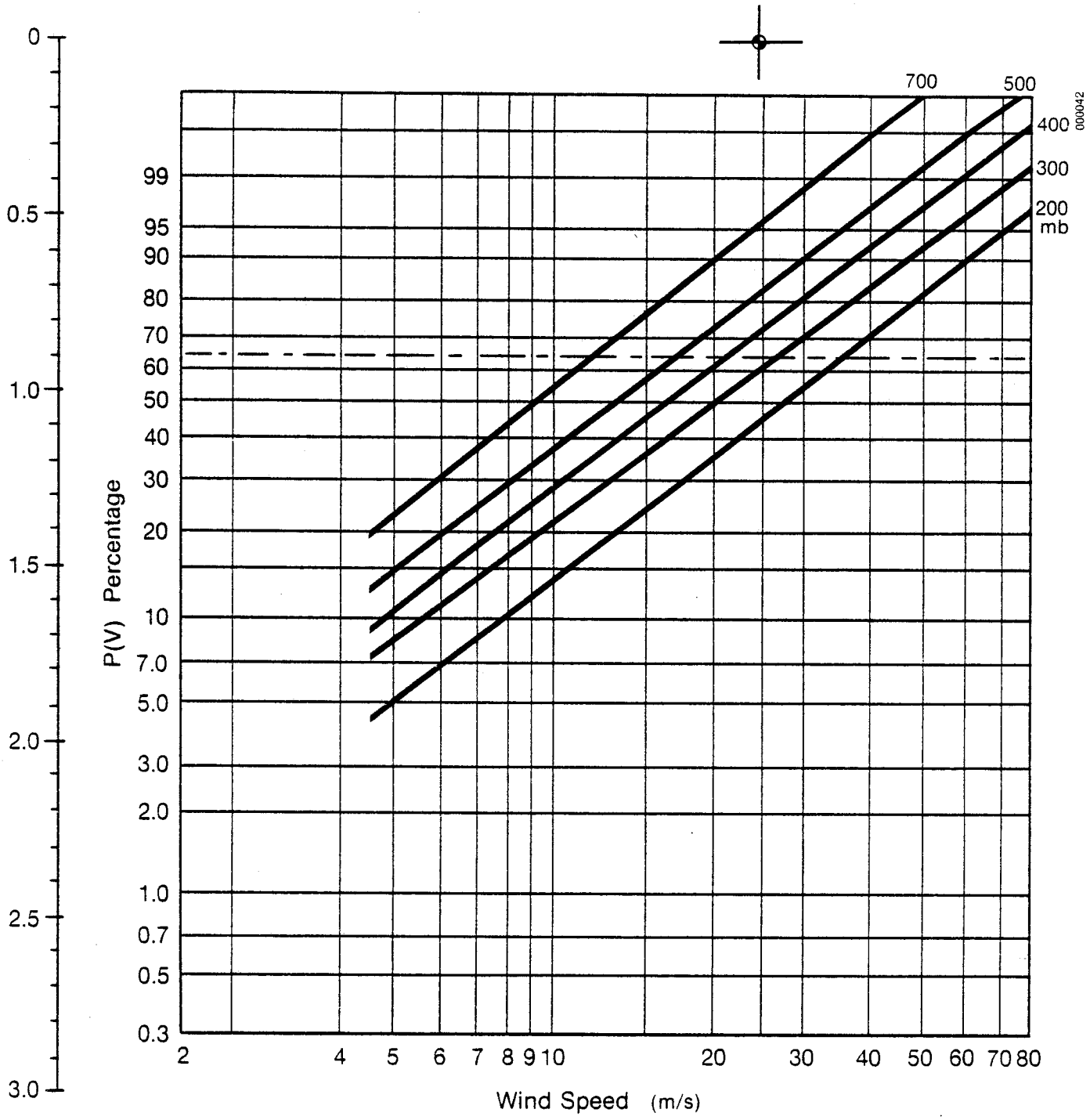

Figure B-28. Annual Probability Distribution of Velocity: Montgomery, AL

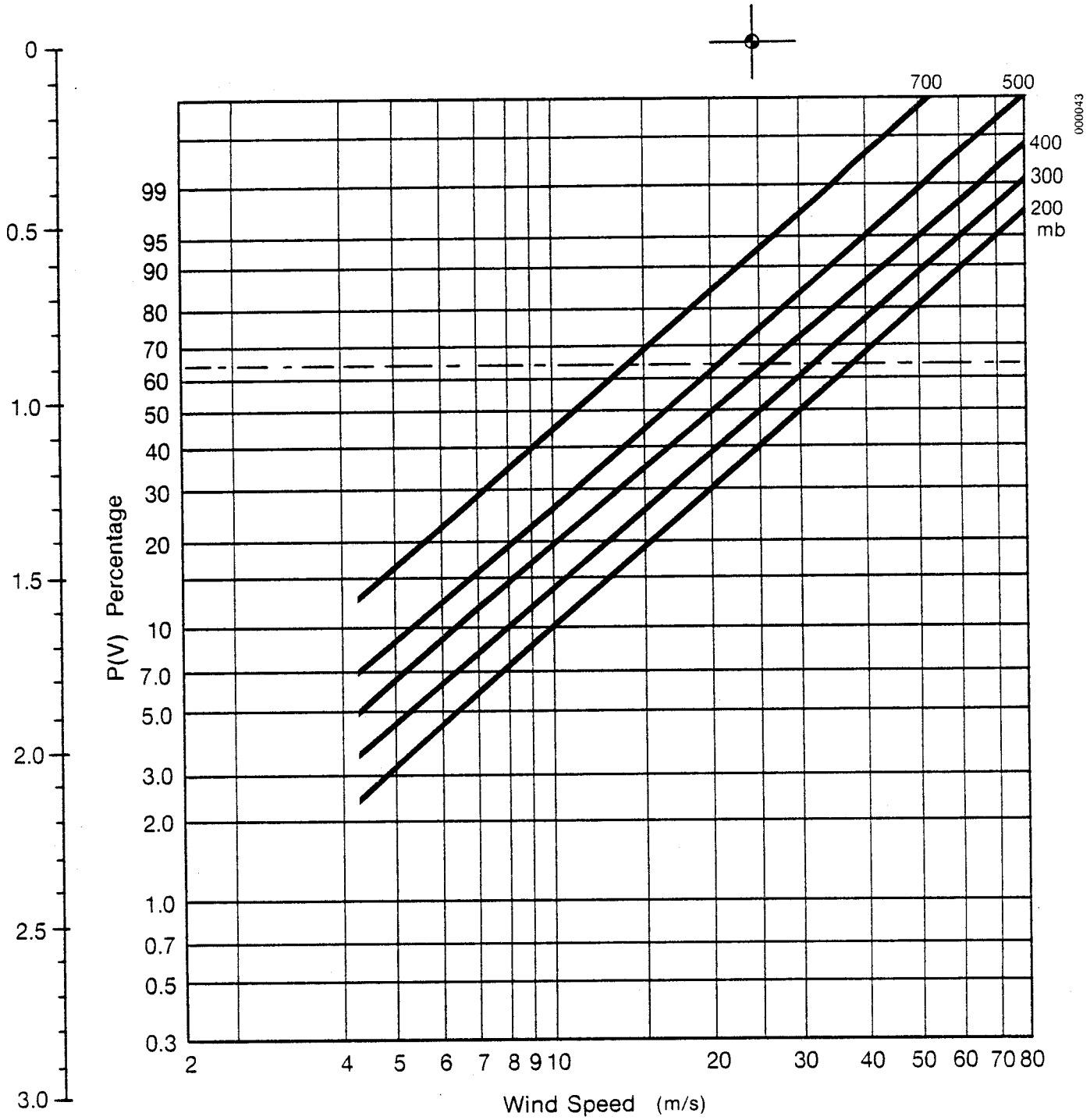

Figure B-29. Annual Probability Distribution of Velocity: Nashville, TN

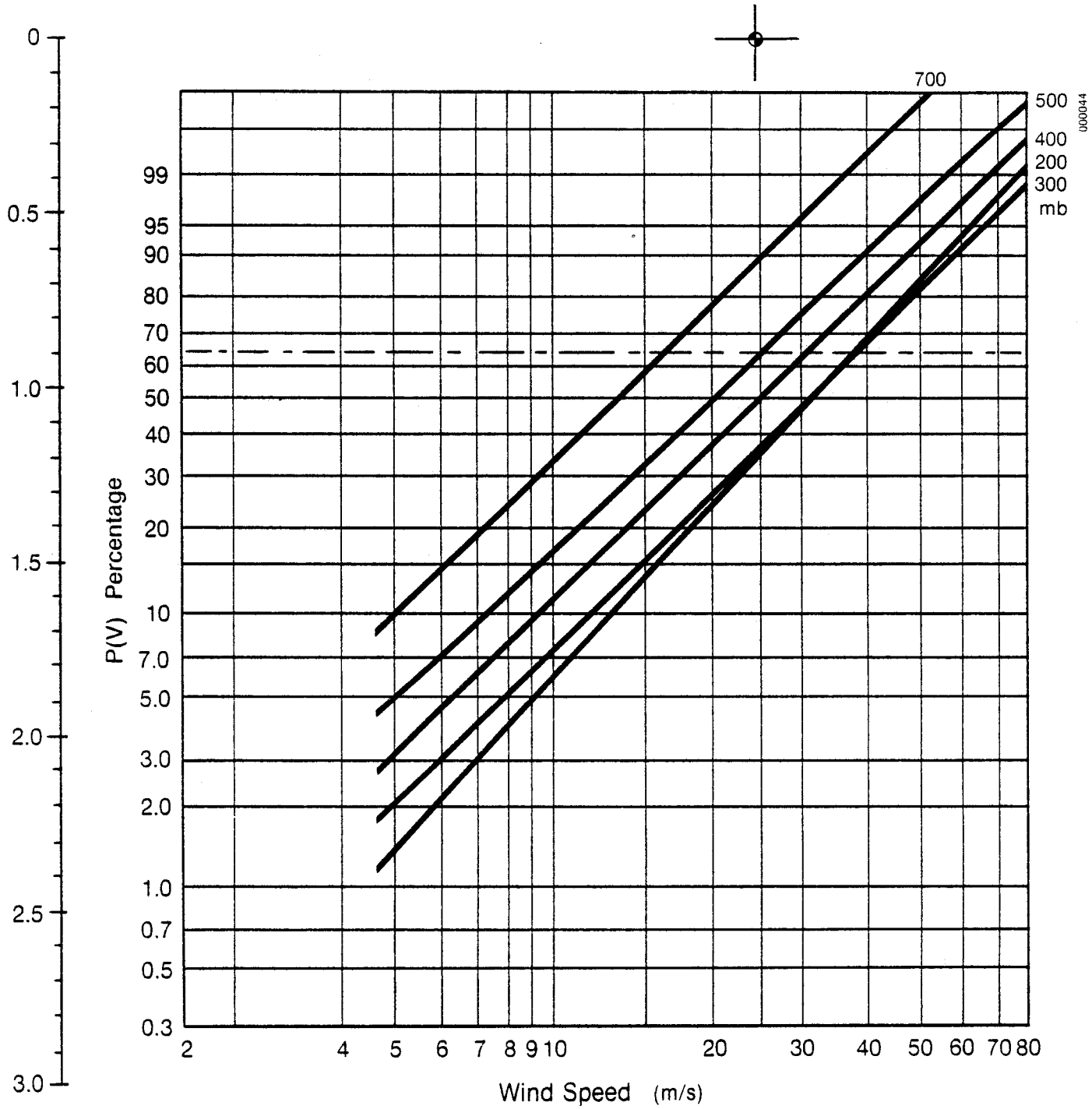

Figure B-30. Annual Probability Distribution of Velocity: New York, NY

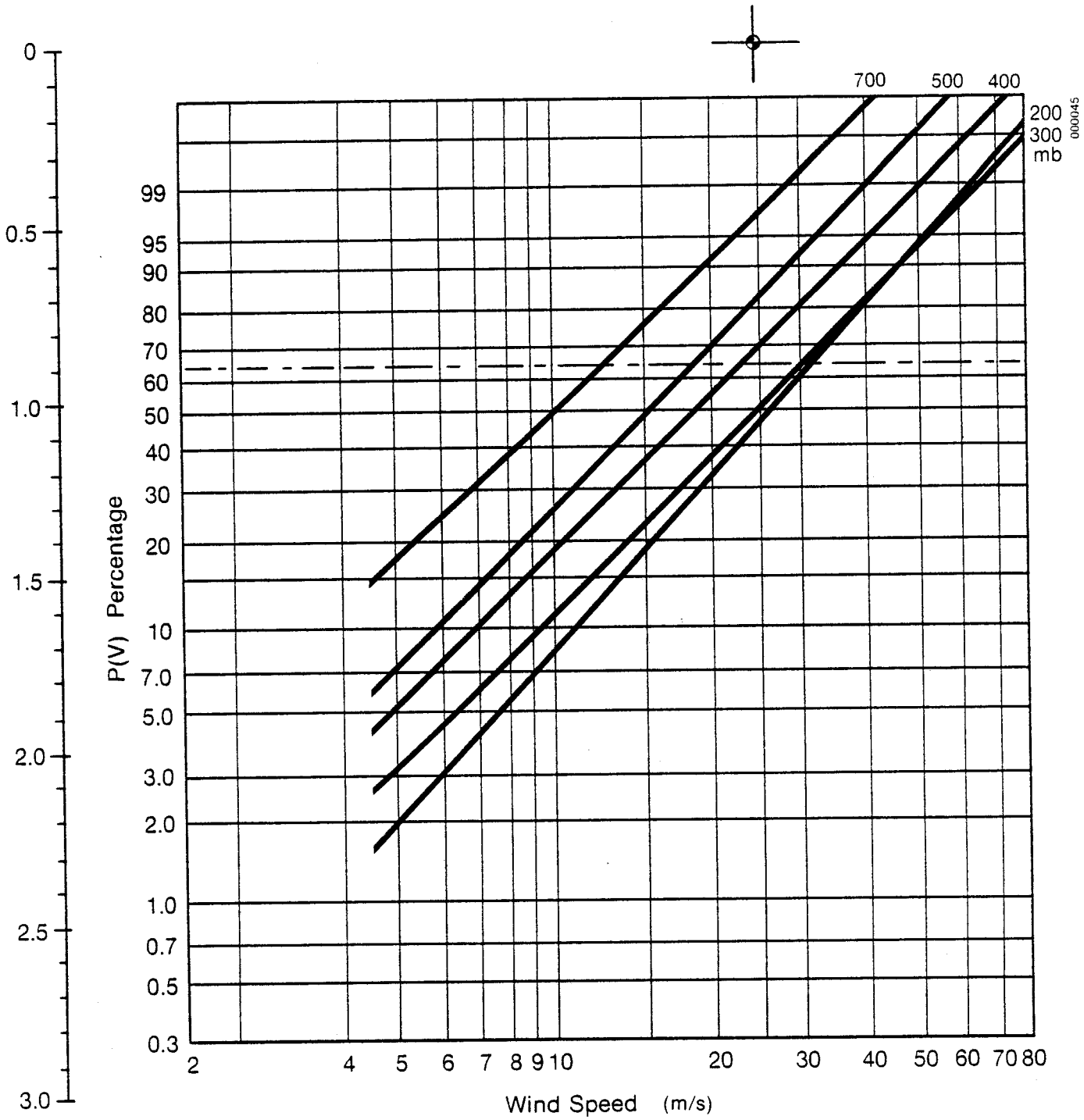

Figure B-31. Annual Probability Distribution of Velocity: North Platte, NE

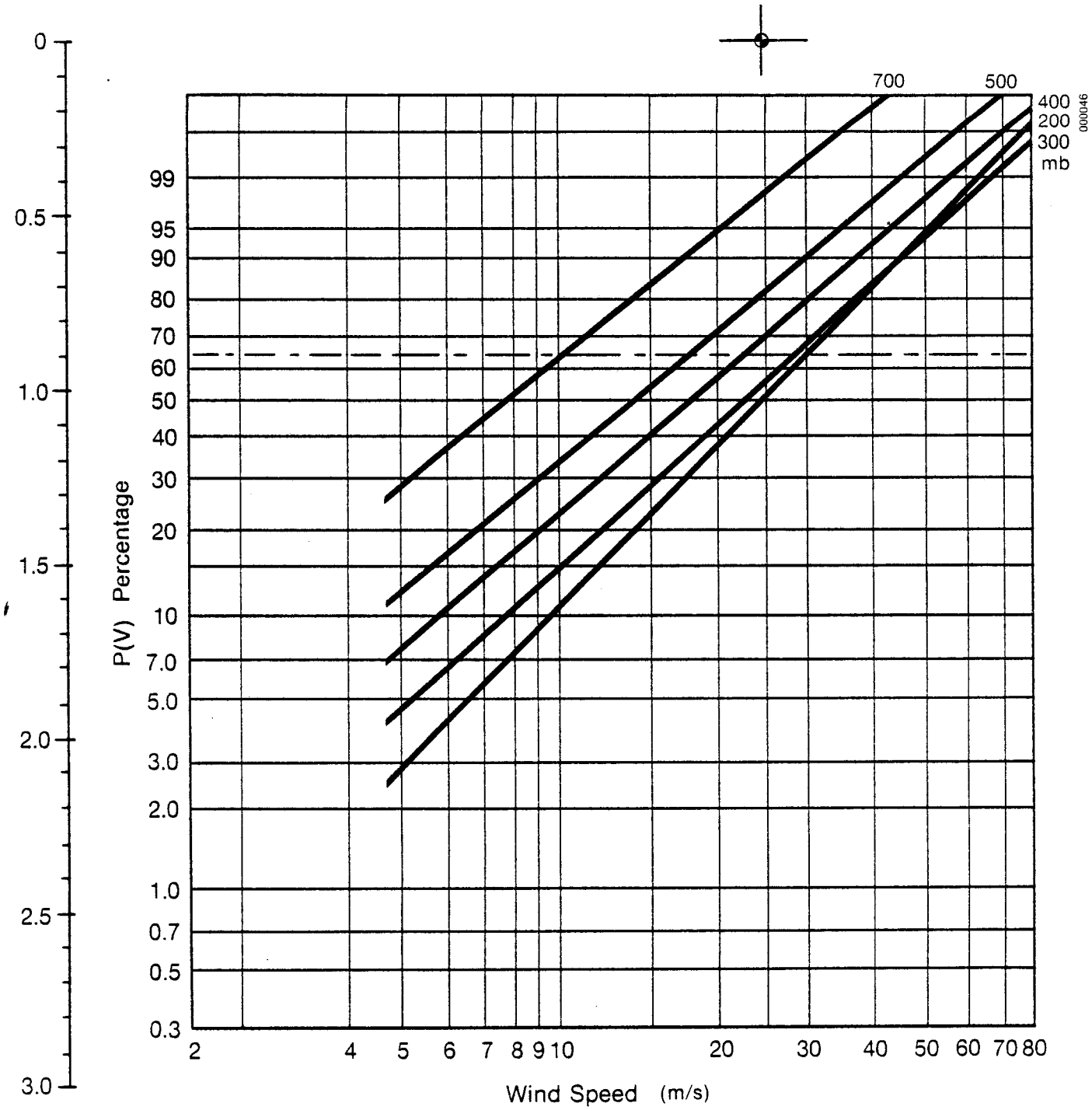

Figure B-32. Annual Probability Distribution of Velocity: Oakland, CA

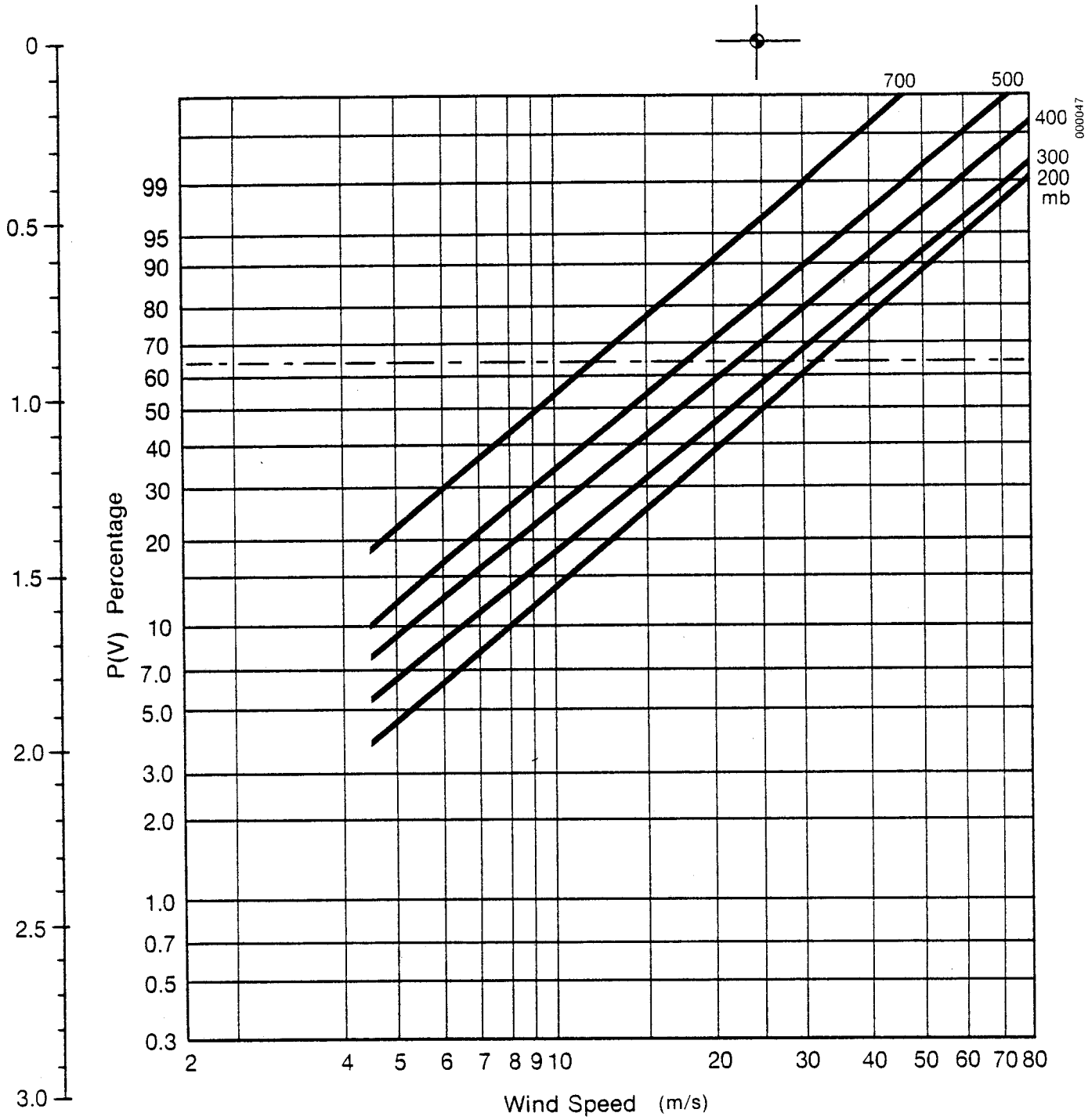

Figure B-33. Annual Probability Distribution of Velocity: Oklahoma City, OK

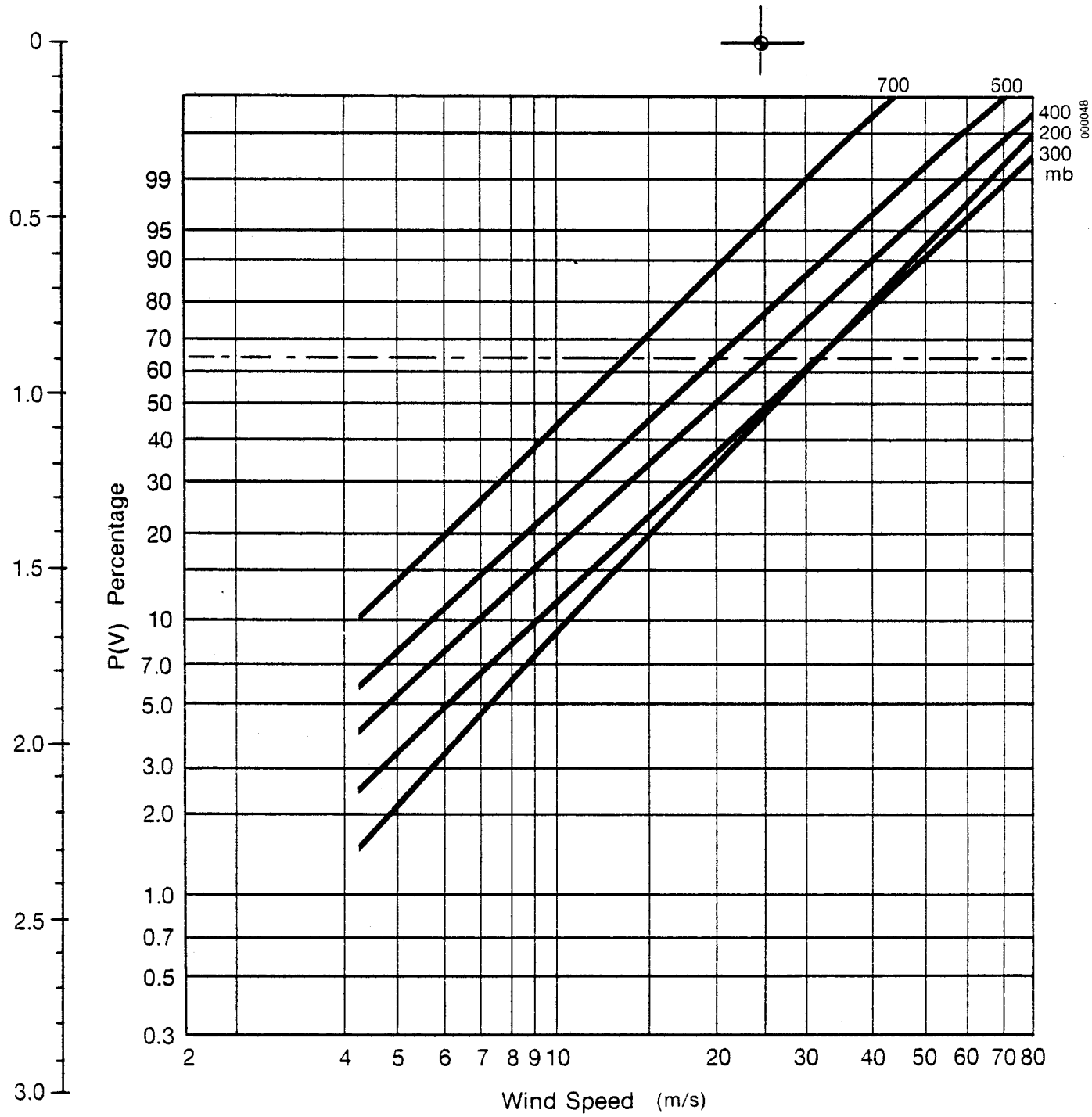

Figure B-34. Annual Probability Distribution of Velocity: Omaha, NB

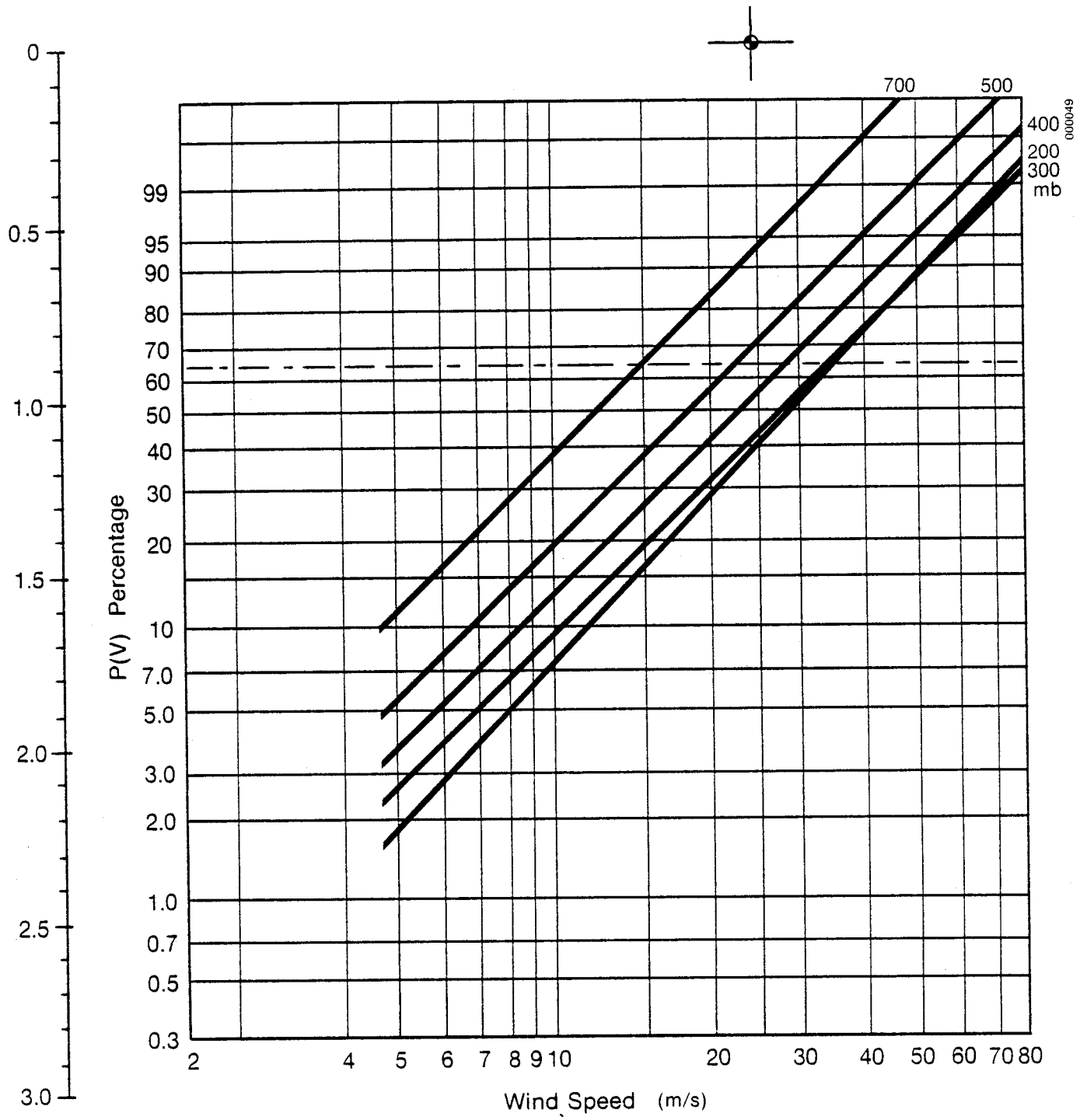

Figure B-35. Annual Probability Distribution of Velocity: Peoria, IL

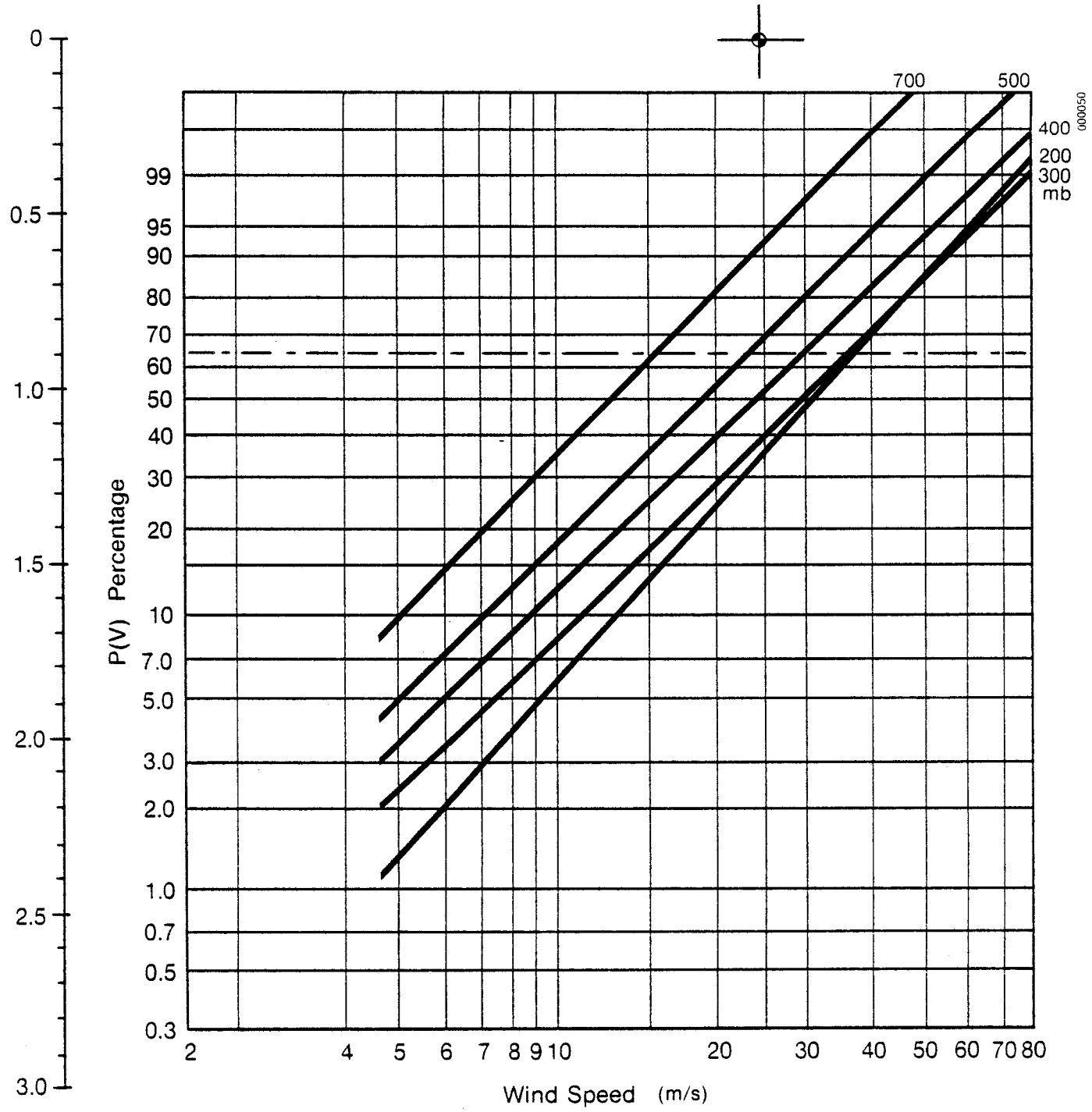

Figure B-36. Annual Probability Distribution of Velocity: Pittsburgh, PA

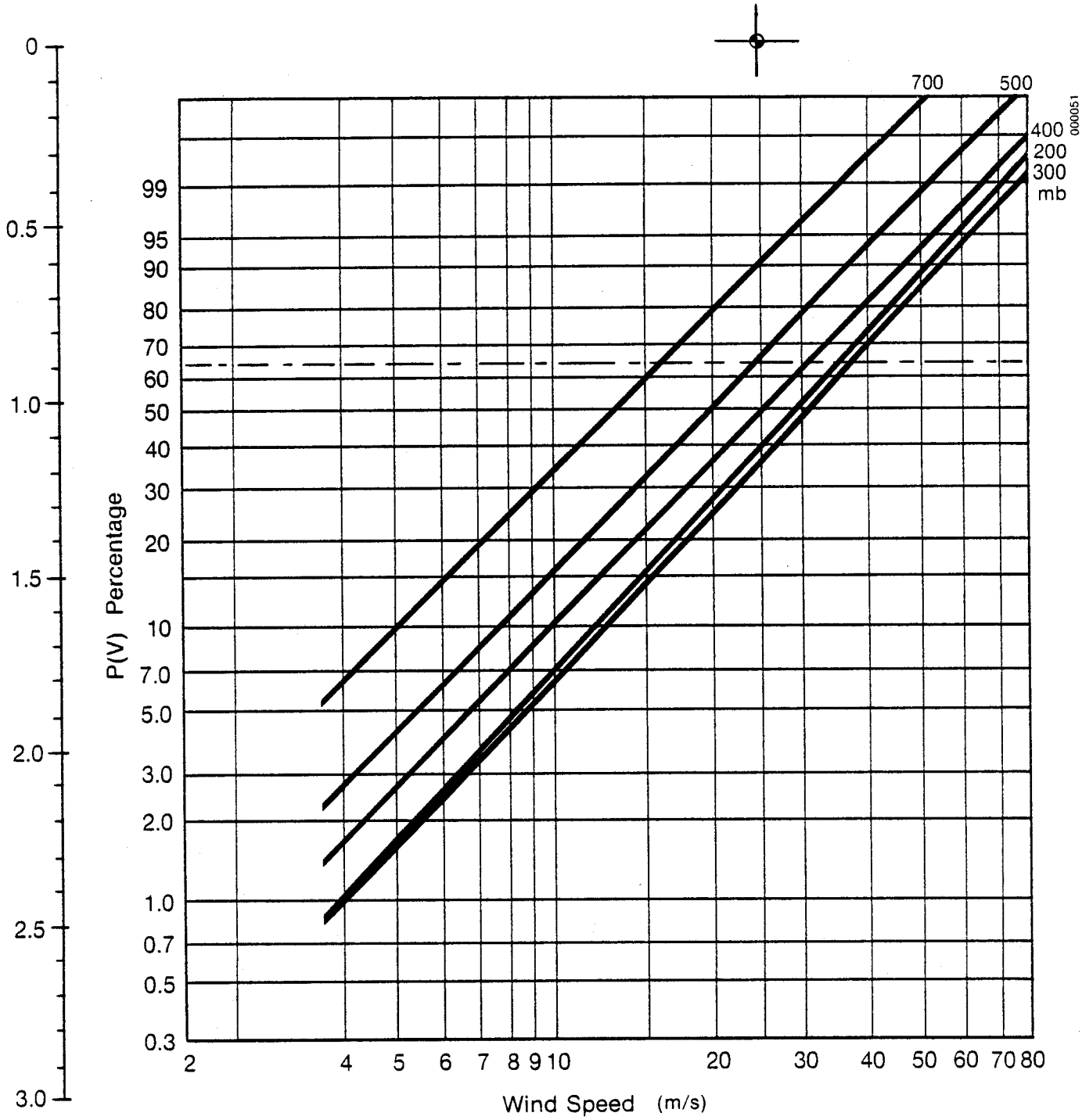

Figure B-37. Annual Probability Distribution of Velocity: Portland, ME

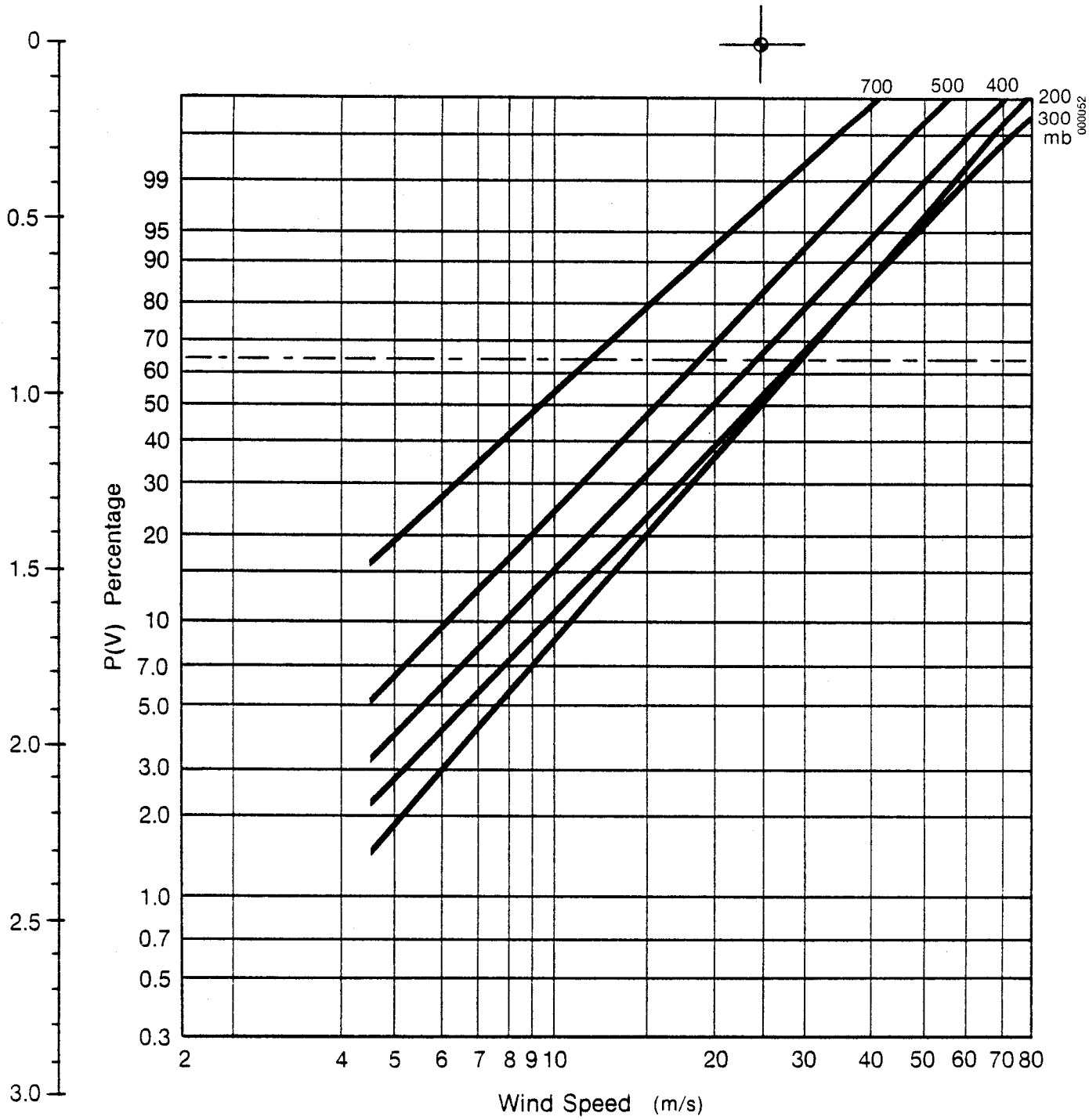

Figure B-38. Annual Probability Distribution of Velocity: Rapid City, SD

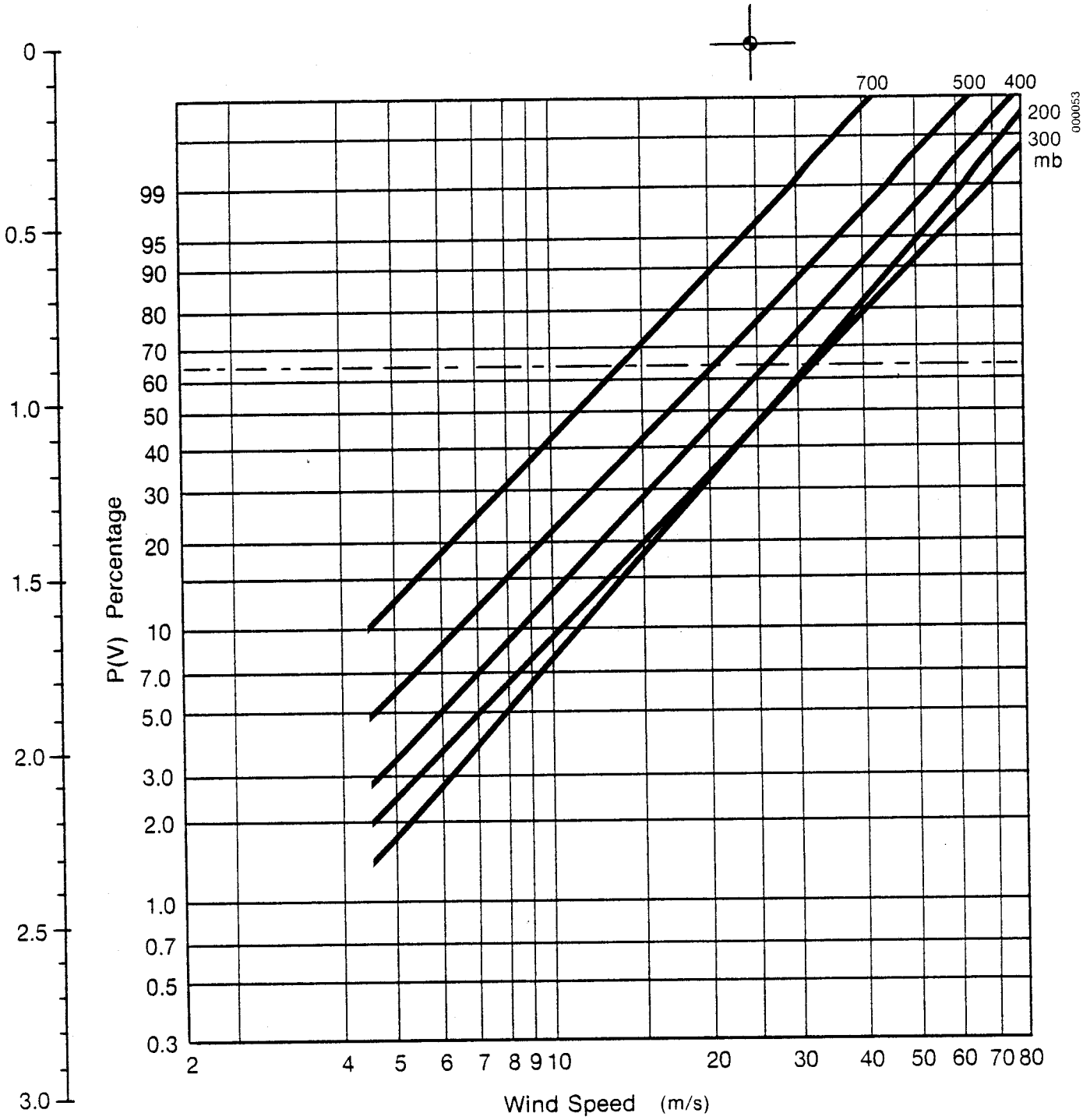

Figure B-39. Annual Probability Distribution of Velocity: St. Cloud, MN

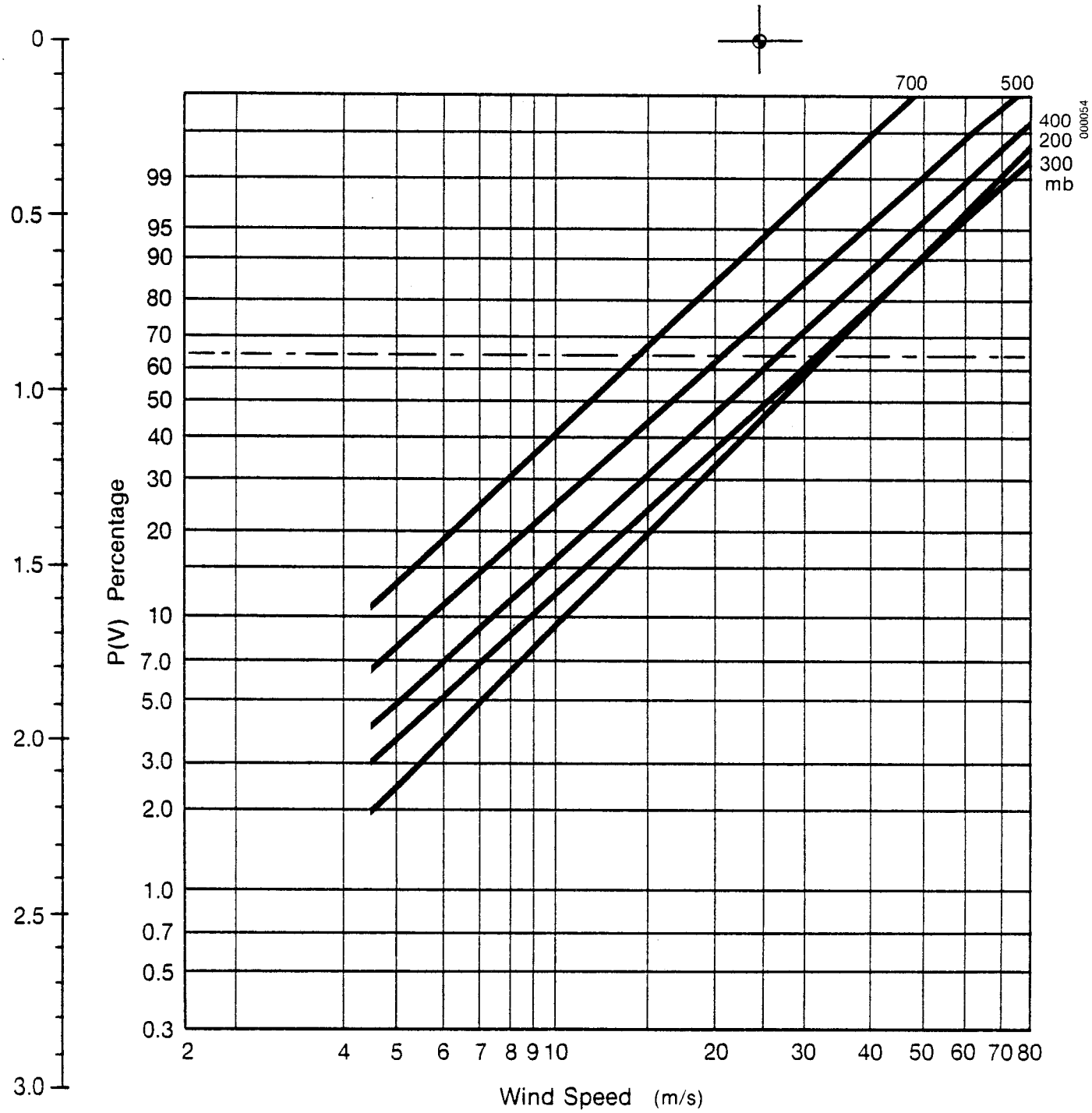

Figure B-40. Annual Probability Distribution of Velocity: Salem, IL

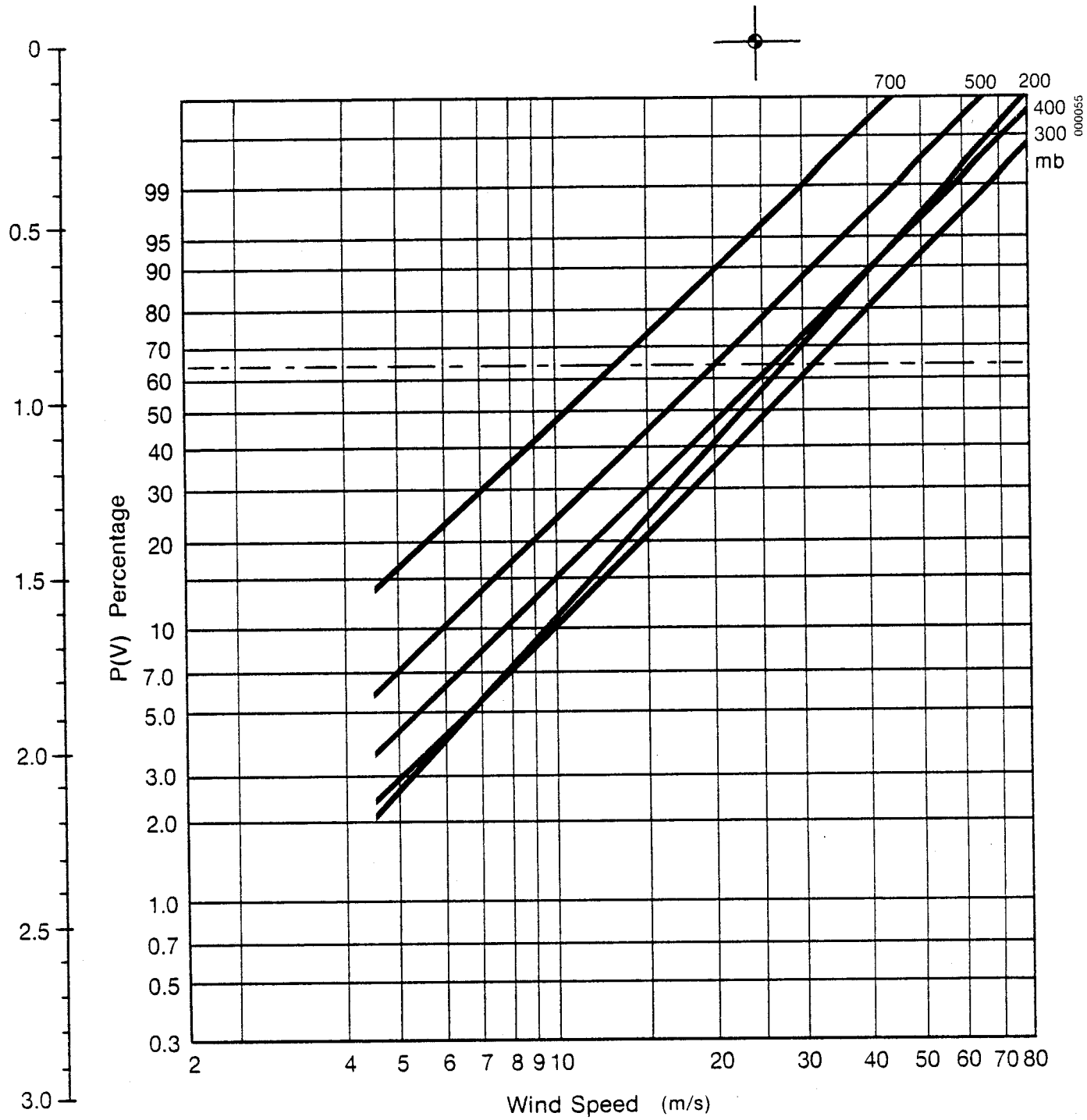

Figure B-41. Annual Probability Distribution of Velocity: Salem, OR

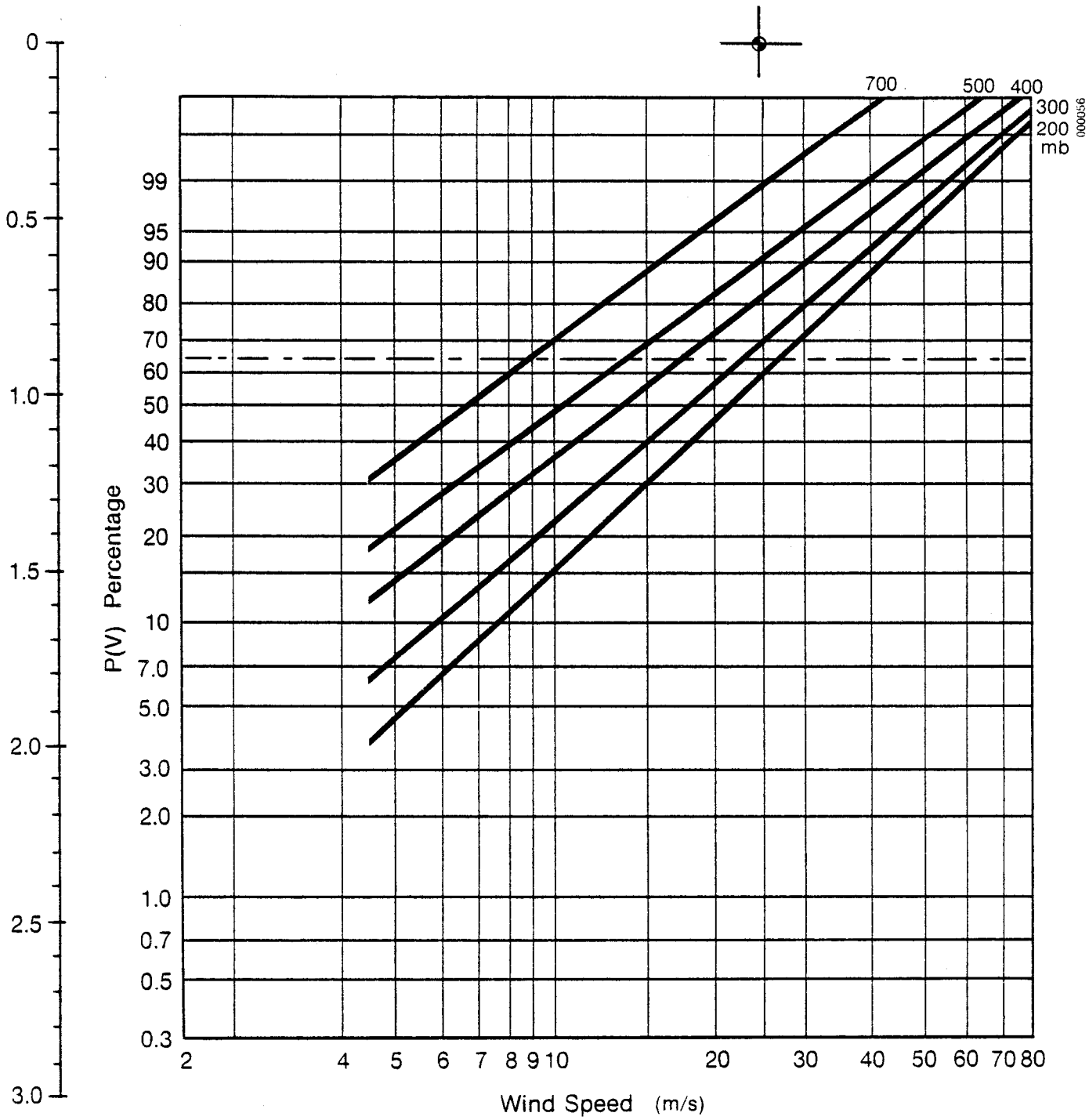

Figure B-42. Annual Probability Distribution of Velocity: San Nichols Island, CA

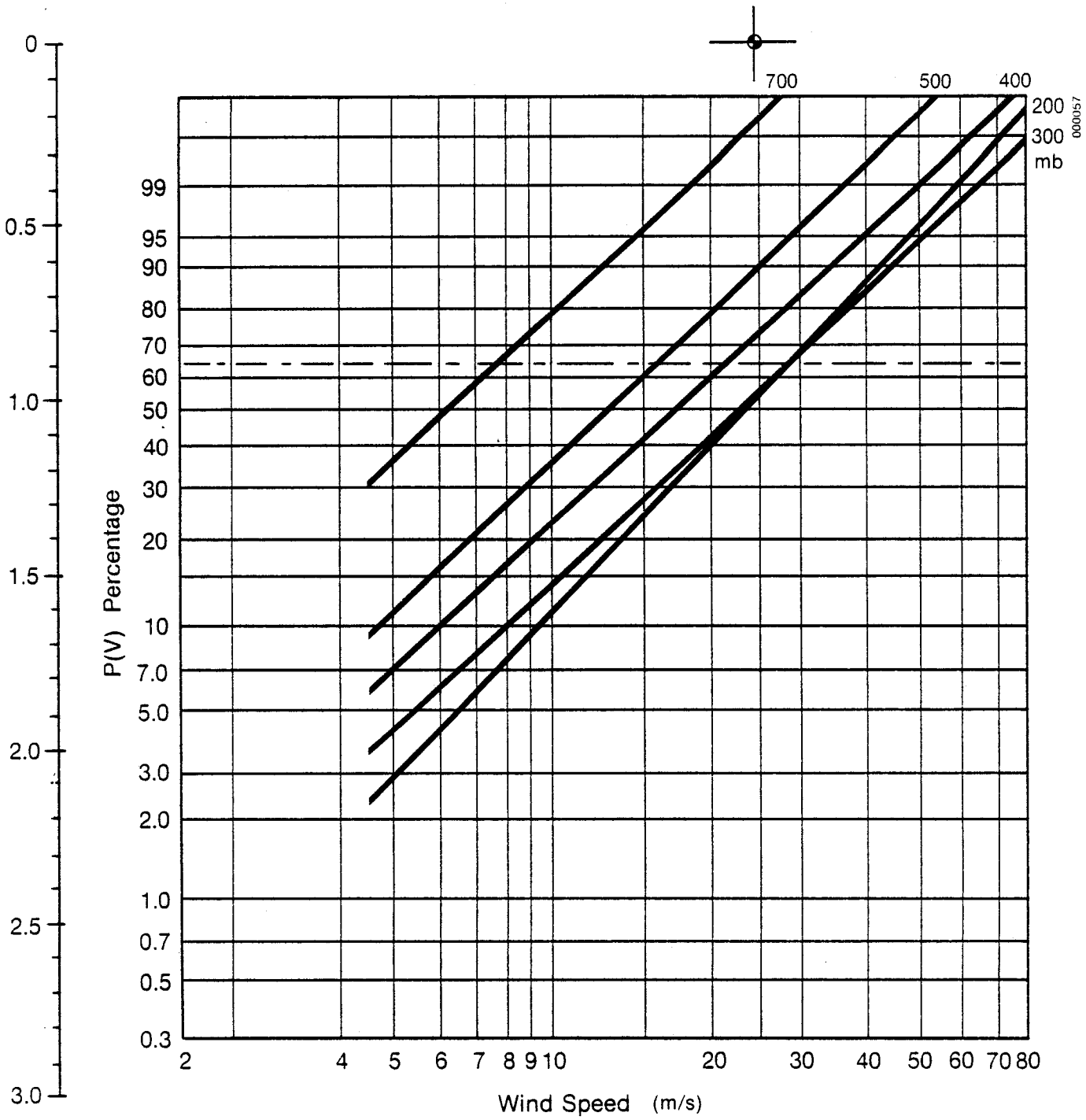

Figure B-43. Annual Probability Distribution of Velocity: Salt Lake City, UT

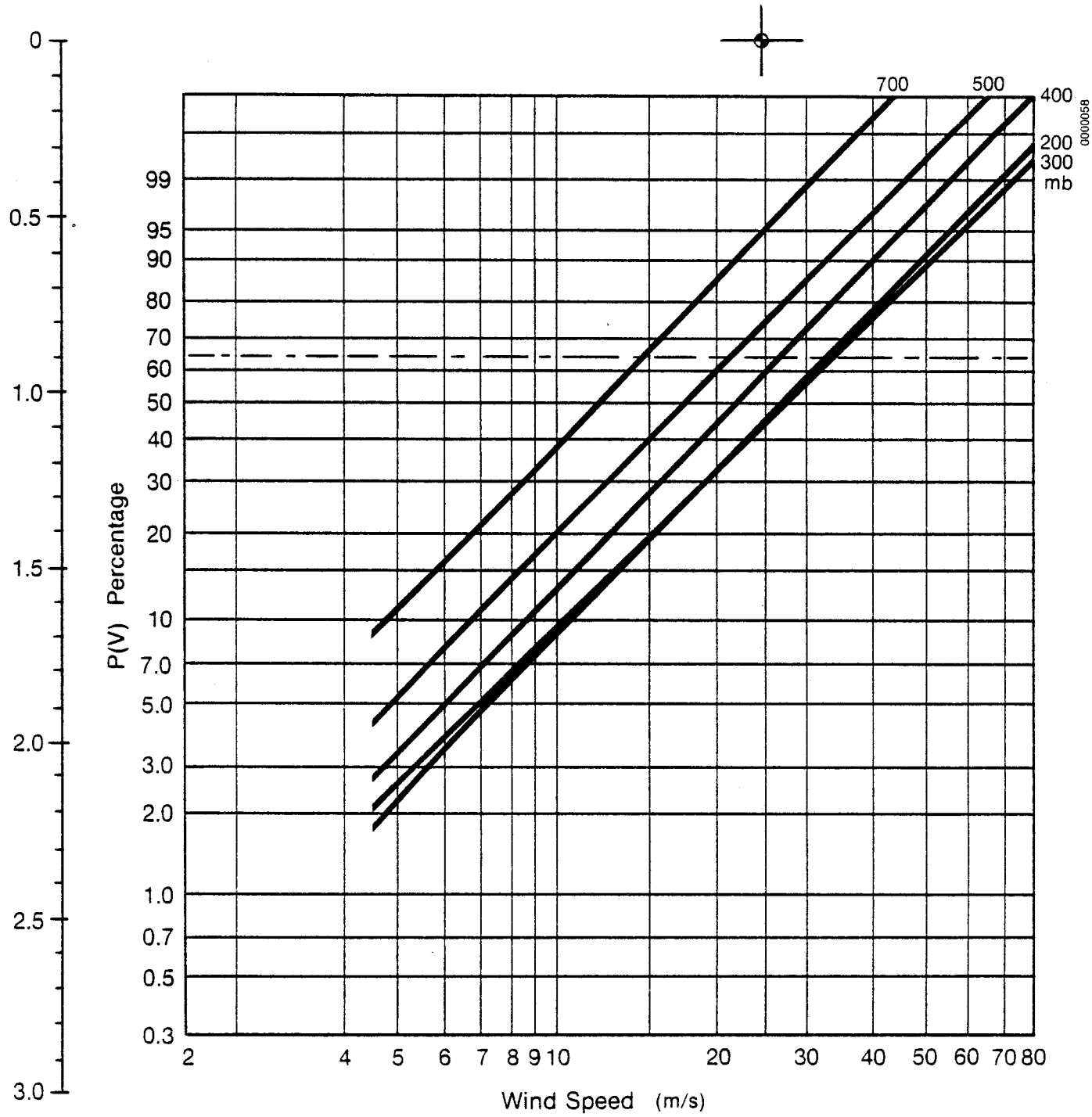

Figure B-44. Annual Probability Distribution of Velocity: Sault Ste. Marie, MI

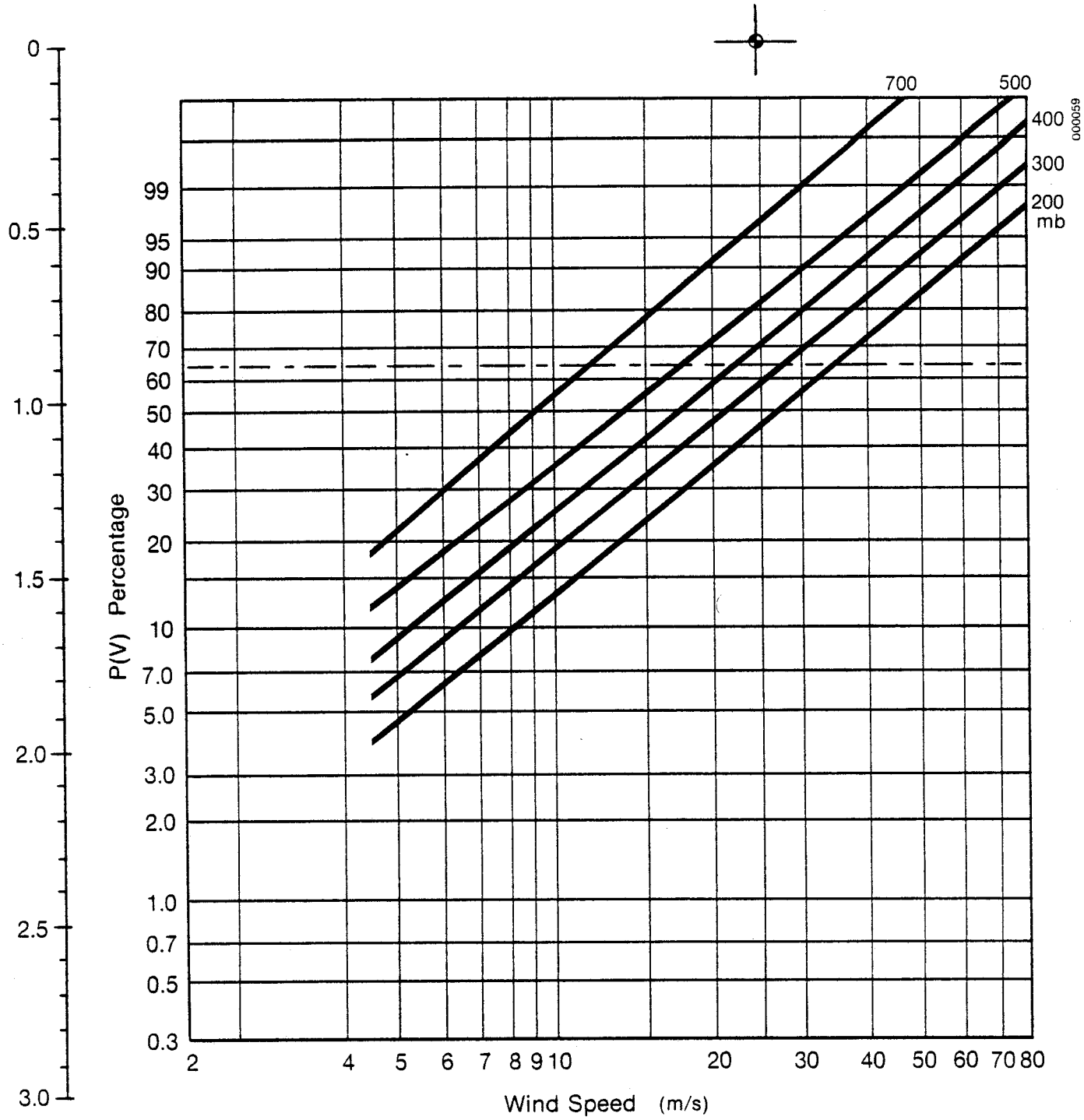

Figure B-45. Annual Probability Distribution of Velocity: Shreveport, LA

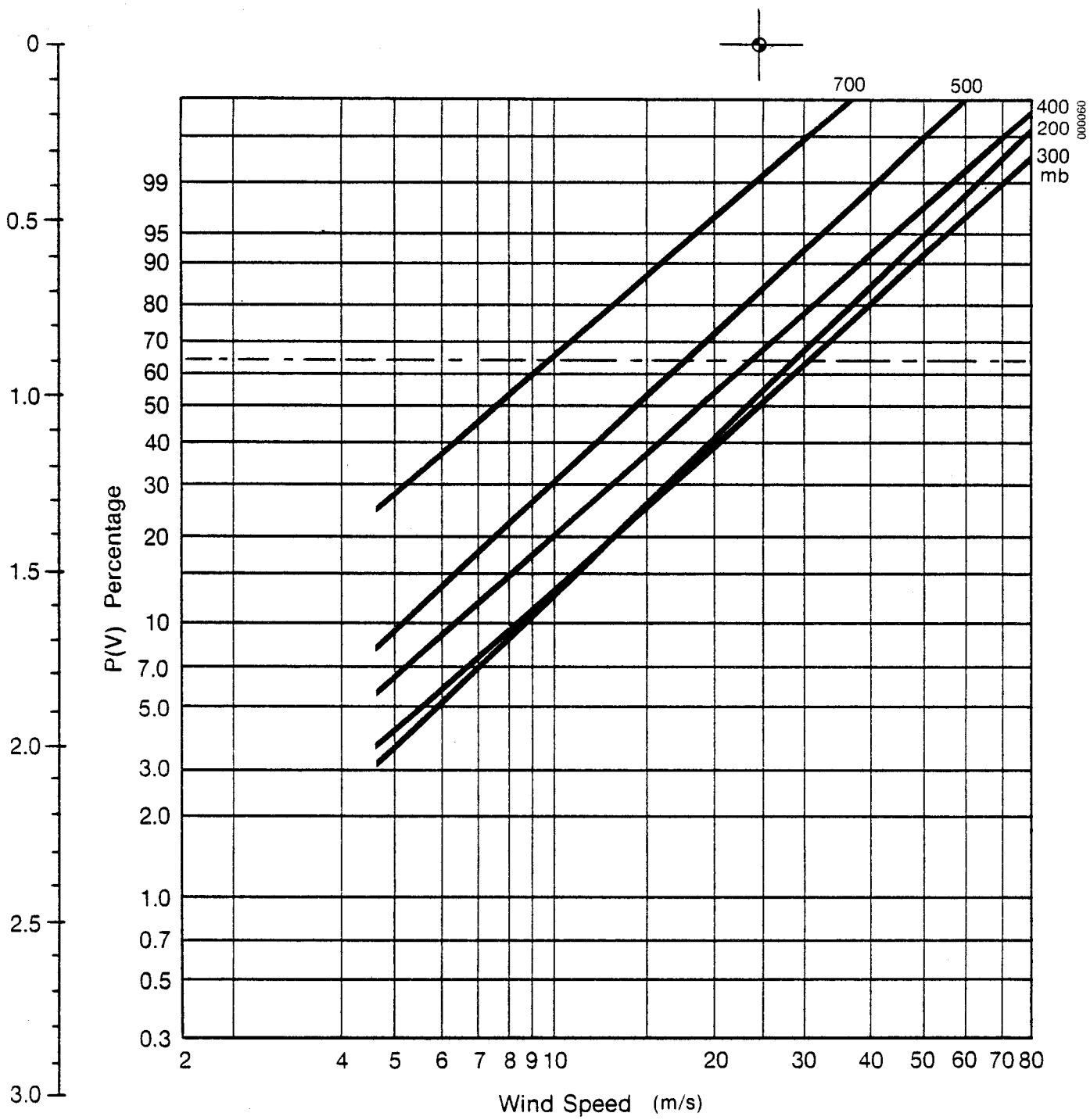

Figure B-46. Annual Probability Distribution of Velocity: Spokane, WA

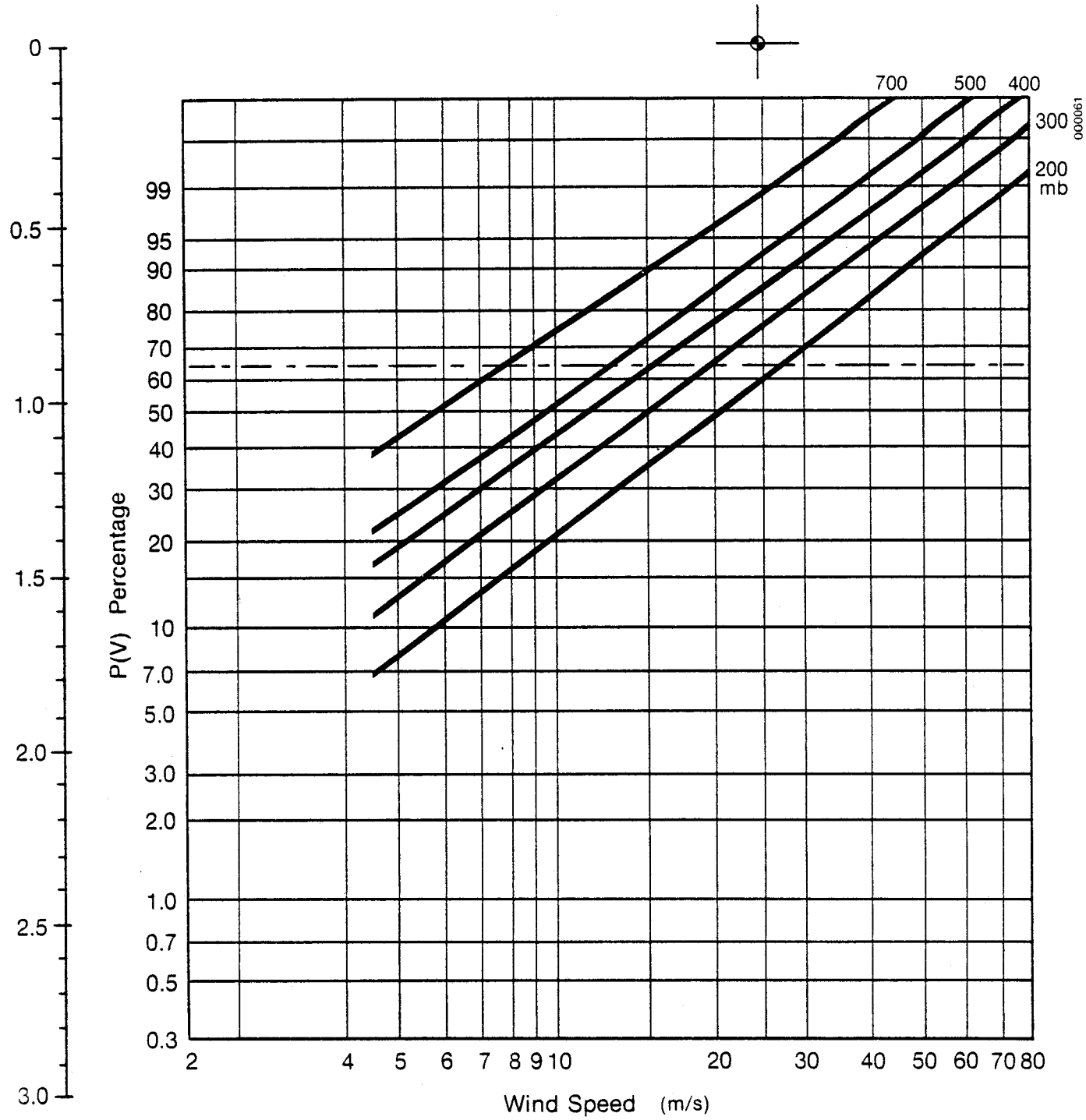

Figure B-47. Annual Probability Distribution of Velocity: Tampa, FL

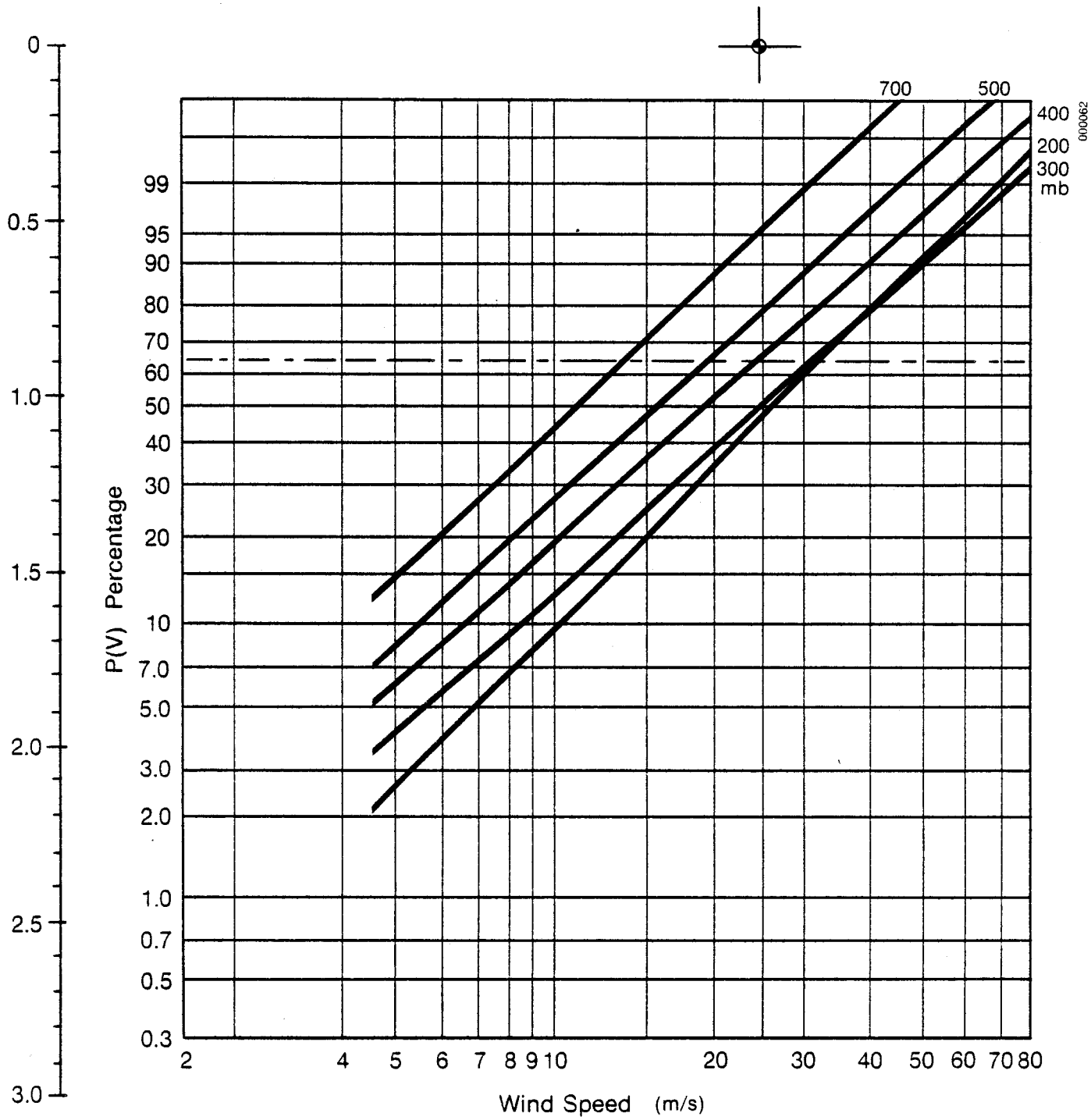

Figure B-48. Annual Probability Distribution of Velocity: Topeka, KS

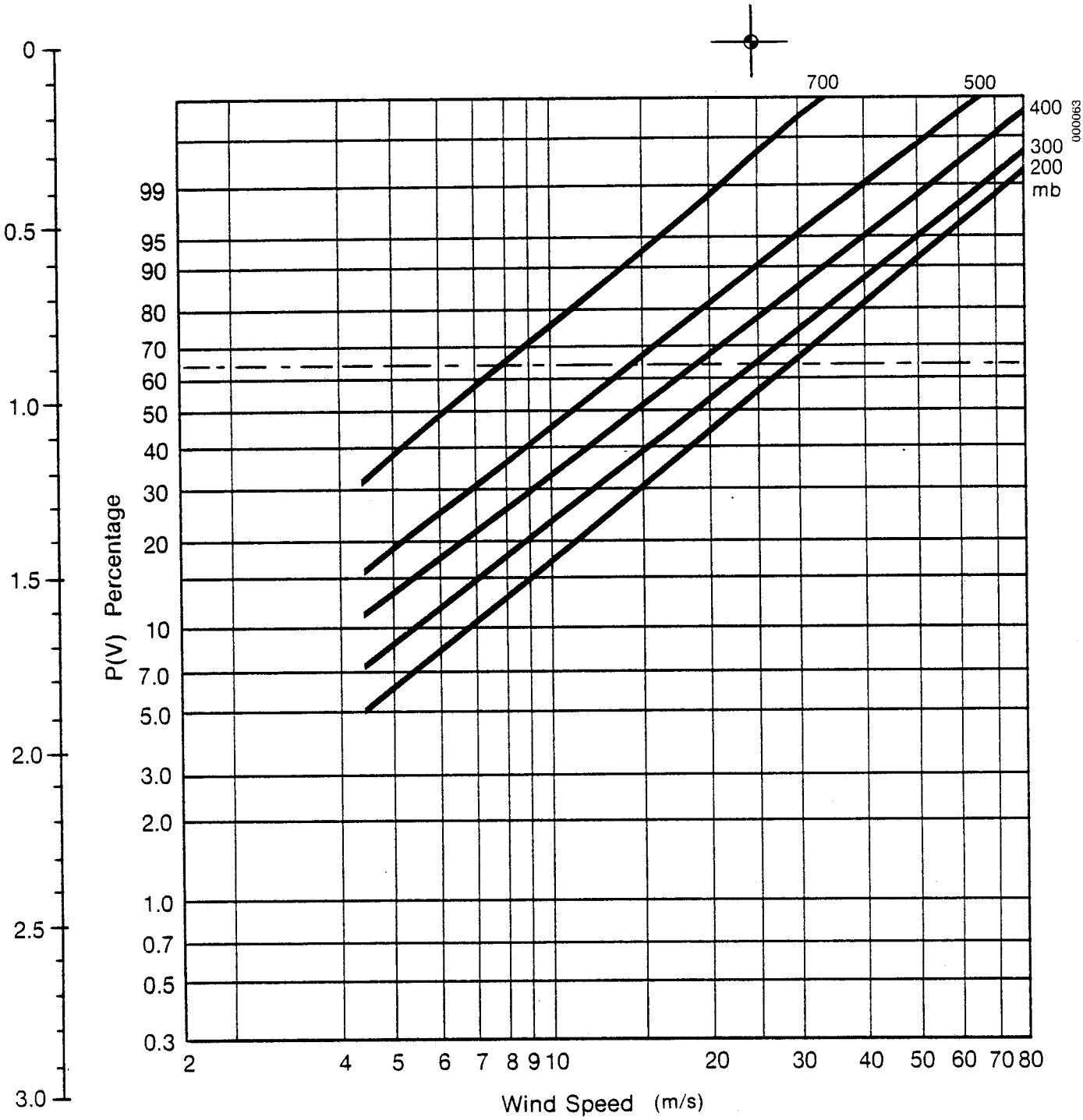

Figure B-49. Annual Probability Distribution of Velocity: Tucson, AZ

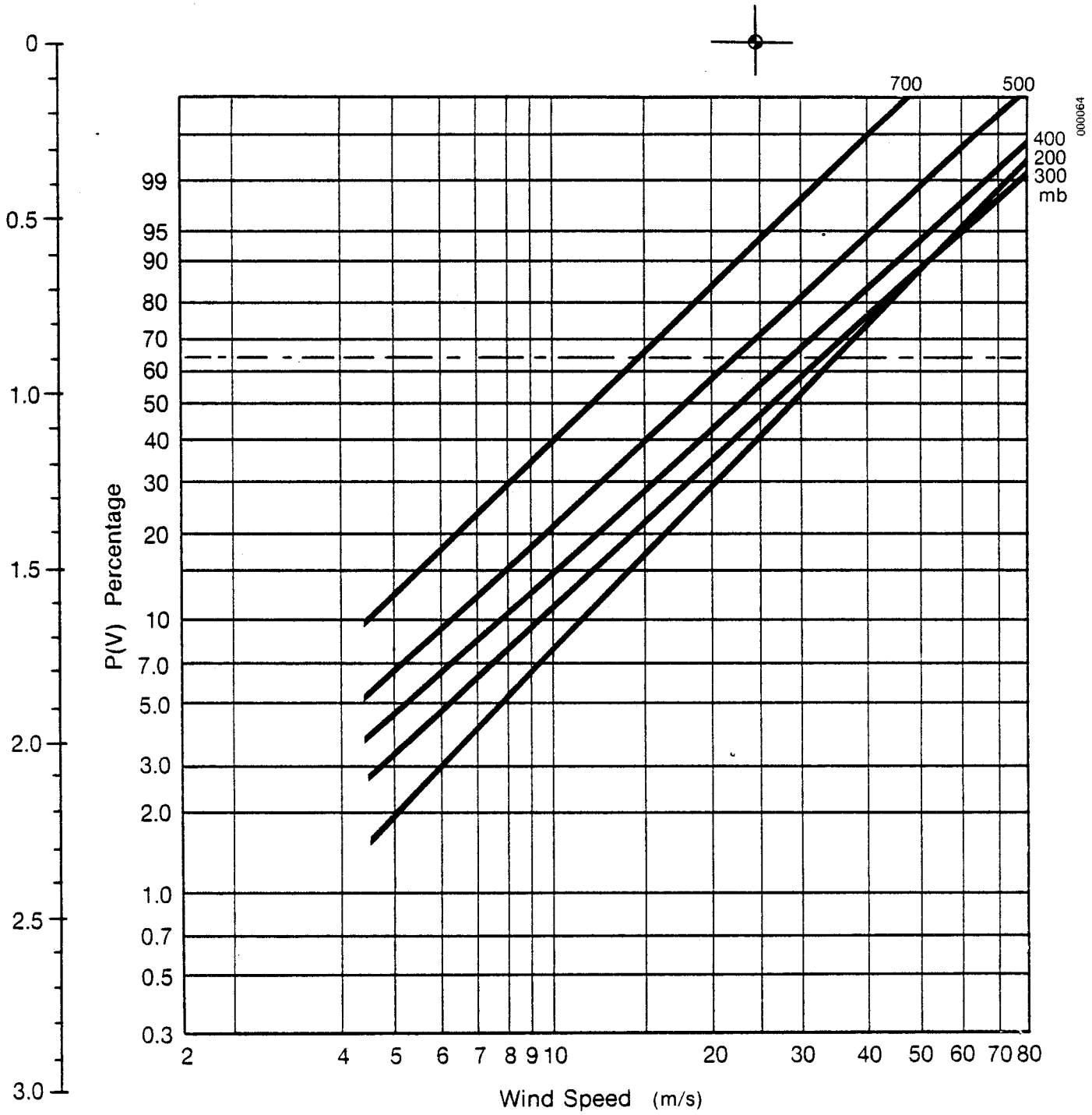

Figure B-50. Annual Probability Distribution of Velocity: Wallops Island, VA

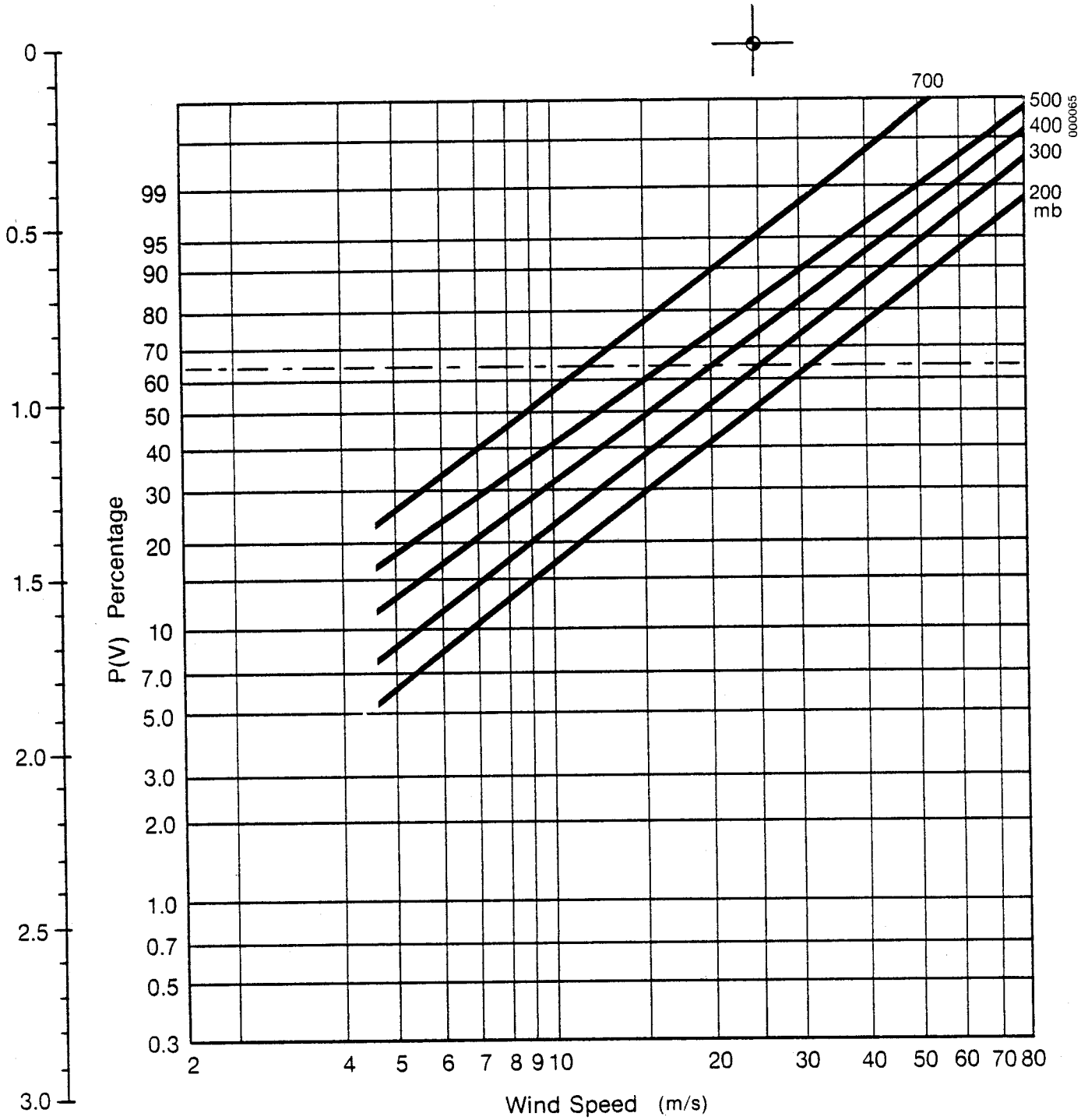

Figure B-51. Annual Probability Distribution of Velocity: Waycross, GA

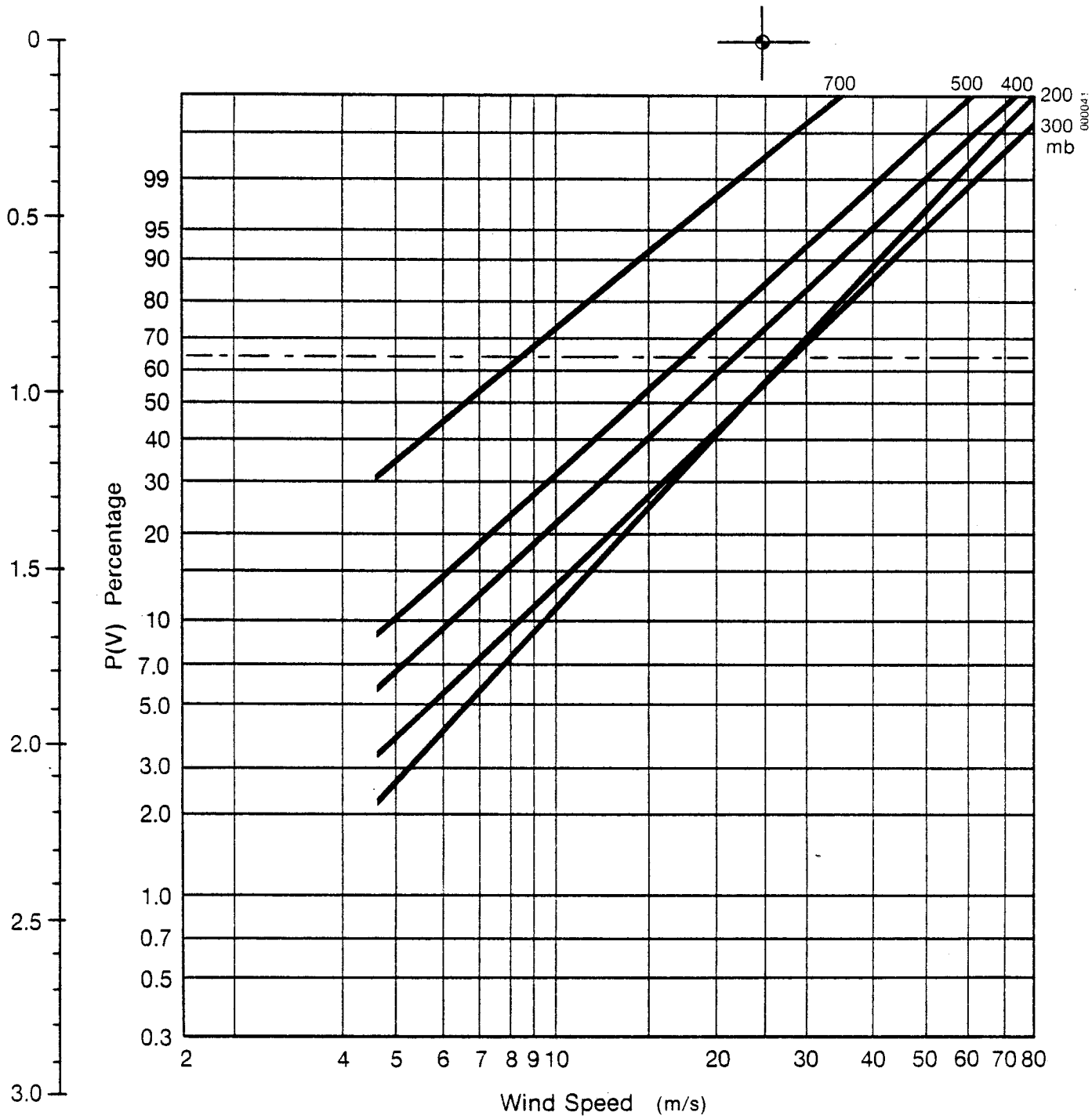

Figure B-52. Annual Probability Distribution of Velocity: Winnemucca, NV

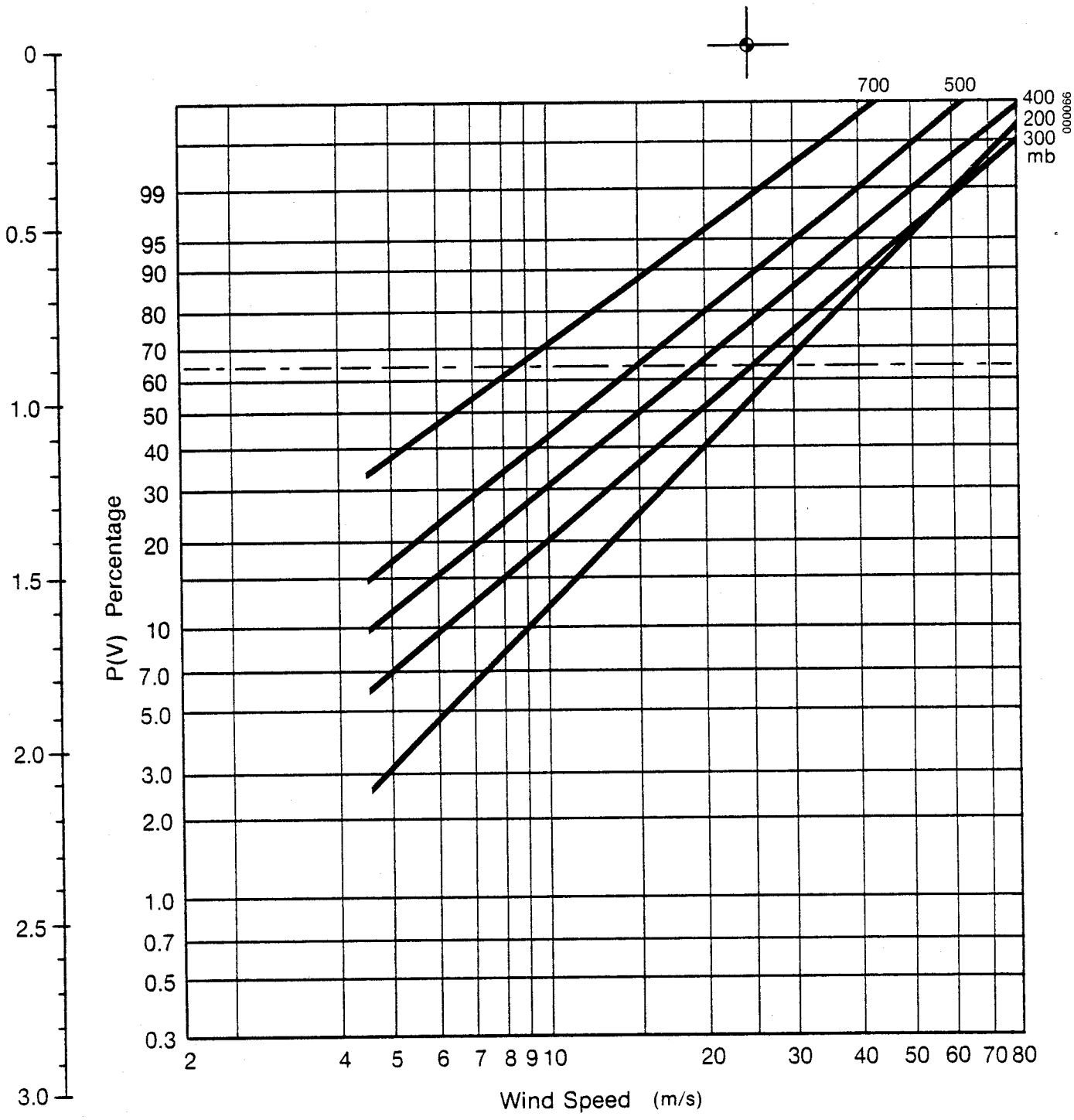

Figure B-53. Annual Probability Distribution of Velocity: Winslow, AZ

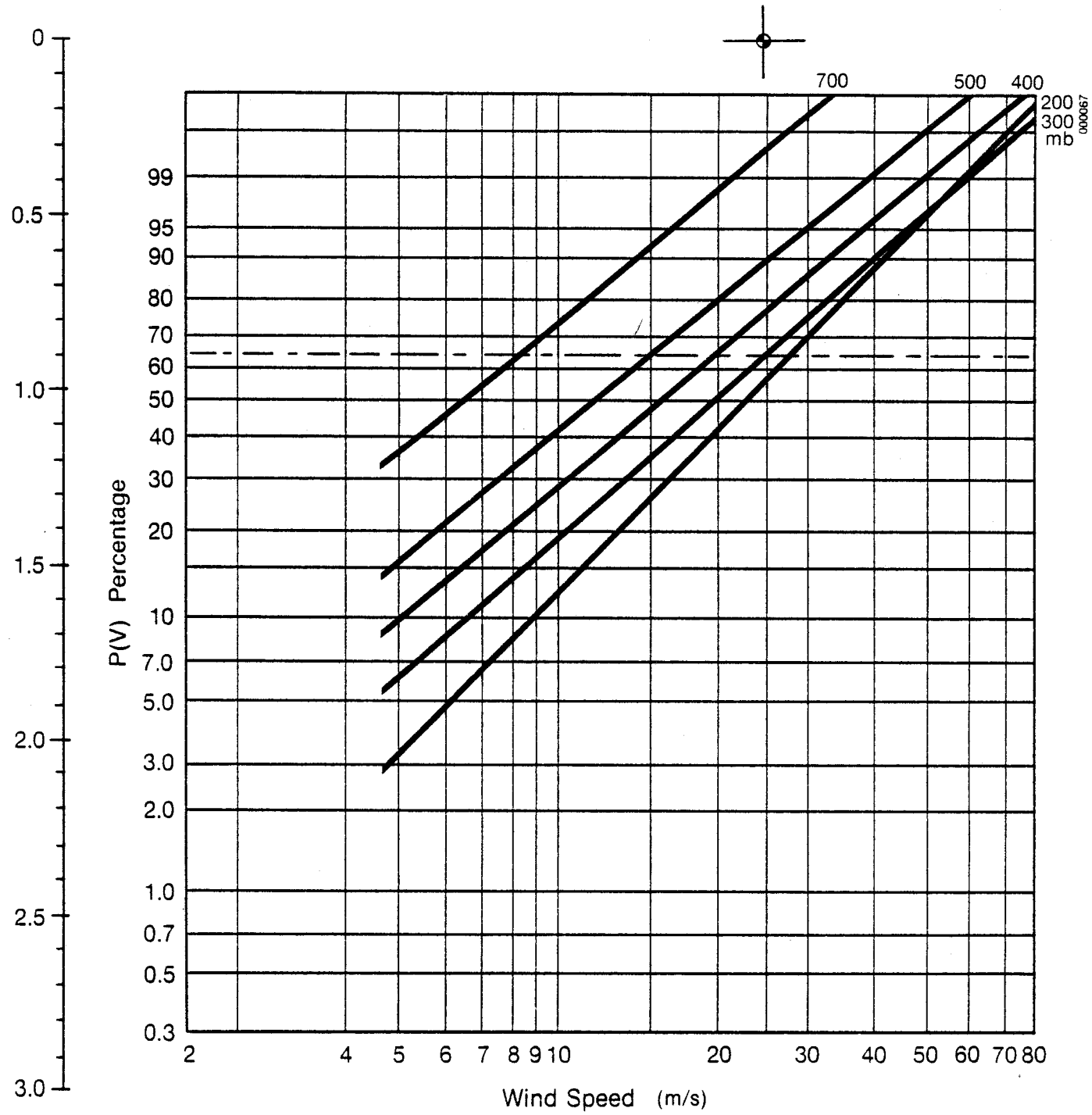

Figure B-54. Annual Probability Distribution of Velocity: Yucca Flats, NV

APPENDIX C

ANNUAL CALM-PERIOD CHARTS

SERI

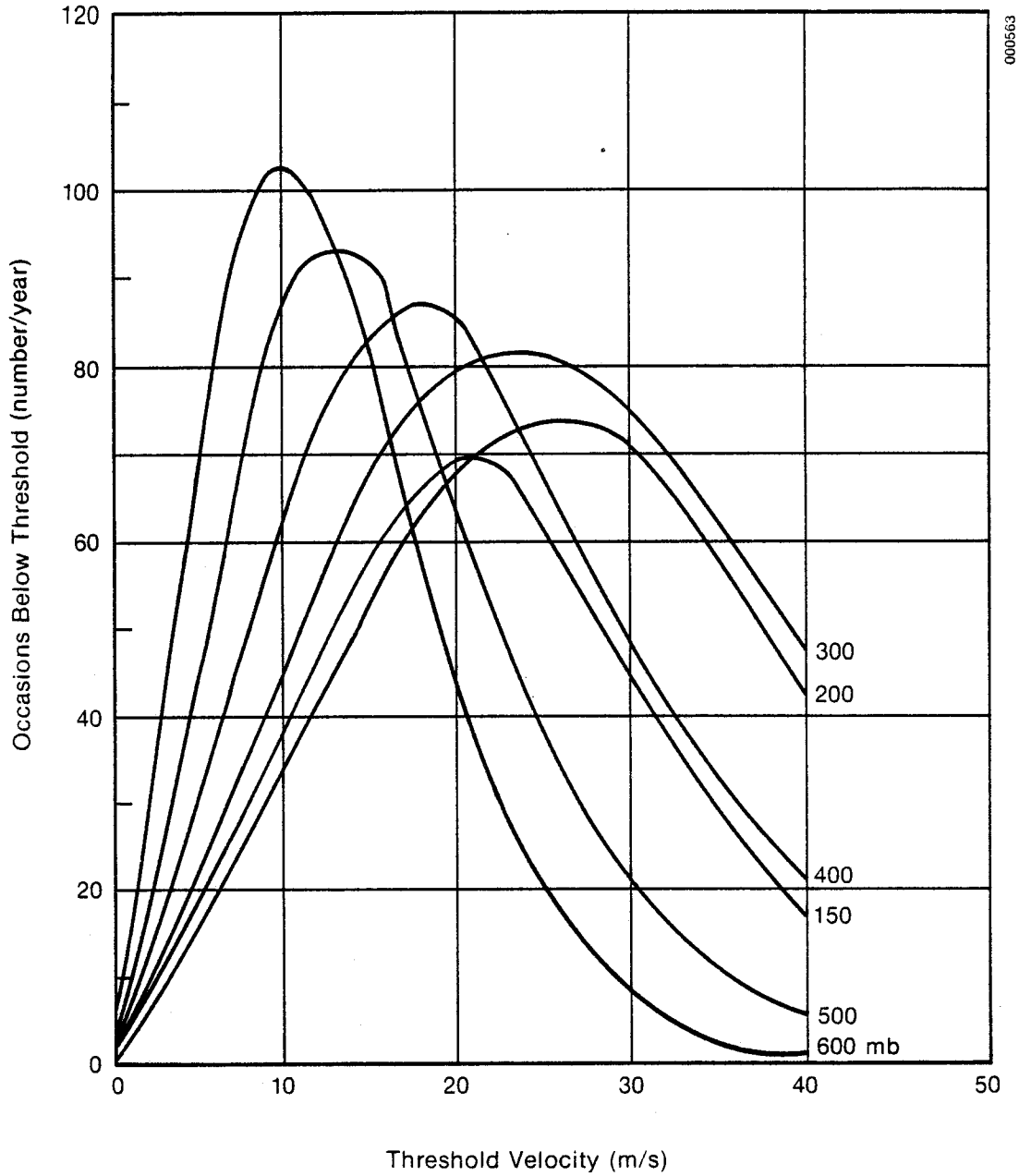

Figure C-1. Annual Calm-Period Analysis: Denver, CO

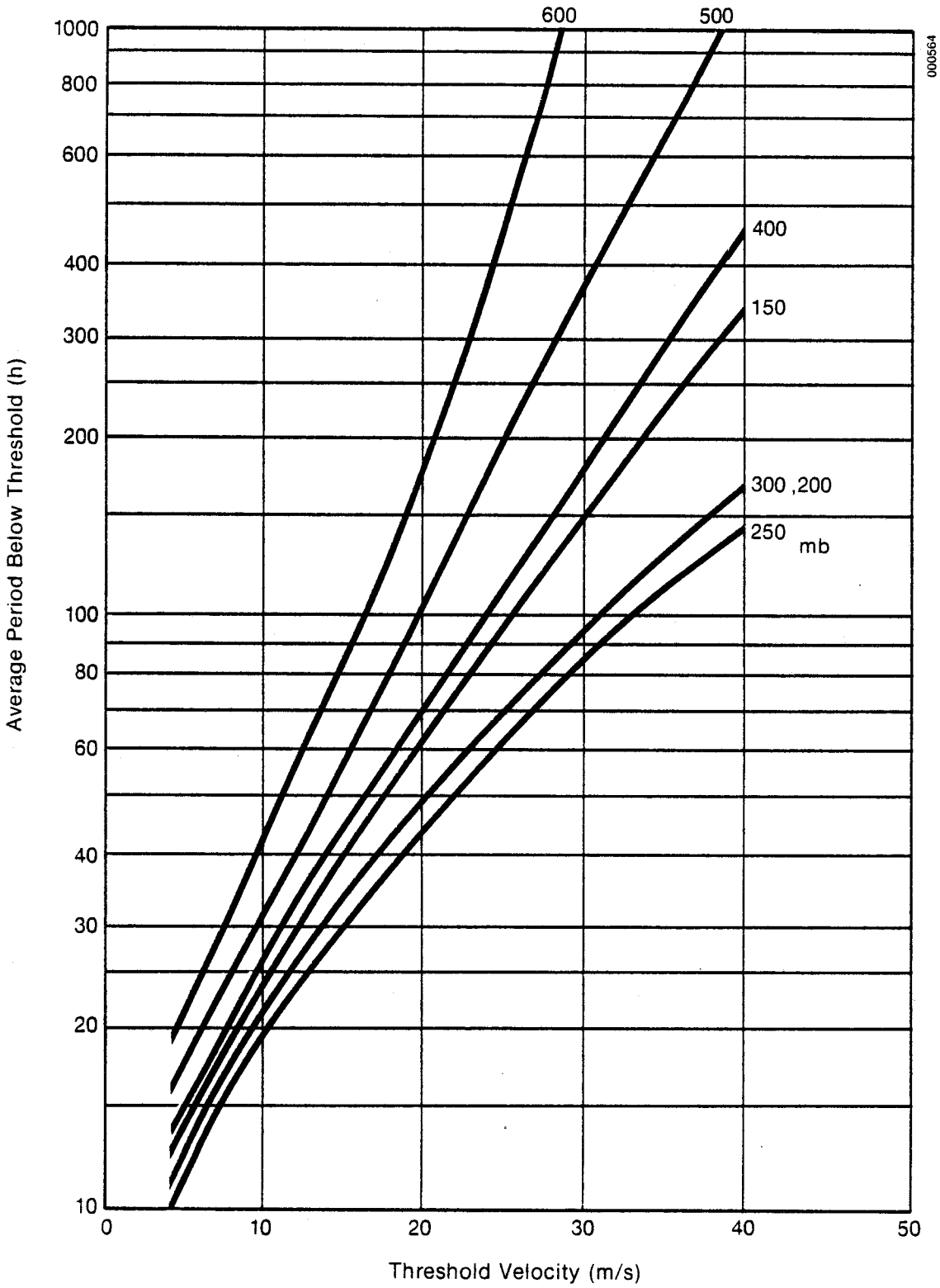

Figure C-2. Annual Calm-Period Analysis: Denver, CO

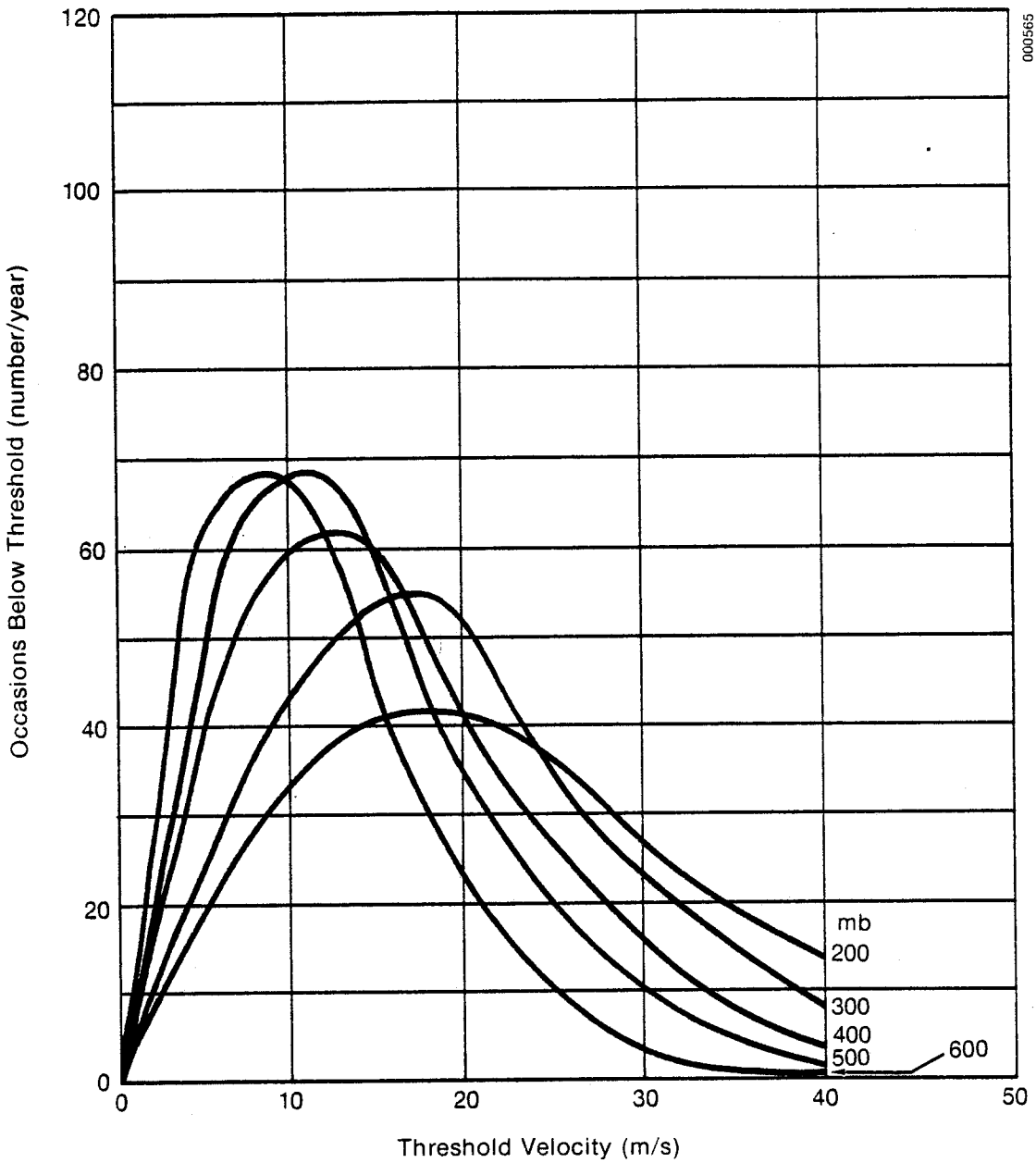

Figure C-3. Annual Calm-Period Analysis: Guadalupe Island, Mexico

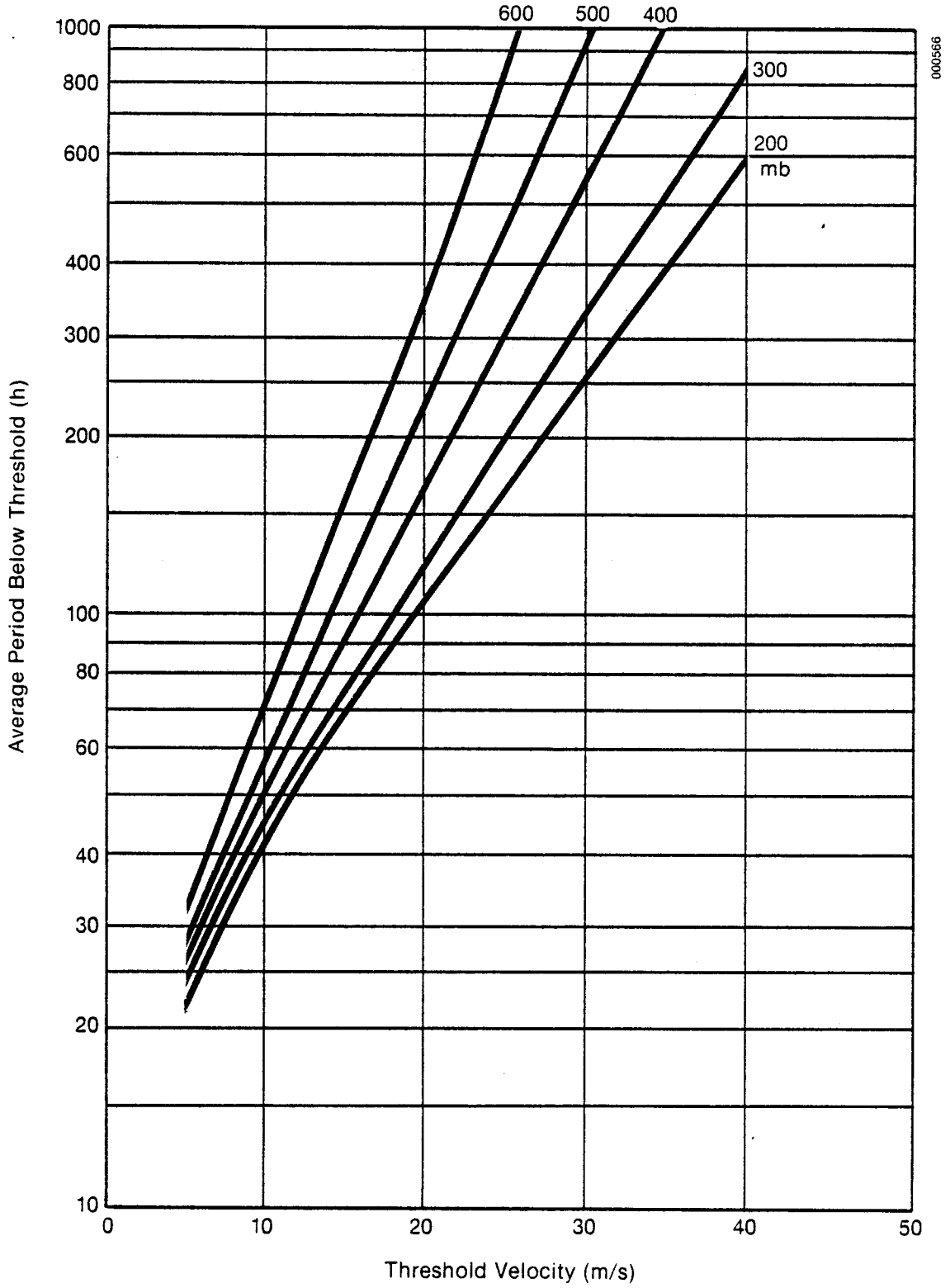

Figure C-4. Annual Calm-Period Analysis: Guadalupe Island, Mexico

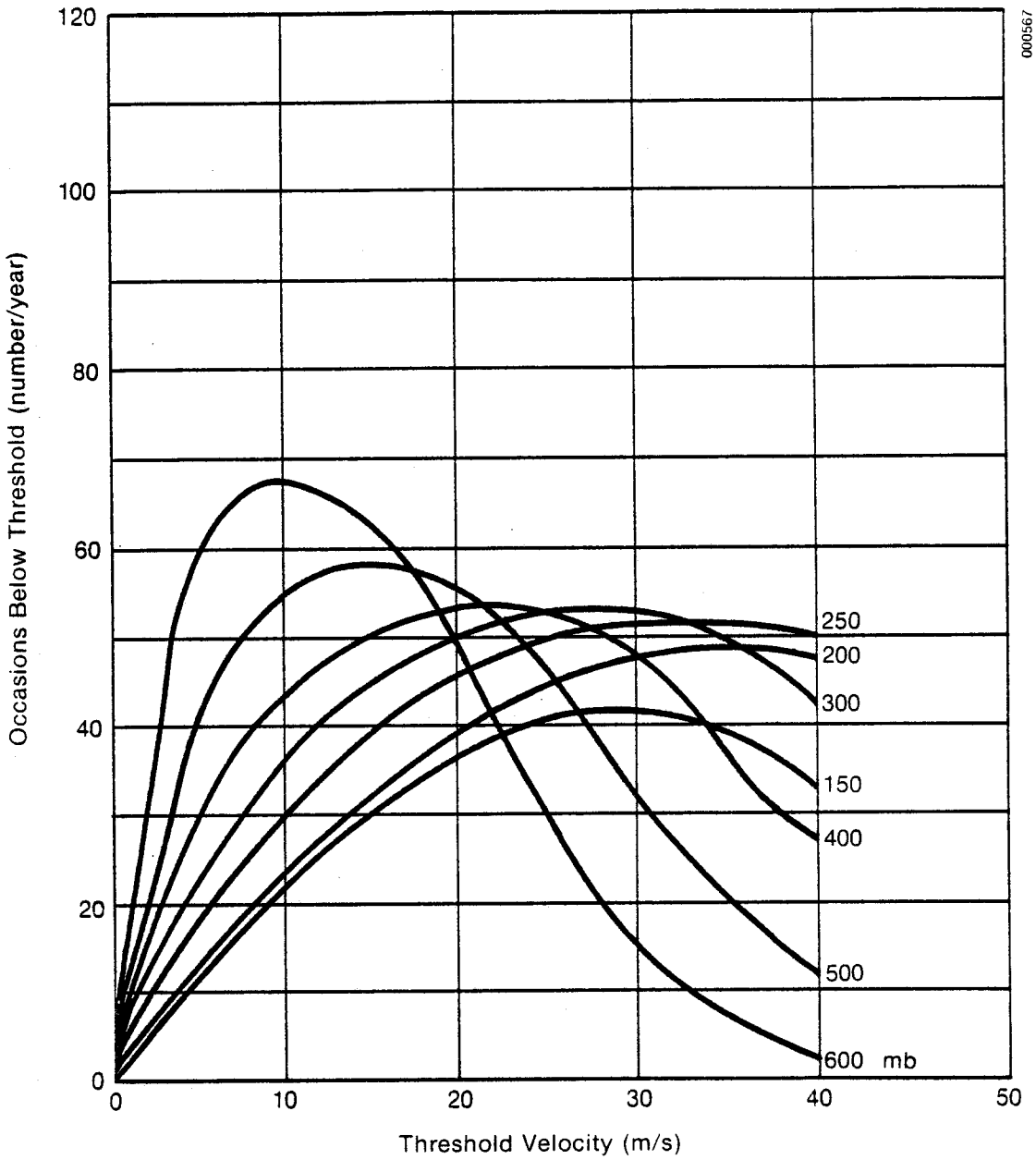

Figure C-5. Annual Calm-Period Analysis: Midland, TX

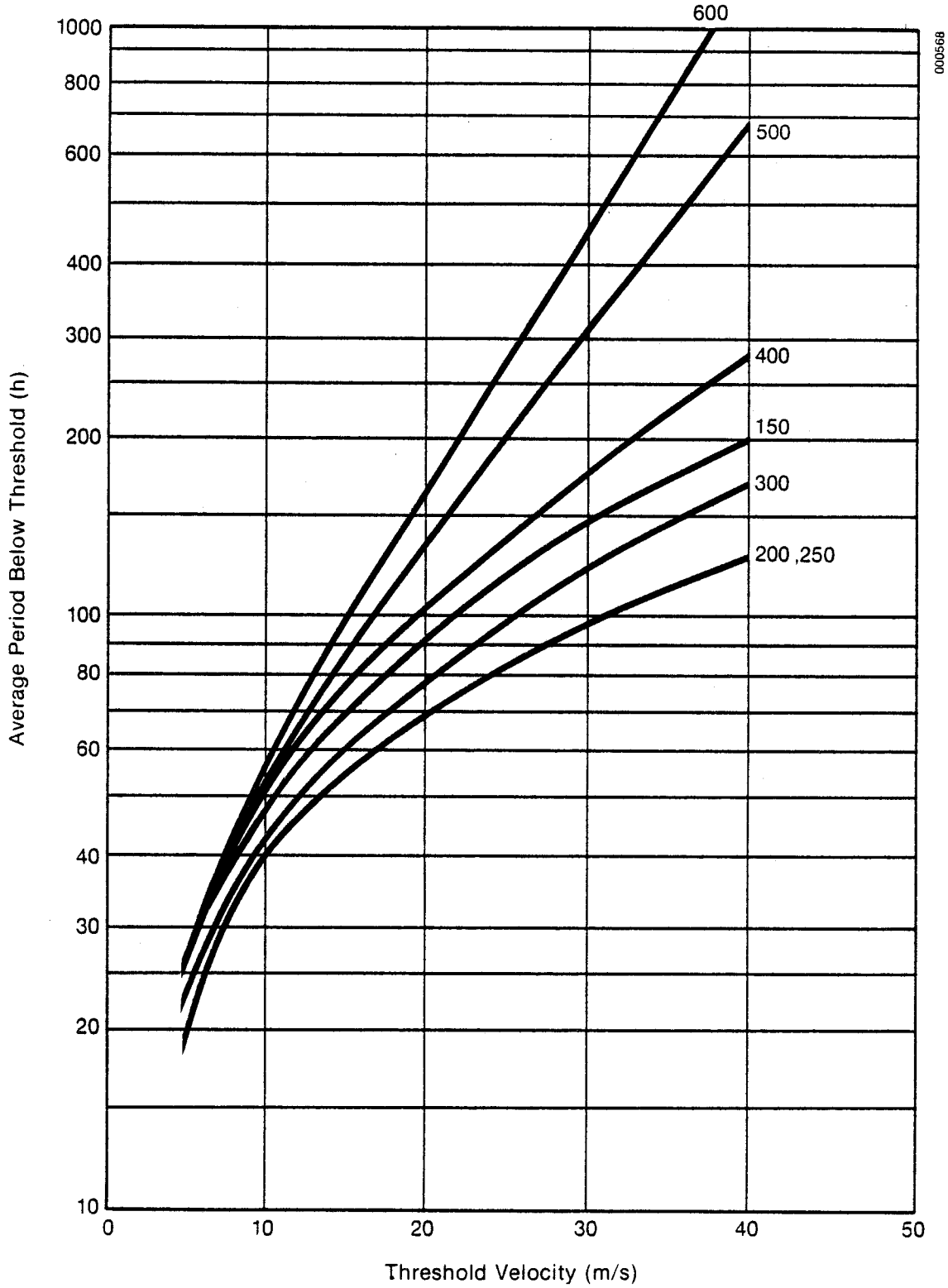

Figure C-6. Annual Calm-Period Analysis: Midland, TX

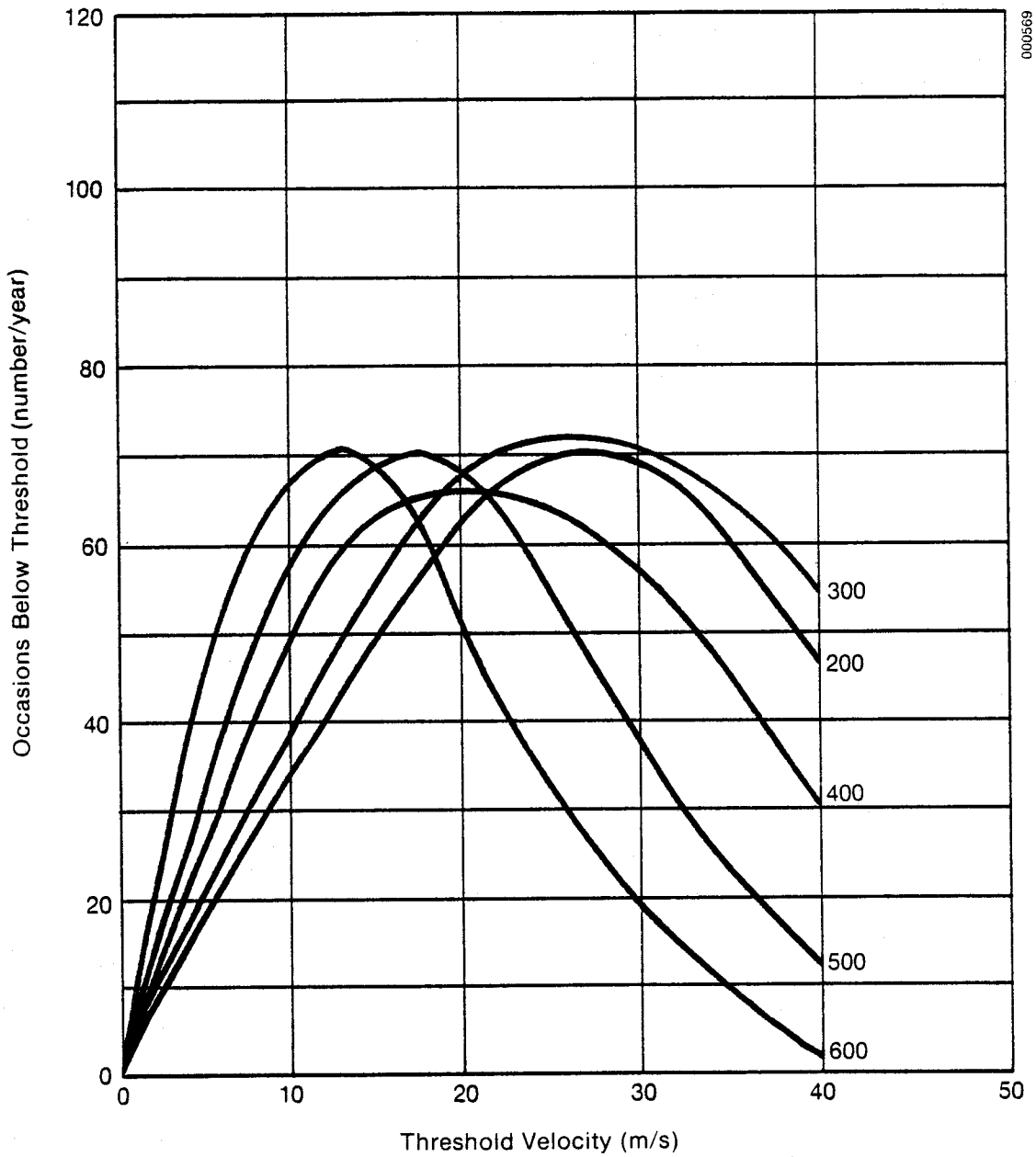

Figure C-7. Annual Calm-Period Analysis: Oakland, CA

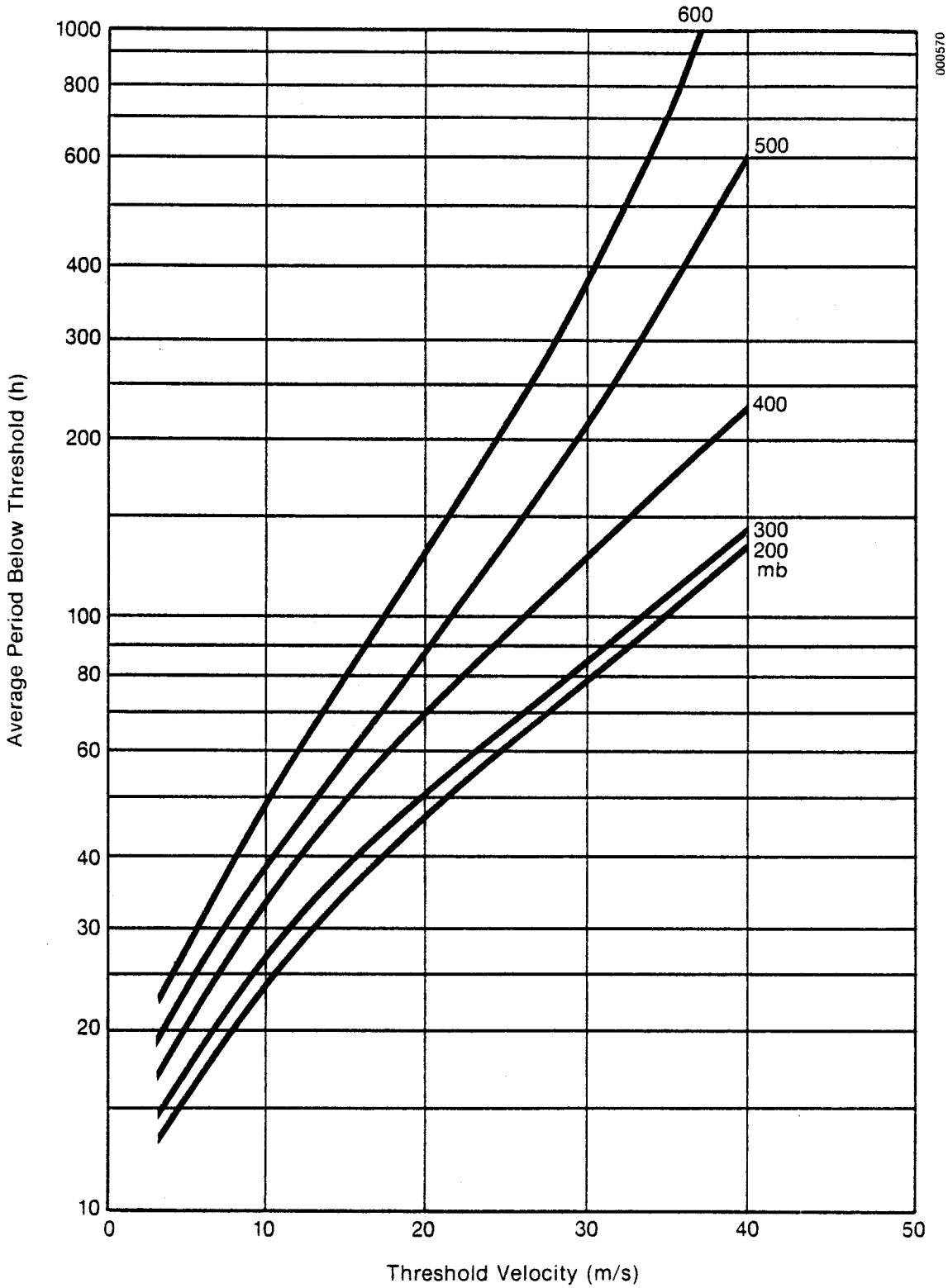

Figure C-8. Annual Calm-Period Analysis: Oakland, CA

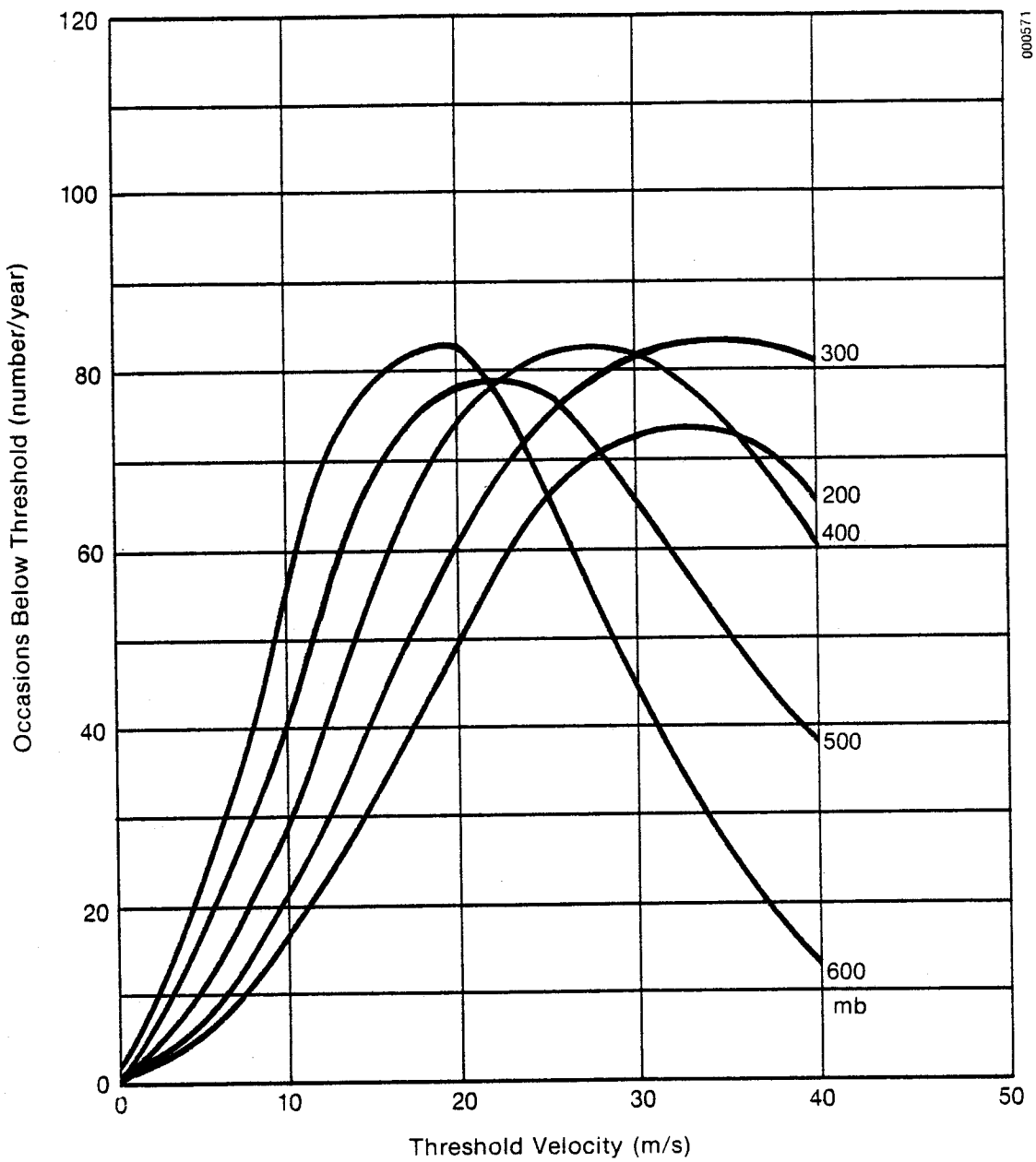

Figure C-9. Annual Calm-Period Analysis: Portland, ME

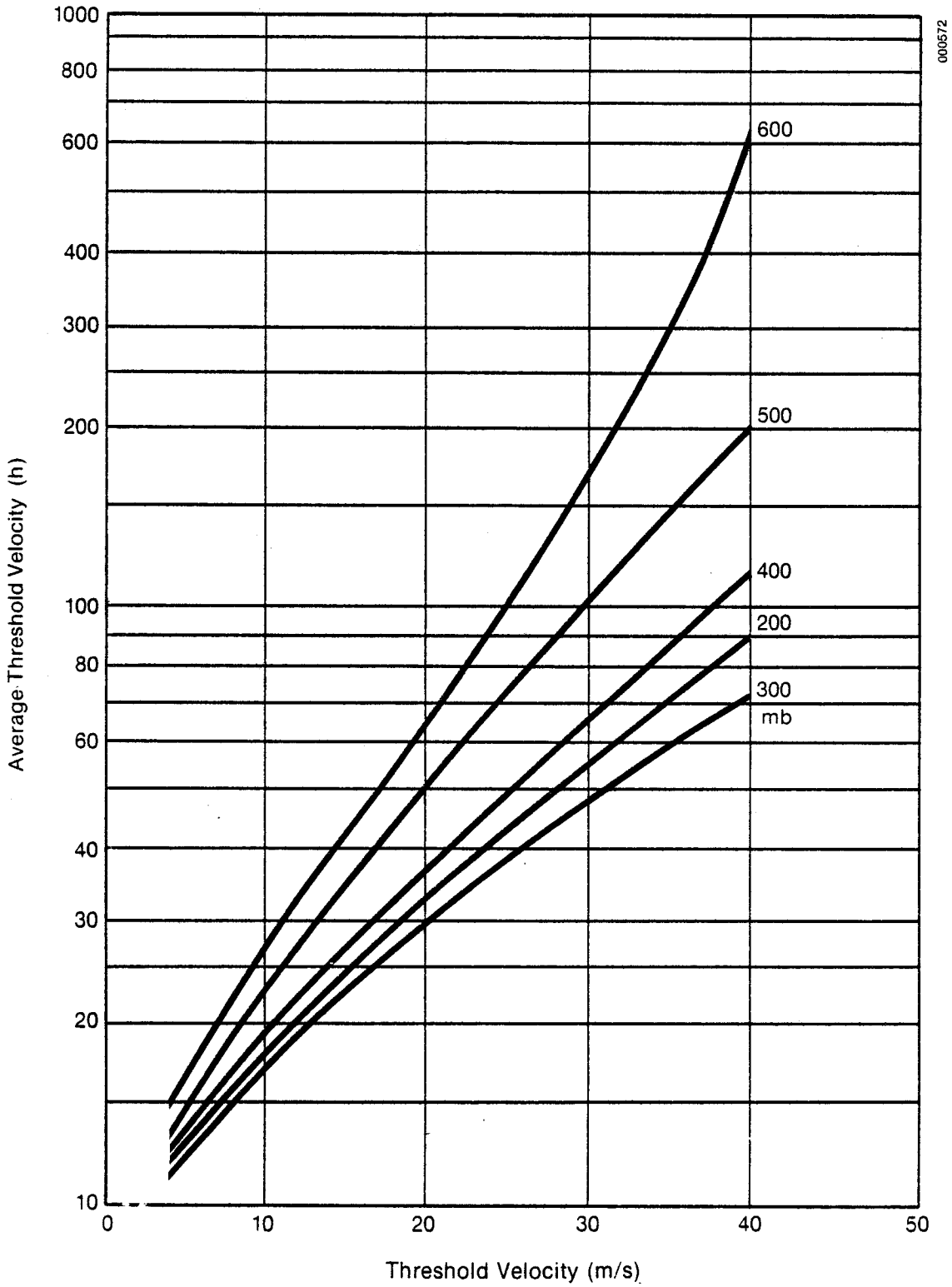

Figure C-10. Annual Calm-Period Analysis: Portland, ME

APPENDIX D

USE OF THE ANNUAL PROBABILITY DISTRIBUTION OF VELOCITY CHARTS

SERI

APPENDIX D

USE OF THE ANNUAL PROBABILITY DISTRIBUTION OF VELOCITY CHARTS

The Annual Probability Distribution of Velocity charts are given in Figs. B-1 through B-54 in App. B. In each of the charts the actual cumulative probabilities P(V) are plotted against V for various pressure levels between 700 mb and 200 mb.

Furthermore the charts have been plotted on special paper known as Weibull paper [3]. On this paper the two-parameter Weibull distribution, given as

$$P(V) = 1 - e^{-(V/V_o)^{\alpha}} \quad V \geq 0 \quad , \tag{1}$$

will appear as a straight-line plot. In this manner, a straight line may be drawn to represent the actual distribution formed from the NCAR data.

The probability distribution given in Eq. 1 uses two parameters, V_o and α. In order to reduce this distribution to a straight-line plot on Weibull graph paper, one needs to compute the natural logarithm of both sides of Eq. 1. Hence it follows that

$$\sqrt{\ell n\{1/[1 - P(V)]\}} = (V/V_o)^{\alpha/2} \quad . \tag{2}$$

If Eq. 2 is plotted on log-log graph paper,

$$\alpha/2 = \log\left(\sqrt{\ell n\{1/[1 - P(V)]\}}\right)/\log(V/V_o) \quad . \tag{3}$$

In this way the slope of the straight-line plot of Fig. 2-7 is exactly $\alpha/2$. In addition the value of V_o is found from $V = V_o$ when $P(V) = (1 - 1/e) = 0.633$.

Finally α is approximately 2 in our work, so that the slope of the straight line is approximately 45° because $\alpha/2 \approx 1$.

Figure 2-7 of the text gives the Weibull probability distributions for Portland, Me., at altitudes of 700, 500, 400, 300, and 200 mb. The intersection of the appropriate Weibull straight line with the dotted horizontal line at P(V) = 63.3% gives the corresponding value of V_o, as read on the abscissa of the chart. The values of V_o are tabulated in Table D-1 as read from Fig. 2-7 to an accuracy of ±0.5 m/s.

To determine the value of α, first choose the required straight-line distribution. Then draw another straight line parallel to this line so that it passes through the center of the target symbol near the top right corner of the figure. Next extend this parallel line to cross the vertical line at the extreme left side of the figure. This latter intersection gives the value of α. The relevant values of α from Fig. 2-7 are given in Table D-1 to a reading accuracy of about ±0.01.

Table D-1. Values of V_o in Portland, Maine

Pressure (mb)	V_o (m/s)	α
700	16.5	1.98
500	25.5	2.07
400	31.5	2.07
300	37.0	2.22
200	35.5	2.21

It is possible to show from the Weibull distribution given in Eq. 1 that the average annual wind speed $\overline{V}$ and the average annual power density $\overline{P}$ are the following functions of V_o and α:

$$\overline{V} = V_o\Gamma(1 + 1/\alpha) \quad , \tag{4}$$

and

$$\overline{P} = 1/2\ \rho V_o^3\Gamma(1 + 3/\alpha) \quad , \tag{5}$$

where $\Gamma(x)$ is the gamma function that is widely tabulated.

Next, compare the mean velocities and power densities using Table D-1 with the actual computed values of $\overline{V}$ and $\overline{P}$ using the NCAR data. The comparison in Table D-2 verifies the validity or otherwise of our Weibull model. The first of the columns $\overline{V}$ and $\overline{P}$ are for the Weibull model, while the second columns of $\overline{V}$ and $\overline{P}$ are formed from the NCAR data.

According to the results in Table D-2, the Weibull model gave good estimates of the mean wind speeds and the mean power densities.

We feel that the two-parameter Weibull model is generally satisfactory, which is in line with other wind energy results from workers such as Justus, Hennessey, and others.

Table D-2. Weibull Model vs. Actual Data for Values of $\overline{V}$ and $\overline{P}$ in Portland, Maine

Pressure (mb)	$\Gamma(1 + 1/\alpha)$	$\Gamma(1 + 3/\alpha)$	ρ (kg/m^3)	$\frac{1}{2}\rho V_o^3$ (kW/m^2)	Weibull Model		Actual Data	
					$\overline{V}$ (m/s)	$\overline{P}$ (kW/m^2)	$\overline{V}$ (m/s)	$\overline{P}$ (kW/m^2)
700	0.886	1.348	0.913	2.05	14.6	2.76	14.8	2.84
500	0.886	1.285	0.695	5.76	22.6	7.40	22.5	7.53
400	0.886	1.285	0.580	9.06	27.9	11.6	27.6	11.4
300	0.886	1.203	0.460	11.65	32.8	14.0	32.8	14.1
200	0.886	1.210	0.323	7.23	31.5	8.74	31.2	7.90

Document Control Page	1. SERI Report No. TR-211-1400	2. NTIS Accession No.	3. Recipient's Accession No.

4. Title and Subtitle
The Application of U.S. Upper Wind Data in the Design of Tethered Wind Energy Systems

5. Publication Date
February 1982

6.

7. Author(s)
R. J. O' Doherty

8. Performing Organization Rept. No.

9. Performing Organization Name and Address
Solar Energy Research Institute
1617 Cole Boulevard
Golden, Colorado 80401

10. Project/Task/Work Unit No.
1067.10

11. Contract (C) or Grant (G) No.
(C)
(G)

12. Sponsoring Organization Name and Address

13. Type of Report & Period Covered
Technical Report

14.

15. Supplementary Notes

16. Abstract (Limit: 200 words)
This report assesses the upper atmospheric wind resource for the continental United States, Hawaii, and Alaska. The document is intended for Solar Energy Research Institute contractors interested in tethered wind energy systems. The raw data were obtained from the National Center for Atmospheric Research, Boulder, Colo. The probability distributions of velocity are presented for 54 sites, and detailed calm wind analyses have been undertaken for five of these locations. On the average, the wind lulls about one day per week for a period in excess of about 30 hours. The report shows that the average power density of this wind resource can be as high as 16 kW/m^2 at northeastern U.S. sites. This power density is at a maximum around the 300-mb pressure level.

17. Document Analysis
a. Descriptors wind ; earth atmosphere ; altitude ; wind power ; velocity ; statistics ; numerical analysis ; power density ; statistical data

b. Identifiers/Open-Ended Terms

c. UC Categories
60

18. Availability Statement
National Technical Information Service
U.S. Department of Commerce
5285 Port Royal Road
Springfield, Virginia 22161

19. No. of Pages
139

20. Price
$7.25

Form No. 8200-13 (6-79)